



Review

# Comprehensive Review on Synthesis, Properties, and Applications of Phosphorus (P<sup>III</sup>, P<sup>IV</sup>, P<sup>V</sup>) Substituted Acenes with More Than Two Fused Benzene Rings

Marek Koprowski <sup>1,\*</sup>, Krzysztof Owsianik <sup>1</sup>, Łucja Knopik <sup>1</sup>, Vivek Vivek <sup>1</sup>, Adrian Romaniuk <sup>1</sup>, Ewa Różycka-Sokołowska <sup>2</sup> and Piotr Bałczewski <sup>1,2,\*</sup>

<sup>1</sup> Division of Organic Chemistry, Center of Molecular and Macromolecular Studies, Polish Academy of Sciences, Sienkiewicza 112, 90-363 Łódź, Poland

<sup>2</sup> Institute of Chemistry, Faculty of Science and Technology, Jan Długosz University in Częstochowa, Armii Krajowej 13/15, 42-200 Częstochowa, Poland

\* Correspondence: mkopr@cbmm.lodz.pl (M.K.); pbalczew@cbmm.lodz.pl (P.B.)

**Abstract:** This comprehensive review, covering the years 1968–2022, is not only a retrospective investigation of a certain group of linearly fused aromatics, called acenes, but also a presentation of the current state of the knowledge on the synthesis, reactions, and applications of these compounds. Their characteristic feature is substitution of the aromatic system by one, two, or three organophosphorus groups, which determine their properties and applications. The (P<sup>III</sup>, P<sup>IV</sup>, P<sup>V</sup>) phosphorus atom in organophosphorus groups is linked to the acene directly by a P-C<sub>sp2</sub> bond or indirectly through an oxygen atom by a P-O-C<sub>sp2</sub> bond.

**Keywords:** acene; anthracene; phosphine; phosphonate; phosphonium salt; phosphorane; phosphate; diphosphene; tri-, tetra-, pentacoordinated phosphorus; properties



**Citation:** Koprowski, M.; Owsianik, K.; Knopik, Ł.; Vivek, V.; Romaniuk, A.; Różycka-Sokołowska, E.; Bałczewski, P. Comprehensive Review on Synthesis, Properties, and Applications of Phosphorus (P<sup>III</sup>, P<sup>IV</sup>, P<sup>V</sup>) Substituted Acenes with More Than Two Fused Benzene Rings. *Molecules* **2022**, *27*, 6611. <https://doi.org/10.3390/molecules27196611>

Academic Editor: Jakub Adamek

Received: 9 September 2022

Accepted: 27 September 2022

Published: 5 October 2022

**Publisher's Note:** MDPI stays neutral with regard to jurisdictional claims in published maps and institutional affiliations.



**Copyright:** © 2022 by the authors. Licensee MDPI, Basel, Switzerland. This article is an open access article distributed under the terms and conditions of the Creative Commons Attribution (CC BY) license (<https://creativecommons.org/licenses/by/4.0/>).

## 1. Introduction

Organophosphorus-substituted acenes are an increasingly important group of aromatic hydrocarbons due to the unique properties of the phosphorus atom, which can form tri-, tetra-, and pentacoordinated compounds. This creates the possibility of tuning the electronic properties of the aromatic system of acenes by substituting with organophosphorus groups with different electron characters, from electron-donating phosphine groups to strongly electron-accepting phosphonium groups. The acenes of this type, especially anthracenes, have usually been synthesized with the intention of applying them to organic light-emitting diodes (OLEDs) [1,2]. Other uses of these acenes include the synthesis of ligands for metal catalysts in the hydroformylation reaction [3] or in the Diels–Alder reaction as dienes [4]. Anthrylphosphonic acids and their derivatives have also been employed in the synthesis of self-assembled monolayers [5,6] and anthrylbisphosphonates were used to synthesize fluorescent organic nanoparticles as apoptosis inducers of cancer cells [7].

**Scope:** Acenes, as defined, are a group of aromatic compounds containing linearly fused benzene rings. In the literature, compounds with angularly fused benzene rings, such as phenanthrene, and compounds with fused heteroaromatic five- and six-membered rings are sometimes included in this group, and they are specifically called angularly fused acenes and heteroacenes, respectively. Both groups, due to the large number of combinations of ring types and the ring positioning in the fused acene, in addition to derivatives of the simplest linearly fused acene, naphthalene, are not the subject of this review. By virtue of their chemical structure, organophosphorus groups have not been restricted and include all groups containing three-, four-, and five-coordinate phosphorus atoms. In the compounds reviewed, organophosphorus groups contain a phosphorus atom,

which is linked to the acene directly by a P-C<sub>sp2</sub> bond or indirectly through an oxygen atom by a P-O-C<sub>sp2</sub> bond, such as in phosphates.

This review of the literature covers the period of 1968–2021 and reveals a lack of aromatics that contain more than three fused benzene rings (tetracenes, pentacenes, etc.). Therefore, the subject of this review is anthracenes substituted with any organophosphorus groups.

In addition to the synthesis, this review discusses the reactions that these compounds undergo, and therefore, due to the difficulty of separating the two categories, “synthesis and reactions” are combined together in sections and subsections. Moreover, this review discusses the properties and applications of the synthesized derivatives as well.

This manuscript is divided into five main sections covering phosphines, P<sup>III</sup> acids derivatives, diphosphenes, phosphonates and phosphonic acids, phosphates, and the hetero analogs of the mentioned compounds. In the subsections, groups of compounds that can be obtained directly from the precursor included in the main section are identified, e.g., phosphine oxides, phosphonium salts, and phosphoranes can be obtained from phosphines by oxidation, alkylation, and halogenation, respectively, and therefore they are included in the section devoted to the synthesis and reactions of phosphines and derivatives.

Finally, a comment on Section 3 is necessary. Phosphines ( $\lambda^3$ -phosphanes), by definition, are P<sup>III</sup> compounds containing a combination of three P-Z bonds (Z = C,H). Halophosphines AnthPX<sub>2</sub> and Anth<sub>2</sub>PX (X = F, Cl), which contain at least one P-C bond and one or two halogen atoms, are here classified as halides of the corresponding lower P<sup>III</sup> acids [8]. Additionally included in this group are other representatives of the lower P<sup>III</sup> acids, i.e., phosphonous acid diamides AnthP(NR<sub>2</sub>)<sub>2</sub> (diaminophosphines) and phosphorous acid esters (phosphites).

As a consequence of this division, phosphonous acid P<sup>IV</sup> tautomers (*H*-phosphinic acids) and phosphinous acid P<sup>IV</sup> tautomers (*H*-phosphine oxides) are also reviewed in this section.

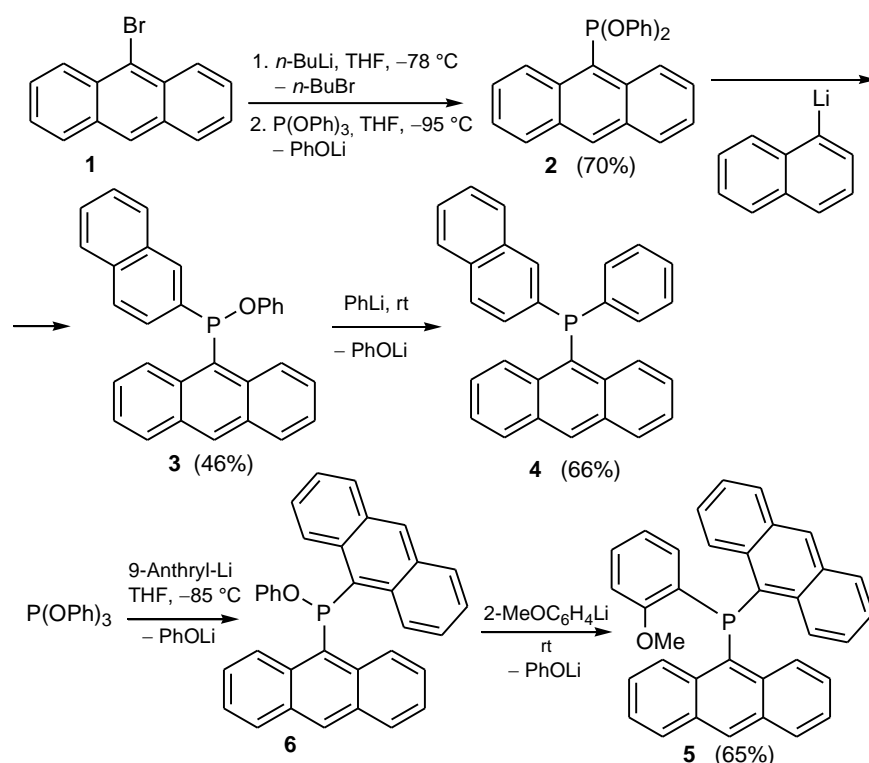
Diphosphenes, as the only compounds with a functional group containing more than one phosphorus atom, are discussed separately in Section 6.

## 2. Synthesis and Reactions of Phosphines (AnthPR<sub>2</sub>) (Anth = Anthryl) and Derivatives

This section discusses phosphines, which contain a three-coordinated phosphorus atom linked to three carbon atoms. The subsections of this chapter include groups of compounds that can easily be obtained from phosphine precursors by direct transformation to give compounds with tetra- and pentacoordinated phosphorus atoms. Phosphine oxides, sulfides, and selenides are placed together in one subsection because most papers simultaneously describe the synthesis and reactions of two or three groups of these derivatives. Secondary phosphine oxides (*H*-phosphine oxides) are discussed in Section 3.5 as phosphinous acid P<sup>IV</sup> tautomers.

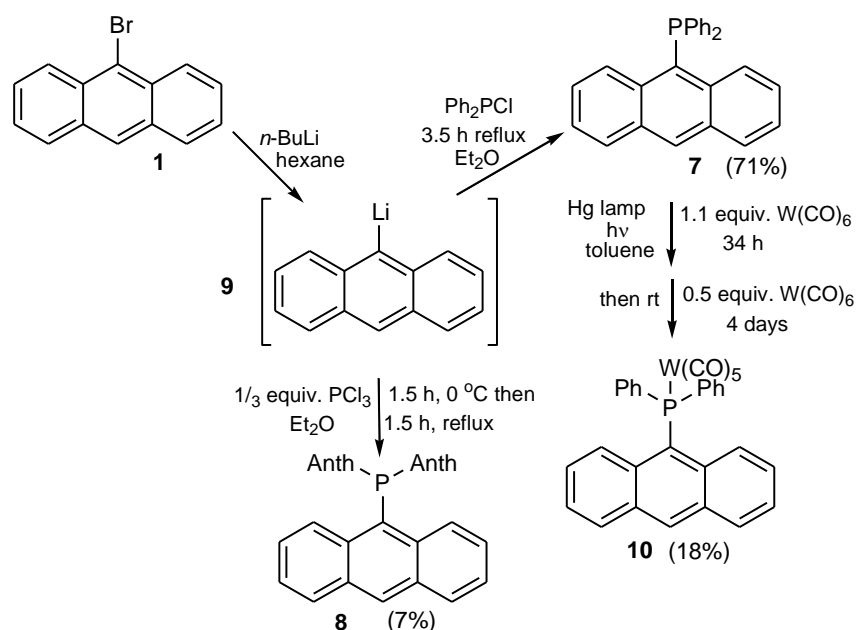
9-Bromoanthracene **1** is the most frequently used starting material for the syntheses of anthryl phosphines and other derivatives (cf. other subsections throughout this review).

A number of sterically shielded phosphorus ligands for metal catalysts were synthesized by Straub and co-workers via a selective stepwise nucleophilic substitution reaction at the phosphorus atom in triphenyl phosphite (Scheme 1). Thus, first, diphenyl 9-anthrylphosphonite **2** was obtained in a 70% yield by substitution of one phenoxy group by anthryllithium, generated from 9-bromoanthracene **1** and *n*-butyllithium. Next, the second phenoxy group in triphenyl phosphite was replaced by 1-naphthyllithium to afford phenyl 9-anthryl(1-naphthyl)phosphinite **3** in an overall yield of 46%. Finally, the third least reactive phenoxy group was replaced by phenyllithium to give (anthryl)(naphthyl)(phenyl)phosphine **4** in a 66% isolated yield over three steps. In another synthetic sequence, [di(9-anthryl)](2-methoxyphenyl)phosphine **5** was obtained from triphenyl phosphite via phenyl phosphinite **6** by reacting triphenyl phosphite first with 9-anthryllithium, followed by 2-methoxyphenyllithium at −85 °C. Since phosphorus ligands, employed in homogeneous catalysis, often contain at least one sterically demanding substituent, this method delivers a strategy for the rapid and cost-efficient synthesis of such ligands [9].



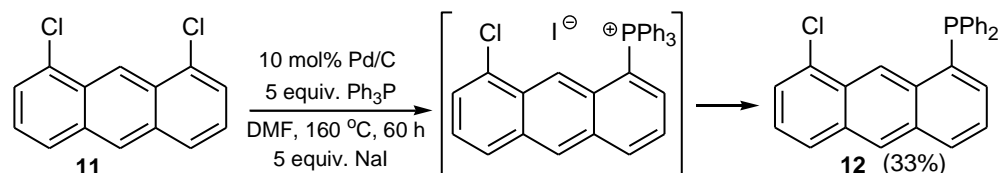
**Scheme 1.** The synthesis of sterically hindered phosphine ligands 4 and 5.

Schmutzler et al. reported the synthesis of (anthryl)(diphenyl)phosphine 7 and trianthrylphosphine 8 starting from 9-bromoanthracene 1, which was lithiated to give the intermediate 9-lithioanthracene 9. The latter was reacted with 1 equiv. of chlorodiphenylphosphine or 1/3 equiv. of  $\text{PCl}_3$  in diethyl ether at reflux to give 7 or 8 in 71% and 7% yields, respectively. The irradiation of 7 in the presence of  $\text{W}(\text{CO})_6$  with a mercury lamp for 34 h formed the pentacarbonyltungsten complex 10 in an 18% yield (Scheme 2) [10].



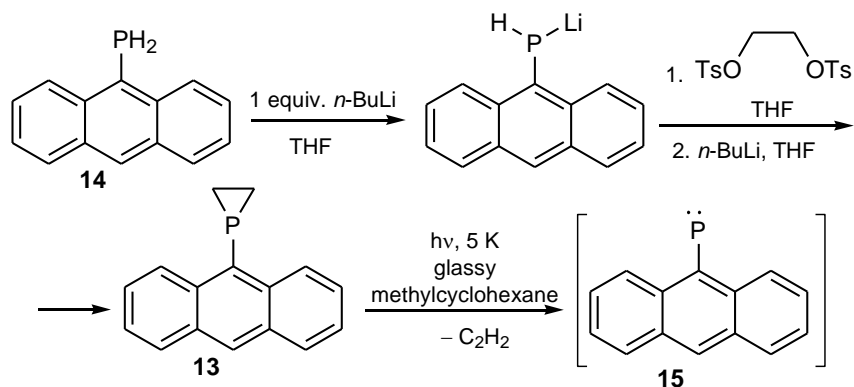
**Scheme 2.** The synthesis of (anthryl)(diphenyl)phosphine 7 and trianthrylphosphine 8 and the pentacarbonyltungsten complex 10.

Chan and co-workers reported a simple monophosphinylation reaction of 1,8-dichloroanthracene **11**, leading to 8-chloro-1-(diphenylphosphino)anthracenes **12** in a 33% yield (Scheme 3) [11]. This reaction was carried out in DMF at 160 °C for 60 h and catalyzed by 10 mol% of palladium supported on charcoal in the presence of 5 equiv. of triphenylphosphine. The addition of 5 equiv. of sodium iodide improved both the rate and yield of the reaction. The second chlorine atom in **11** was not substituted in this reaction and only the mono-derivative **12** was observed, despite the presence of an excess of triphenylphosphine. The authors claimed that steric hindrance of the diphenylphosphino group in position 1 of anthracene protected against the reaction of the second chlorine atom.



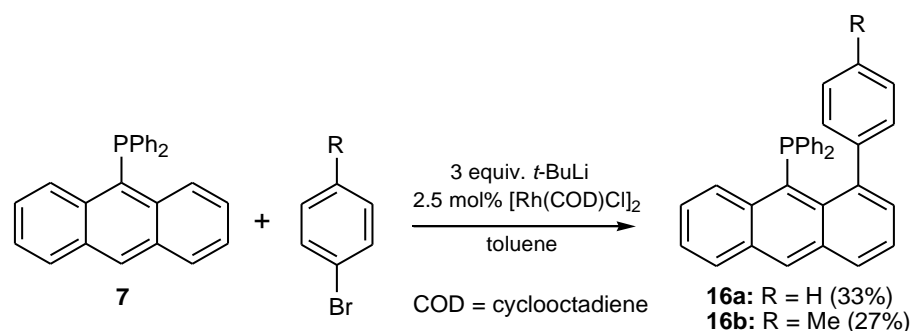
**Scheme 3.** The synthesis of 8-chloro-1-(diphenylphosphino)anthracenes **12**.

Misochko and co-workers [12] obtained 9-(1-phosphirano)anthracene **13** from 9-phosphinoanthracene **14** and ethylene glycol ditosylate as substrates by adapting the procedure of Robinson et al. [13] (Scheme 4). In the next step, 9-(1-phosphirano)anthracene **13** was subjected to UV photolysis to receive a stable triplet anthrylphosphinidene **15**, which could be characterized by electron paramagnetic resonance (EPR).



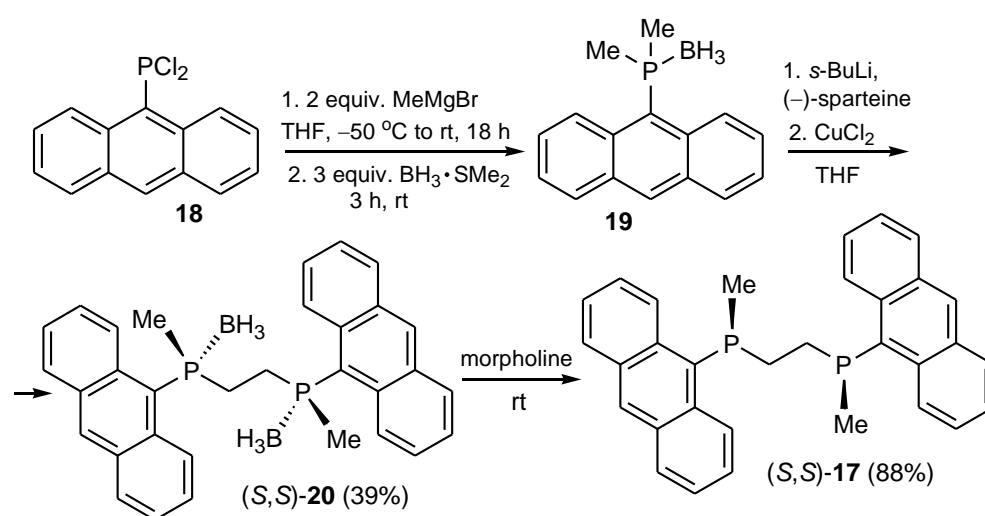
**Scheme 4.** Synthesis of 9-(1-phosphirano)anthracene **13**, a precursor of the phosphinidene **15**.

Che and co-authors reported the rhodium(I)-catalyzed C–H arylation of 9-(diphenylphosphino)anthracene **7**, as an example of functionalization of phosphines, to give 1-aryl-substituted derivatives **16a** and **16b** (Scheme 5) [14]. The presented strategy provided access to *peri*-substituted (naphth-1-yl)phosphines as well.



**Scheme 5.** The Rh-catalyzed arylation of 9-(diphenylphosphino)anthracene **7** with different aryl bromides.

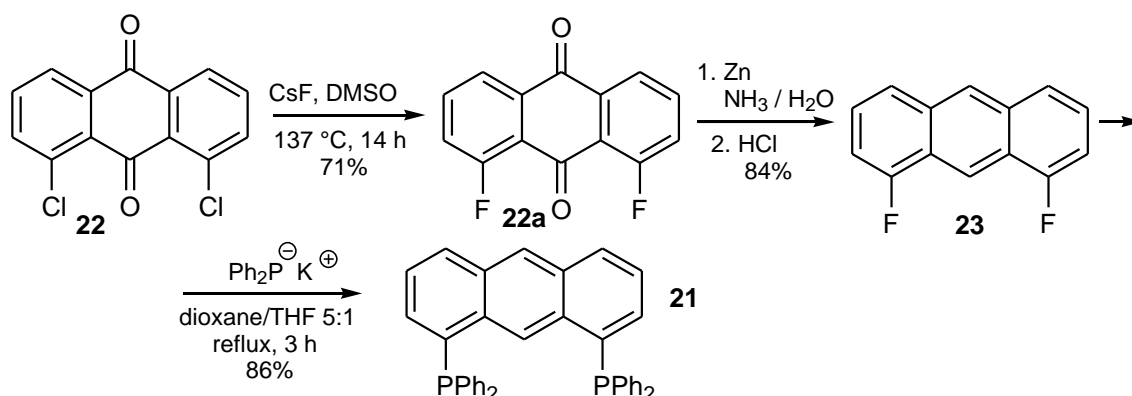
The synthesis of optically active 1,2-ethylene bis(phosphine) (*S,S*)-**17**, presented by Maienza and co-workers, is the only example of a molecule containing two anthrylphosphino moieties linked via an alkyl linker [15]. First, 9-(dichlorophosphino)anthracene **18** was utilized in the reaction with methyl magnesium bromide and  $\text{BH}_3 \cdot \text{SMe}_2$  to obtain 9-anthryldimethylphosphine borane **19**. Then, **19** was enantioselectively deprotonated in the presence of (–)-sparteine with *s*-BuLi and then oxidatively coupled with Cu (II) to give a mixture of enantiomers of 1,2-ethylene bis(phosphine) diboranes (*S,S*)-**20** and (*R,S*)-**20** in a 6:1 ratio and 70% total yield (Scheme 6). Diastereomerically pure (*S,S*)-**20** was received by crystallization from a  $\text{CH}_2\text{Cl}_2/\text{Et}_2\text{O}$  mixture in a 39% yield and 18% ee. Finally, the diphosphine borane (*S,S*)-**20** was deprotected by stirring in morpholine at room temperature for 12 h. In this reaction, the 1,2-ethylene bis(phosphine) (*S,S*)-**17** was obtained and its enantiomeric excess was determined based on the corresponding phosphine oxide, which was prepared by oxidation of **17** with an excess of  $\text{H}_2\text{O}_2$ .



**Scheme 6.** The synthesis of 1,2-ethylene bis(phosphine) **17**.

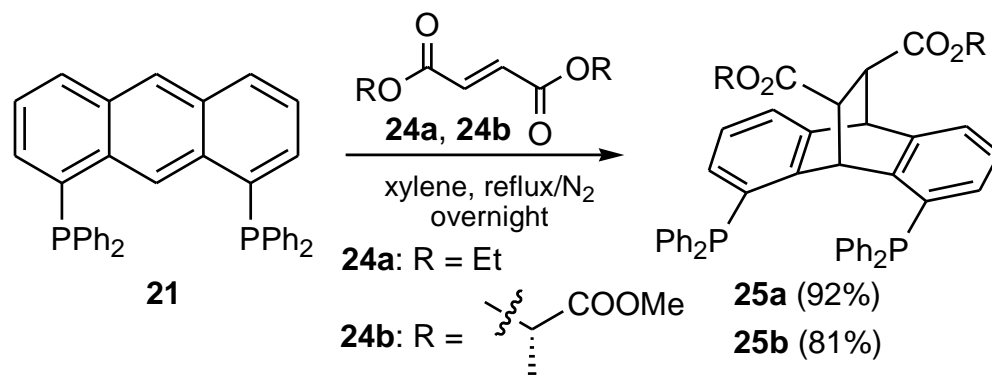
In the reviewed literature, the synthesis, transformations, and utilization of anthracenes with two phosphino groups on the aromatic moiety were found and are presented below.

1,8-Bis(diphenylphosphino)anthracene **21** was synthesized in a three-step reaction in a 51% overall yield starting from 1,8-dichloro-9,10-anthraquinone **22** by Haenel and co-workers (Scheme 7). The anthraquinone **22** was converted to 1,8-difluoroanthracene **23** by chlorine-fluorine exchange to give **22a** followed by reduction with zinc, from which **21** was obtained by reacting it with potassium diphenylphosphide [16].



**Scheme 7.** The synthesis of 1,8-bis(diphenylphosphino)anthracene **21** from 1,8-dichloro-9,10-anthraquinone **22**.

Gelman and co-workers presented the quantitative Diels–Alder cycloaddition of 1,8-bis-(diphenylphosphino)anthracene **21** to diethyl fumarate **24a**. The adduct **25a** was used for the synthesis of bifunctional PCsp<sup>3</sup>P pincer catalyst for the acceptorless dehydrogenation (CAD) of the primary and secondary alcohols to give carbonylic and carboxylic compounds (Scheme 8) [17].



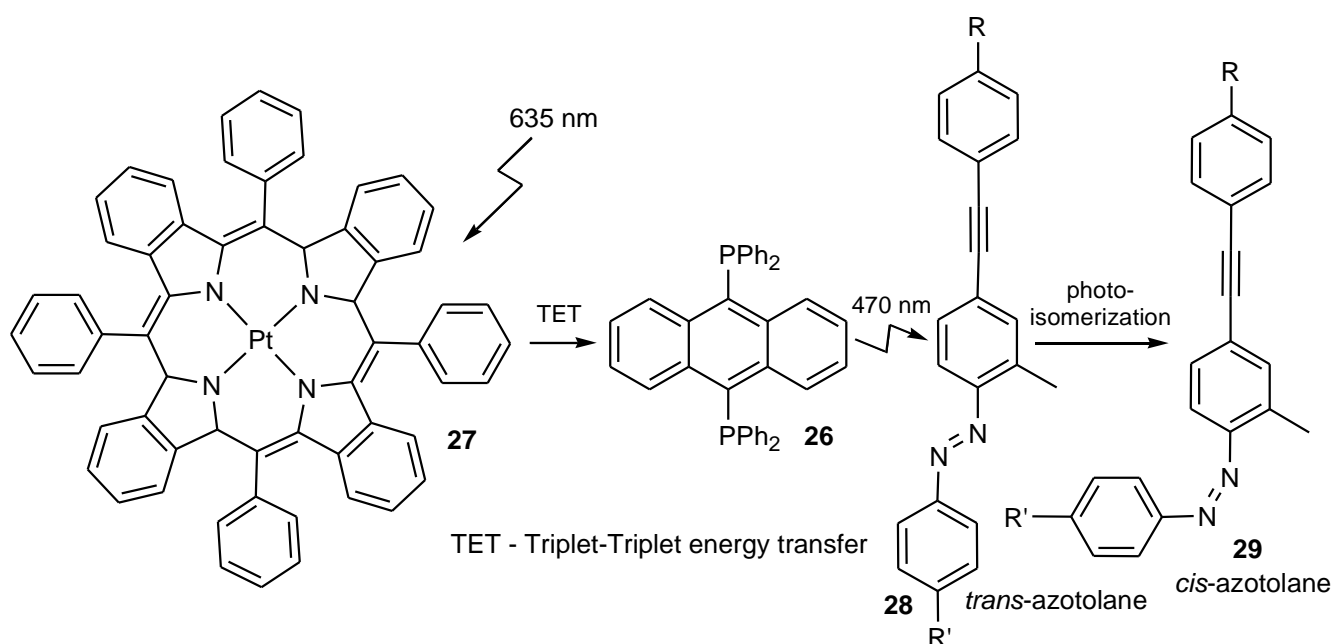
**Scheme 8.** The Diels–Alder cycloaddition reaction of 1,8-bis-(diphenylphosphino)anthracene **21** with dialkyl fumarates.

The same research group reported a synthetic scheme that relied on the carbo-Diels–Alder reaction cycloaddition of 1,8-bis-(diphenylphosphino)anthracene **21** to enantiomerically pure bis-(methyl-(*S*)-lactyl) fumarate **24b**, leading to the formation of chromatographically resolvable diastereomers **25b** that could be converted into a pair of enantiomerically pure antipodes (Scheme 8) [18].

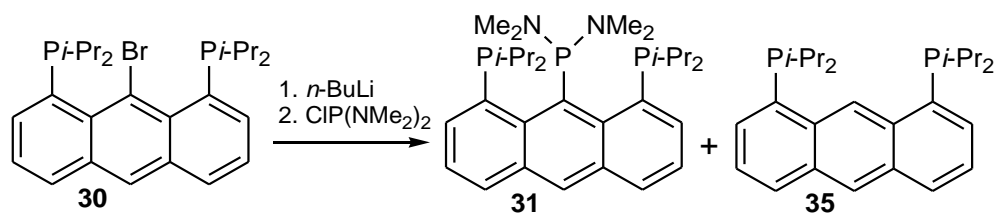
Jiang and co-workers [19] showed a practical utilization of 9,10-bis(diphenylphosphino)anthracene **26**. They obtained a red-light-controllable soft actuator, which was driven by the low-power excited triplet–triplet annihilation-based upconversion luminescence. This system consisted of 9,10-bis(diphenylphosphino)anthracene **26** and the Pt(II) tetraphenyl-tetrabenzoporphyrin complex **27** (Scheme 9). It was then incorporated into a rubbery polyurethane film and assembled with an azotolane-containing film to study its possible utilization as a highly effective phototrigger of photodeformable cross-linked liquid-crystal polymers. In this system, the Pt(II) complex **27** acted as a sensitizer, whereas **26** was an annihilator, which induced *trans-cis* photoisomerization of azotolane **28** and **29**. The authors achieved a highly effective red-to-blue triplet-triplet annihilation-based upconversion layout with a low-energy excitation light source, large anti-Stokes shift (165 nm), and high absolute quantum yield (9.3%).

In the literature reviewed, the chemistry of anthracenes with two or three phosphino groups and their mixed tetracoordinated derivatives was also found and is presented below.

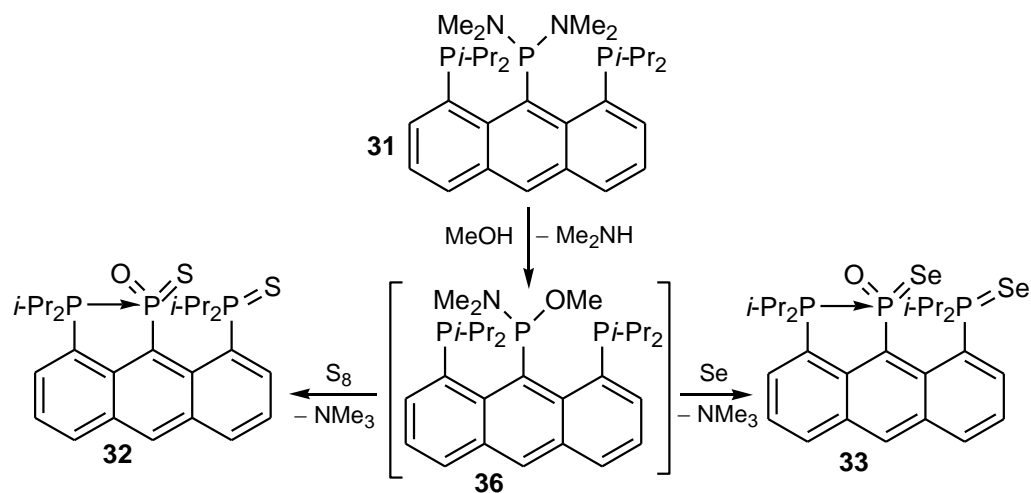
Thus, 9-bromo-1,8-bis(diisopropylphosphino)anthracene **30**, repulsively interacting with 1,8,9-tris(phosphino)anthracene **31** (Scheme 10), single donor stabilized 8-diisopropylphosphino-1-thiophosphinoyl-9-metathio/metaselephosphono)anthracenes **32** and **33** (Scheme 11), and doubly phosphine donor stabilized phosphonium salt **34** (Scheme 12), were synthesized by Kilian and co-workers [20]. The attempted introduction of the third phosphorus atom at the position 9 via Br/Li exchange followed by the reaction with chlorobis(dimethylamino)phosphine resulted in formation of 1,8,9-tris- and 1,8-bis(phosphino)anthracenes **31** and **35**, respectively. The derivative **31** had two relatively inert and bulky diisopropylphosphino groups at positions 1 and 8 whilst the third reactive phosphino group with two P–N bonds on the middle ring opened up the possibility of various transformations on this phosphorus atom, situated in a very crowded surrounding.



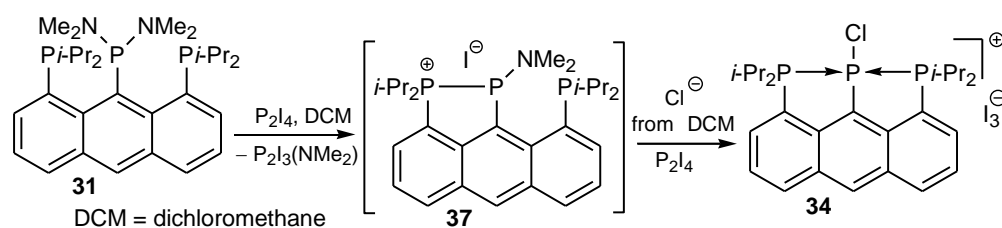
**Scheme 9.** An example of the application of 26 in a red-light-controllable soft actuator system (photoisomerization of azotolane).



**Scheme 10.** Synthesis of repulsively interacting 1,8,9-tris(phosphino)anthracene 31 and 1,8-bis(phosphino)anthracene 35.



**Scheme 11.** The synthesis of single donor stabilized anthracenes 32 and 33 with metathio/selenophosphono groups.



**Scheme 12.** Synthesis of the doubly phosphine stabilized phosphonium salt **34**.

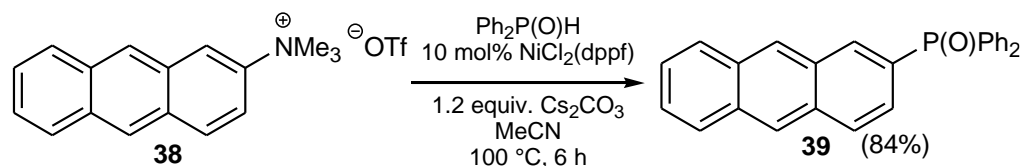
Alcoholysis of **31**, leading to the intermediate **36**, followed by oxidation with sulfur or selenium, afforded phosphine donor stabilized anthracenes **32** or **33** with metaphosphono groups, respectively.

Further reaction of **31** with diphosphorus tetraiodide in 1,2-dichloromethane gave the chlorophosphonium cation **34** stabilized by two phosphino donors at positions 1 and 8, forming a linear P–P–P arrangement. In the first step, the phosphino-phosphonium cation **37** was formed as a transient species. In the next step, the dimethylaminophosphino group was substituted by the chloride anion, which was available from the I/Cl halogen exchange reaction in chlorinated solvent (DCM). Iodide and iodine ( $I_2$ ) and triiodide originated from disproportionation reaction of  $P_2I_4$ .

### 2.1. Phosphine Oxides ( $AnthP(=O)R_2$ ), Phosphine Sulfides ( $AnthP(=S)R_2$ ), Phosphine Selenides ( $AnthP(=Se)R_2$ )

Phosphine oxides, sulfides, and selenides are placed together in one subsection because most papers simultaneously describe the synthesis and reactions of two or three groups of these derivatives. All of them were obtained directly from the corresponding phosphines.

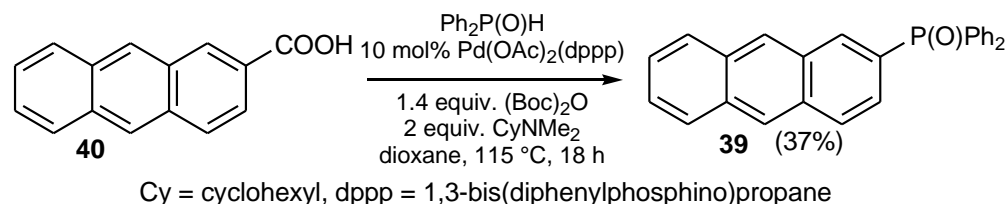
A new method for the synthesis of phosphine oxides was published by Yang et al. [21]. They employed a cross-coupling reaction and showed that aryl, vinyl, and benzyl-ammonium triflates reacted with the corresponding phosphorus-based nucleophiles in the presence of the nickel catalyst  $NiCl_2/dppf$ , ( $dppf = 1,1'$ -bis(diphenylphosphino)ferrocene) (Scheme 13).



**Scheme 13.** The synthesis of 2-(diphenylphosphinoyl)anthracene **39** using anthryl ammonium triflate **38**.

The counterion played a minor role in this reaction, so it could be replaced with chloride, bromide, iodide, mesylate, or tosylate anions without a significant loss of yield. A considerable advantage of this synthesis was that ammonium salts are cheap and readily viable.

Another method, which was developed by Zhang et al. [22], involved a direct transformation of aromatic acids into the corresponding phosphine oxides in the presence of palladium(II) salts. Several substrates were shown to react in this manner, including 2-anthric acid **40**, which was transformed to 2-(diphenylphosphinoyl)anthracene **39** (Scheme 14), providing an alternative to the synthesis of the latter from anthryl ammonium triflate **38** (Scheme 13), although in significantly lower yields.

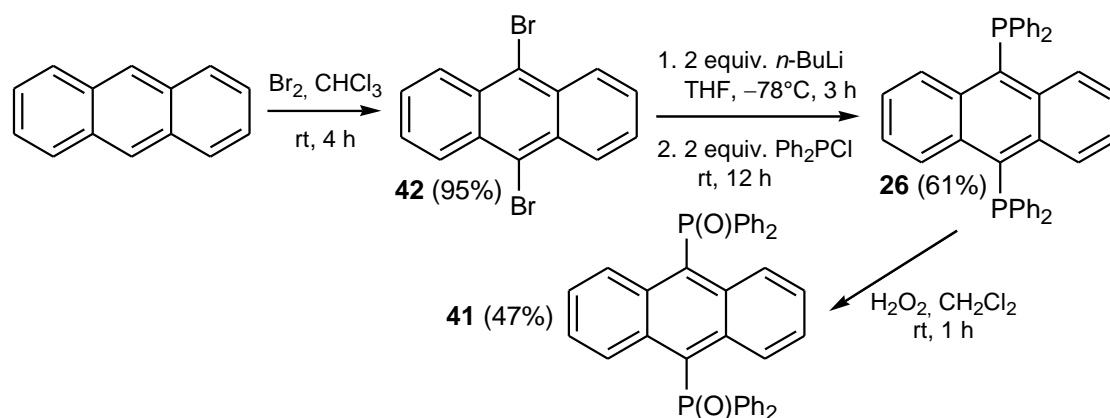


**Scheme 14.** The synthesis of 2-(diphenylphosphinoyl)anthracene **39** using 2-anthric acid **40**.



The optimal temperature for the reaction was 115 °C. Changing the temperature reduced the yield, as did changing the solvent to a highly polar one (DMF, *N,N*-dimethylformamide).

Another study carried out by Zhao and coworkers [1] showed that 9,10-bis(diphenylphosphinoyl)anthracene **41** could readily be synthesized from 9,10-dibromoanthracene **42** by substitution of chlorine in chlorodiphenylphosphine with 9,10-dilithioanthracene obtained from a double Br/Li exchange in **42** followed by oxidation of the resulting bis(diphenylphosphino)anthracene **26** with hydrogen peroxide to yield **41** in a 47% yield. 9,10-Dibromoanthracene **42** was obtained by bromination of anthracene in chloroform (Scheme 15).

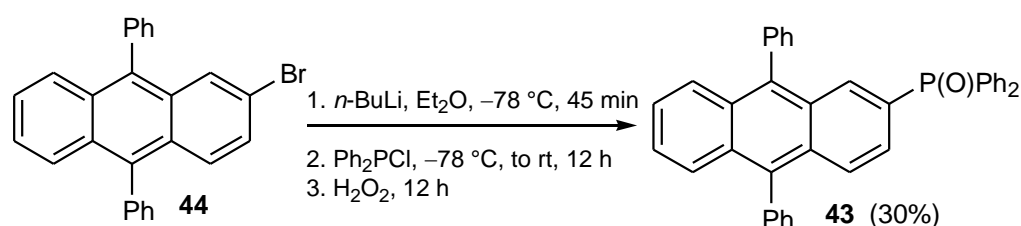


**Scheme 15.** The synthesis of 9,10-bis(diphenylphosphinoyl)anthracene **41** from 9,10-dibromoanthracene **42**.

The product **41** has been synthesized with the intention of applying it in organic light-emitting diodes (OLEDs). Zhao et al. found that **41** was a yellow-green solid with a melting point that reached 265 °C. A similar study by Tao and co-workers [23] confirmed the fluorescent properties of **41**, which could be used in the construction of OLEDs. The authors also claimed that the conversion from **26** to **41** was the first reported triplet-triplet annihilation system activated by hydrogen peroxide.

Furthermore, Xu and co-workers [24] linked the increase in fluorescence properties within the **26**/ $\text{H}_2\text{O}_2$  system to the degree of photooxidation. This system could be used as an indicator of the reaction time, oxygen exposure, and light irradiation or a time-oxygen and light indicator (TOLI). The compound **41** was also the subject of interest in another study by Xu et. al. [25], who used it to investigate the properties of a samarium complex  $\text{Sm}(\text{hfac})_3(\mathbf{41})_3$  (hfac = hexafluoroacetylacetonato).

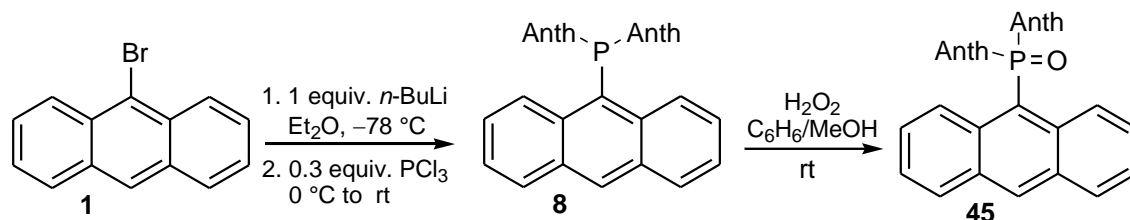
Wu and co-workers [2] showed the synthesis and properties of (9,10-diphenyl-2-phosphinoyl)anthracene **43** with the intention of using it as a true-blue OLED material. The synthesis was similar to the one proposed by Zhao and coworkers [1]: it included treatment of 2-bromo-9,10-diphenylanthracene **44** with *n*-BuLi, followed by the addition of chlorodiphenylphosphine and subsequent oxidation (Scheme 16).



**Scheme 16.** The synthesis of (9,10-diphenyl-2-phosphinoyl)anthracene **43** from 2-bromo-9,10-diphenylanthracene **44**.

The compound **43**, which readily crystallized as a light-yellow solid, was obtained in a 30% yield. It exhibited red-shift fluorescence compared to 9,10-diphenylanthracene. This study showed that **43** was not suitable for the true-blue OLED material due to the fact that the compound exhibited a red shift.

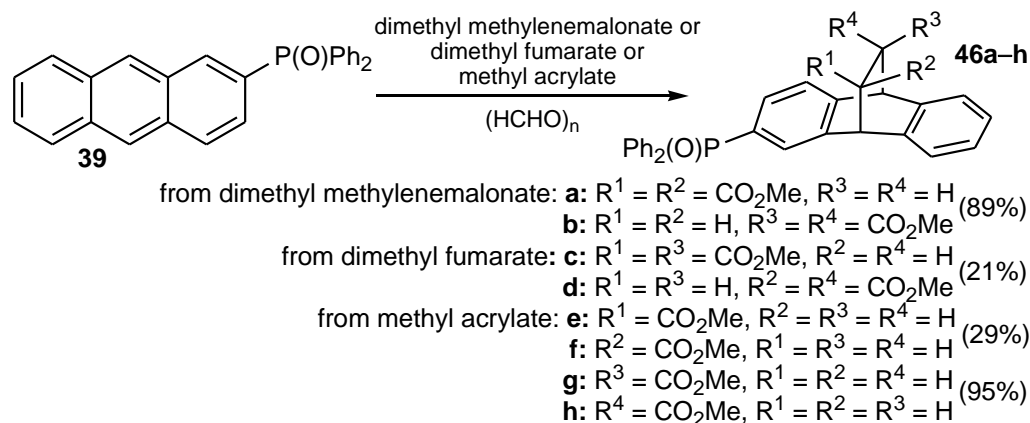
Yamaguchi et al. [26] reported a synthesis and photochemical characterization of tri(9-anthryl)phosphine **8** and tri(9-anthryl)phosphine oxide **45** (Scheme 17).



**Scheme 17.** The synthesis of trianthryl-substituted derivatives **8** and **45** reported by Yamaguchi and coworkers.

Tri(9-anthryl)phosphine **8** was synthesized from 9-bromoanthracene **1** by treatment with *n*-butyllithium, followed by the addition of phosphorus trichloride. Tri(9-anthryl)phosphine oxide **45** was obtained by oxidation of **8** with hydrogen peroxide (Scheme 17). The tri-coordinated **8** and tetra-coordinated derivative **45** exhibited a weak fluorescence.

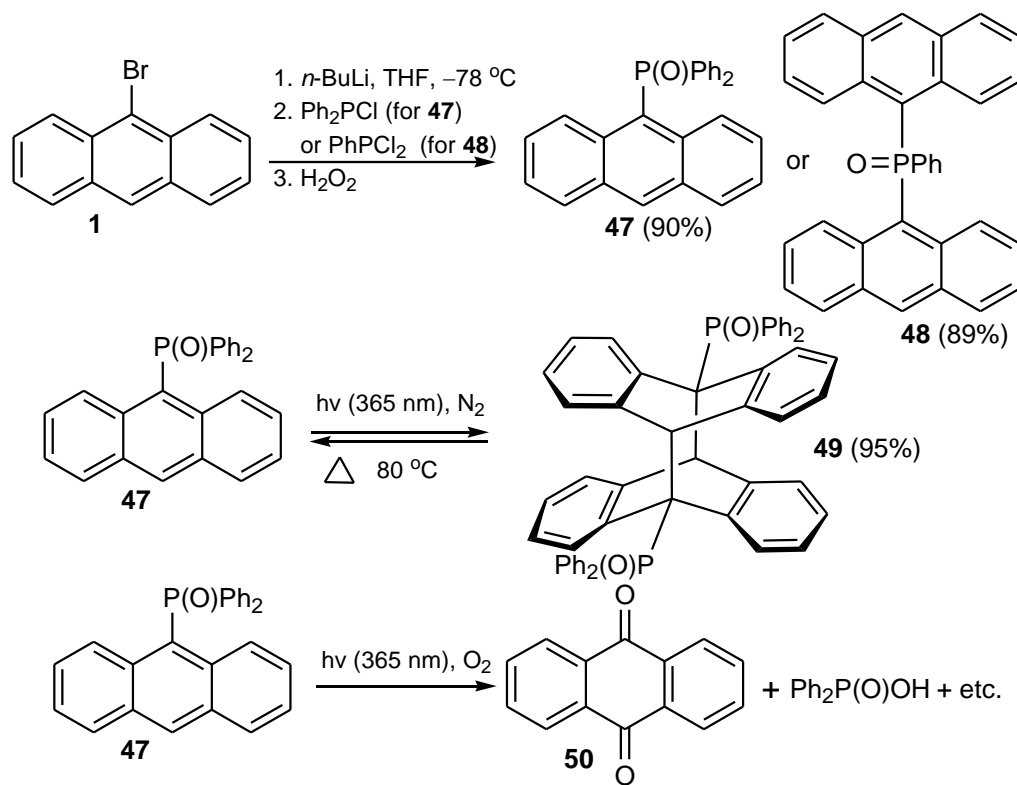
The synthesis of phosphine oxides **46a–h** containing carboxylic acid esters and 9,10-dihydro-9,10-ethanoanthracene moiety, described by Okada and co-workers, is an example of utilization in the synthesis of 2-(diphenylphosphinoyl)anthracene **39**. The bulky compounds **46a–h** were synthesized in the reaction of **39** with dimethyl methylene malonate, dimethyl fumarate, or methyl acrylate and paraformaldehyde in 21–95% yields. (Scheme 18) [27].



**Scheme 18.** Synthesis of phosphine oxides **46a–h** moiety containing carboxylic acid esters from 2-(diphenylphosphinoyl)anthracene **39**.

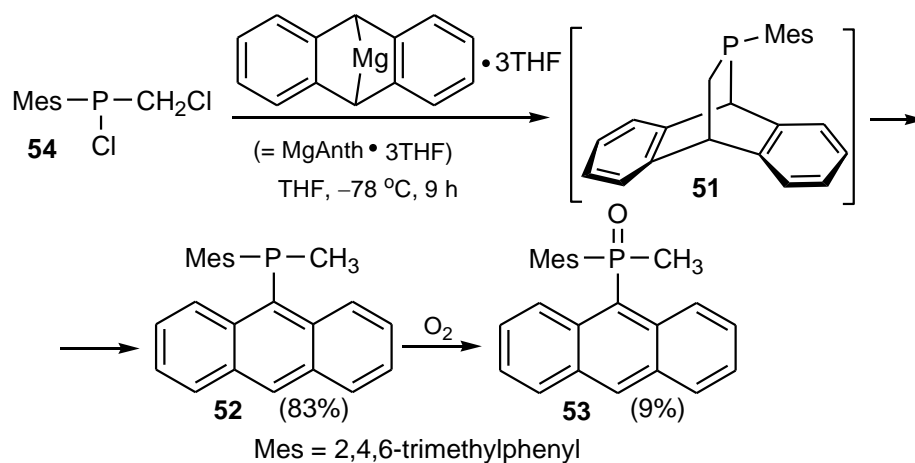
Katagiri et al. [28] synthesized 9-(diphenylphosphinoyl)anthracene **47** and 9-(anthrylphenylphosphinoyl)anthracene **48** from diphenyl chlorophosphine and phenyl dichlorophosphine, respectively (Scheme 19). The synthesis was analogous to the previous method by Schwab and co-workers [29] and first required halogen/lithium exchange and then oxidation with H<sub>2</sub>O<sub>2</sub>. The authors revealed that phosphine oxides **47** and **48** did not lead to the formation of a photodimer in the solid state, whereas in chloroform or acetonitrile under an N<sub>2</sub> atmosphere, at the 365-nm-wavelength irradiation, the [4π + 4π] photodimerization of **47** occurred to give **49**. In addition, the absorption and emission spectra of the compound **47** in acetonitrile showed characteristic absorption and emission bands of anthryl moieties while photodimerization of the anthryl groups led to the disappearance of these bands. The authors reversibly returned **49** to **47** by heating the probe at

80 °C. In contrast, analogous irradiation under an O<sub>2</sub> atmosphere resulted in the formation of anthraquinone **50**.



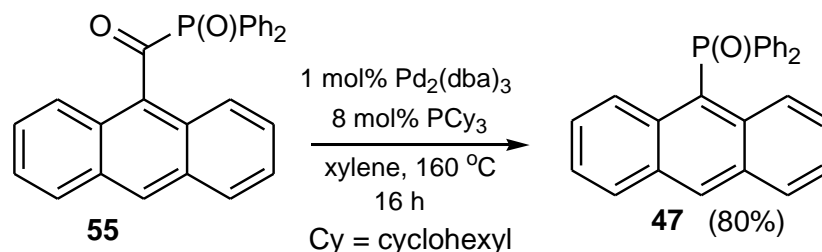
**Scheme 19.** The synthesis of 9-(diphenylphosphinoyl)anthracene **47**, 9-(anthrylphenylphosphinoyl)anthracene **48**, and the products of irradiation of **47** under N<sub>2</sub> and O<sub>2</sub> conditions, respectively.

During attempts to obtain a “masked” version **51** of the phosphalkene Mes-P=CH<sub>2</sub>, Gates and co-workers [30] synthesized 9-[(methyl)(mesityl)phosphino]anthracene **52** and the corresponding 9-[(methyl)(mesityl)phosphinoyl]anthracene **53** in the reaction between (chloro) (chloromethyl) (mesityl) phosphine **54** and the anthracene magnesium (MgAnth•3THF) in THF. The expected adduct **51**, which was initially formed, then decomposed to give the anthracene derivative **52** in an 83% yield. The latter was oxidized to **53** in a 9% yield only (Scheme 20).



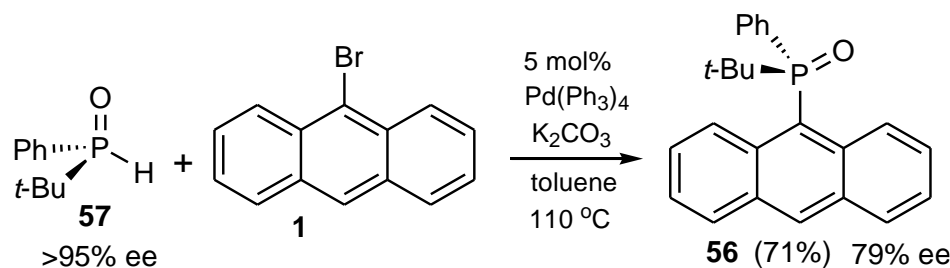
**Scheme 20.** The synthesis of 9-[(methyl)(mesityl)phosphino]anthracene **52** and the corresponding 9-[(methyl)(mesityl)phosphinoyl]anthracene **53**.

Wang and Zhu reported the palladium-catalyzed decarbonylation of 9-[(1-keto diphenylphosphinoyl)]anthracene **55** in the presence of 1 mol% of  $\text{Pd}_2(\text{dba})_3$  and 8 mol% of the phosphine ligand ( $\text{PCy}_3$ ) to give 9-(diphenylphosphinoyl)anthracene **47** in an 80% yield [31] (Scheme 21).



**Scheme 21.** Decarbonylation of 9-[(1-keto diphenylphosphinoyl)]anthracene **55**.

Drabowicz and co-workers synthesized optically active 9-[(*t*-butyl)(phenyl)phosphinoyl]anthracene **56** in a 71% yield in the Hirao reaction of palladium-catalyzed cross-coupling reaction of 9-bromoanthracene **1** with optically active *t*-butylphenylphosphine oxide **57** (Scheme 22) [32]. The formation of carbon–phosphorus bonds took place with retention of the configuration, and the stereoretention of this reaction was confirmed by X-ray analysis.



**Scheme 22.** The synthesis of optically active 9-[(*t*-butyl)(phenyl)phosphinoyl]anthracene **56**.

Stalke and co-workers synthesized three positional isomers of 1-, 2-, and 9-(diphenylthiophosphinoyl)anthracenes **58**, **59**, and **60** that revealed a solid-state fluorescence in three different colors with differences in emission wavelengths of over 100 nm. Analysis of the solid-state structure of **59** and photophysical properties allowed the unusual yellow emission to be attributed to the formation of excimer in the solid state. Therefore, substitution at position 1 of the anthracene fluorophore with suitable substituents may be a promising strategy to obtain long wavelength emission in the solid state using structurally easy to modify compounds (Figure 1) [33].

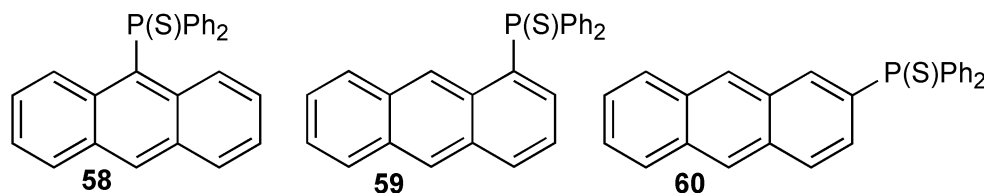
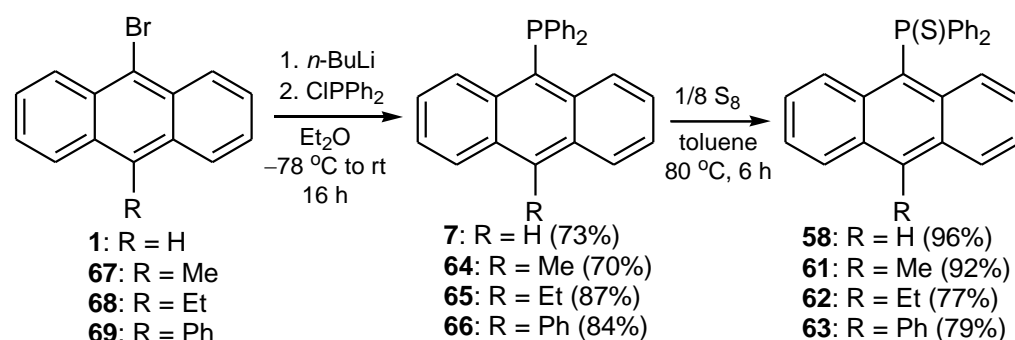


**Figure 1.** Three positional isomers of 1-, 2- and 9-(diphenylthiophosphinoyl)anthracenes **58**, **59**, and **60**.

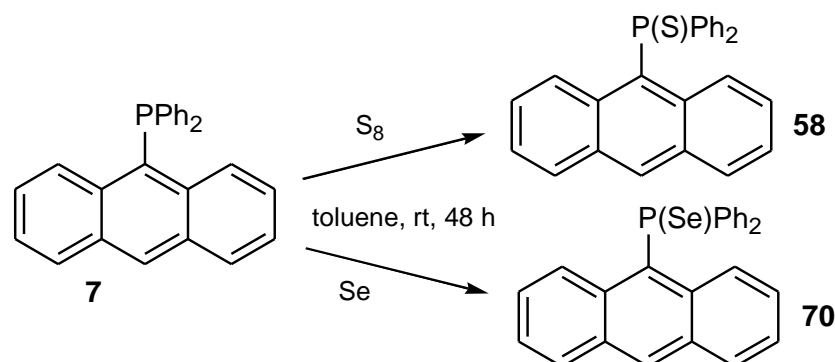
Schillmöller and co-workers [34] synthesized four 9-(diphenylthiophosphinoyl)anthracenes **58** and **61–63** with alkyl and phenyl substituents at the position 10 via sulfuration of 9-(diphenylphosphino)anthracenes **7** and **64–66**. The latter were obtained from the corresponding bromoanthracenes **1** and **67–69** (Scheme 23) [35,36].



**Scheme 23.** The preparation of 9-(diphenylthiophosphinoyl)anthracenes **58** and **61–63**.

The compounds **58** and **61–63** were crystallized and their X-ray structures were then determined. These studies revealed that oxidation of the phosphorus atom with sulfur significantly changed the molecular structural parameters and the crystal packing. This caused a strong bathochromic shift, which resulted in a green solid-state fluorescence. Moreover, the authors prepared four host-guest complexes, with **62** as a host molecule and benzene, pyridine, toluene, and quinoline as guest molecules. This resulted in enhanced emission and up to a five times higher quantum yield in comparison to the pure compound **62**.

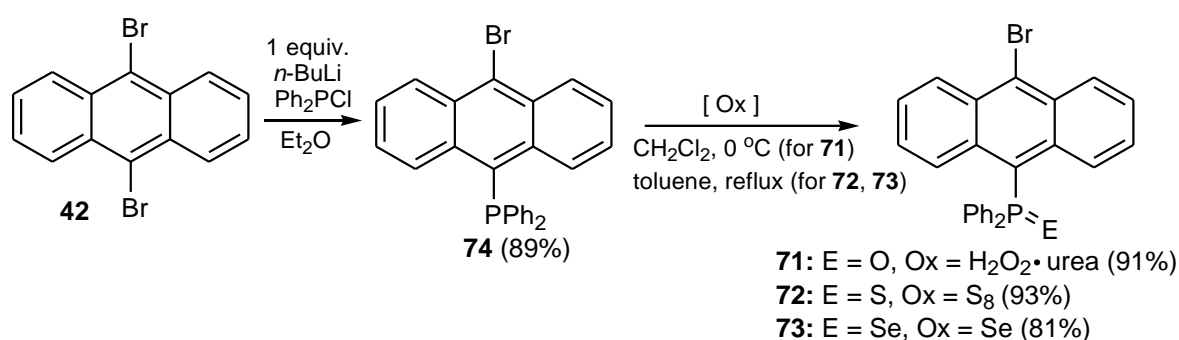
Walensky et al. characterized 9-(diphenylthio- and diphenylselenophosphinoyl)anthracenes **58** and **70**, respectively, by NMR and optical spectroscopy (Scheme 24) [37]. The authors demonstrated that <sup>31</sup>P NMR shifts for **58** and **70** were shifted upfield when compared to the unoxidized analog. This was due to the loss of planarity and relatively greater  $\sigma$ - than  $\pi$ -bonding between the phosphorus atom and the anthracene carbon.



**Scheme 24.** The syntheses of 9-(diphenylthio- and diphenylselenophosphinoyl)anthracenes **58** and **70**.

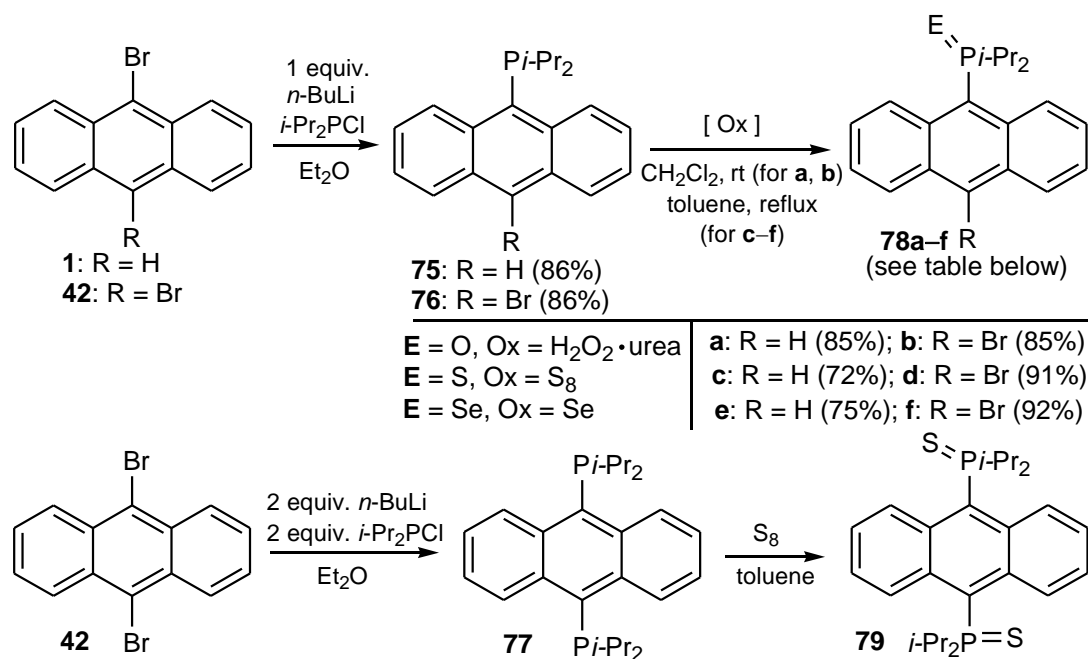
When excited at 310 nm, compounds **58** and **70** showed emission similar to that of unsubstituted anthracene, displaying peaks at 380, 402, 430, and 450 nm. When the excitation wavelength was shifted to 410 nm, the observed emission became structureless and was red-shifted by around 50 nm relative to the typical emission of the unsubstituted anthracene. The authors did not observe excimer formation for these compounds. Moreover, a small deviation from planarity in the anthracene ring was observed for **58** and **70** and the angle of deflection was 3° and 5°, respectively.

Schwab and co-workers [38] obtained 9-bromo-10-(diphenylphosphino)anthracene **71** and its thio- **72** and seleno- **73** derivatives (Scheme 25). In the first stage, 9,10-dibromoanthracene **42** was treated with *n*-BuLi followed by the addition of chlorodiphenylphosphine to give 9-bromo-10-(diphenylphosphino)anthracene **74**. Then, **74** was oxidized to the corresponding oxo-, thio-, and seleno derivatives **71–73** in high yields according to the procedure described by Stalke et al. [39]. Their spectral and structural properties were investigated and shown to be largely consistent with those of the 9,10-diphosphino derivatives **80–82** mentioned below (Scheme 27).



**Scheme 25.** The synthesis of 9-bromo-10-(diphenylphosphino)anthracene **6** and its oxo-, thio-, and seleno derivatives **71–73**.

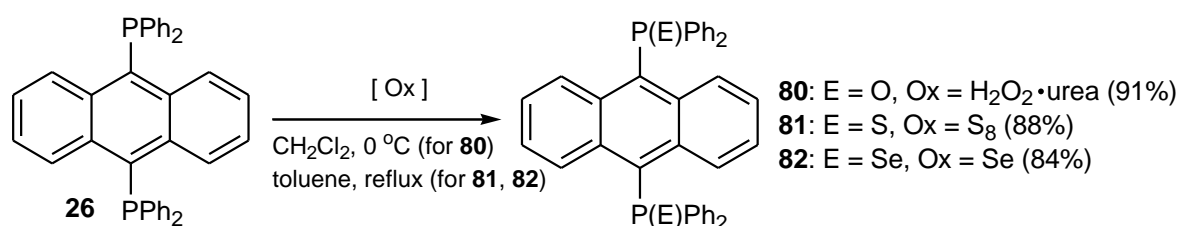
In an analogous manner, the same authors [29] synthesized bulky 9-(diisopropylphosphino)anthracene **75**, 9-bromo-10-(diisopropylphosphino)anthracene **76**, and 9,10-symmetrically-substituted anthracene **77**, which were then oxidized to the corresponding derivatives **78a–f** and **79** (Scheme 26).



**Scheme 26.** The synthesis of phosphinoanthracenes **75**, **76**, and **77** and their oxo-, thio-, and seleno derivatives **78a–f** and **79**.

9,10-Bis(diphenylphosphino)anthracene **80**, 9,10-bis(diphenylthiophosphino)anthracene **81**, and 9,10-bis(diphenylselenophosphino)anthracene **82** were obtained by oxidation (E = O, S, Se) of 9,10-bis(diphenylphosphino)anthracene **26** again using H<sub>2</sub>O<sub>2</sub>·(NH<sub>2</sub>)<sub>2</sub>C=O (urea) (dichloromethane, 0 °C), elemental sulfur (toluene, reflux), and selenium (toluene, reflux), respectively (Scheme 27). The compounds obtained were significantly more soluble in organic solvents than the starting material **26**. The absorption and emission spectra of **80–82** were recorded in solution and in the solid state. In solution, only **80** exhibited a detectable emission whereas **81** did not emit. The latter showed strong fluorescence in the solid state at λ = 508 nm. This molecule formed single crystals possessing a groove suitable for binding toluene reversibly to the anthracene chromophore by means of C-H···π-ring center interactions. Hence, the crystalline **81** was the first solid-state excimer that could serve as a chemosensor to detect toluene selectively. Single crystals of **80** emitted at λ = 482 nm, whereas the selenium derivative **82** did not emit in the solid state. In addition, the crystal structures of compounds **80–82** were analyzed using the single-crystal

X-ray diffraction technique (Scheme 27) [39]. The substrate **26** was obtained based on the procedure described by Prabhavathy and co-workers [40].

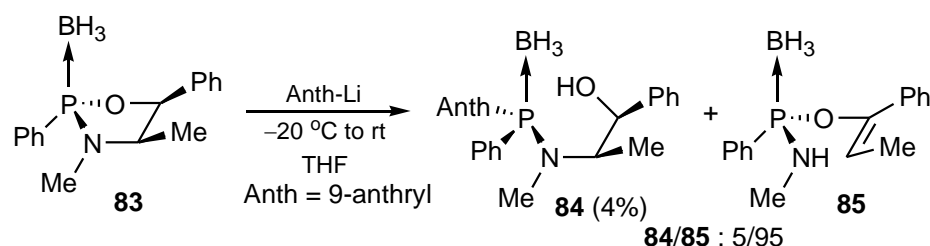


**Scheme 27.** The synthesis of 9,10-bis(diphenylphosphino)anthracene and thio- and seleno derivatives **80–82**.

### 2.2. Phosphine Boranes ( $\text{AnthPR}_2 \bullet \text{BH}_3$ )

In this subsection, the presented syntheses and reactions of phosphine molecules with P-B coordinate (semipolar, dative) bonds are presented.

The ring opening of enantiomerically pure oxazaphospholidineborane **83** with bulky anthryllithium to give phosphineboranes **84** was studied by Stephan and co-workers. The authors proposed an explanation for the low 4% yield of **84**. They reported that in the case when the attack on the phosphorus atom was hindered, deprotonation of the benzylic proton occurred, yielding *trans*-(*N*-methylamino)(phenyl)(1-phenyl-1-propenyloxy) phosphineborane **85** instead of **84** (**84/85** = 5/95) (Scheme 28) [41].



**Scheme 28.** The reaction of enantiomerically pure oxazaphospholidineborane **83** with anthryllithium.

1,8-Bis-(diisopropylphosphino)-9-methoxyanthracene **86**, as a starting material for the synthesis of 9-boron-substituted 1,8-bis-(diisopropylphosphino)anthracene **87a/87b**, was prepared by Akiba and co-workers by treatment of 1,8-dibromo-9-methoxy-anthracene **88**, first with *n*-BuLi and then with diisopropylchlorophosphine. Diphenylchlorophosphine was used as well; however, only the diisopropylphosphine derivative **86** could be successfully transformed into 1,8-bis(diisopropylphosphino)-9-bromoanthracene **30** with LDBB (lithium di-*tert*-butylbiphenylide) followed by treatment with  $\text{BrCF}_2\text{CF}_2\text{Br}$ , as a brominating agent, in a 51% yield. The introduction of a boron substituent at the position 9 in **30** via Br/Li exchange followed by reaction with chloroborane **89** led to the formation of 1,8-bis(diisopropylphosphino)-9-borylanthracene **87a/87b**. The  $^1\text{H}$  and  $^{31}\text{P}$  NMR spectra of **86** showed a symmetrical anthracene pattern at room temperature. This meant that a very rapid bond switching process between **87a** and **87b** occurred in solution (Scheme 29) [42].

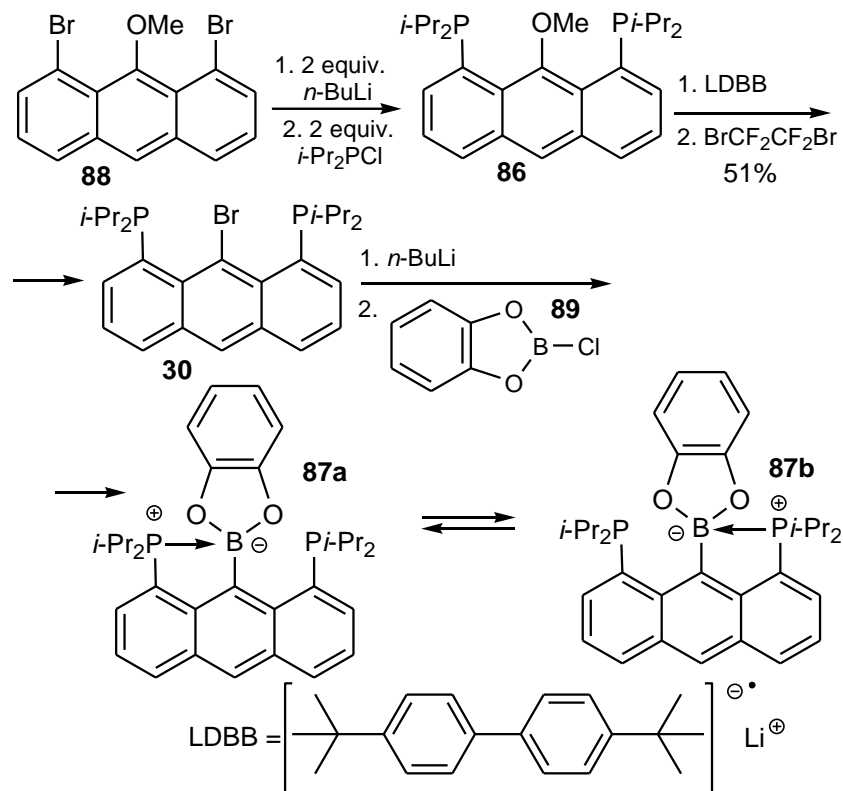
### 2.3. Phosphine–Metal Complexes ( $\text{AnthPR}_2\text{-Metal}$ )

In this subsection, complexes of phosphines possessing at least one anthryl substituent with metals, such as Au, Ag, Au/Ag/Sb, Fe, Pd, Pt, Ir, Lu, Eu, Ru, and Ni, are reviewed.

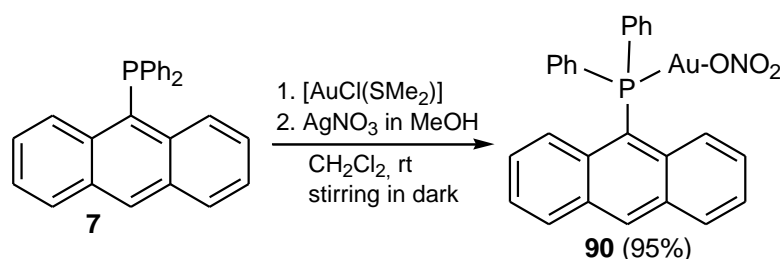
Other metals (W, Os, Co), i.e., the pentacarbonyltungsten complex of 9-diphenylphosphino anthracene, are reported in Section 2 while the triosmiumdodecacarbonyl cluster and dinuclear cobalt complex are discussed in Section 3, respectively.

Gold and platinum(II) complexes of the phosphine ligands  $\text{PAnth}_n\text{Ph}_{3-n}$  (Anth = anthryl) were synthesized by Mingos et al. [43]. The authors recorded  $^{31}\text{P}\{^1\text{H}\}$  NMR chemical shifts for (anthryl)(diphenyl)phosphine, (dianthryl)(phenyl)phosphine and trianthrylphosphine, their

oxo derivatives, and gold (I) halide and gold (I) nitrate complexes. Moreover, a crystal structure of the  $[\text{AuCl}(\text{PAnth}_2\text{Ph})]\cdot\text{CH}_3\text{Cl}$  complex was determined by X-ray analysis. An example of the preparation of the gold (I) complex  $[\text{Au}(\text{NO}_3)(\text{PAnthPh}_2)]$  **90** obtained from 9-(diphenylphosphino)anthracene **7** is shown in Scheme 30.



**Scheme 29.** The synthesis of tridentate anthracene ligand **87a/87b**.



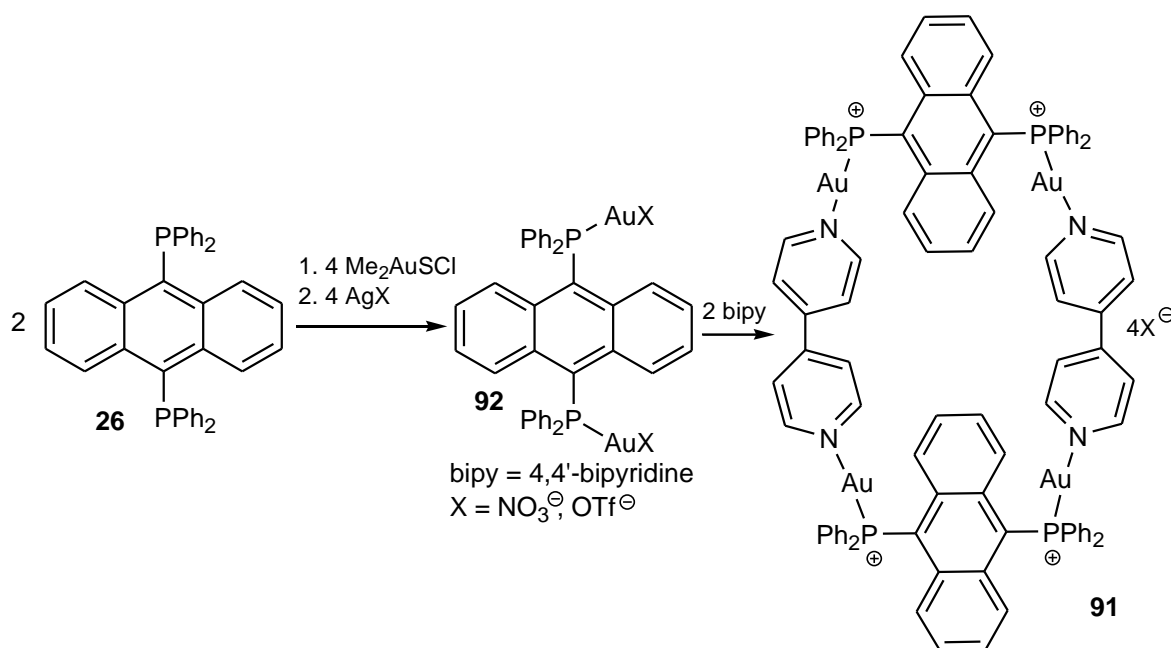
**Scheme 30.** An example of the preparation of the gold (I) complex  $[\text{Au}(\text{NO}_3)(\text{PAnthPh}_2)]$  **90**.

Several other Au and Pt complexes were also synthesized: *trans*- $[\text{PtCl}_2(\text{PAnthPh}_2)_2]$  (64%); *trans*- $[\text{Pt}(\text{CH}_3\text{CN})_2(\text{PAnthPh}_2)_2](\text{BF}_4)_3$  (74%); *trans*- $[\text{Pt}(\text{CH}_3\text{CN})_2(\text{PAnth}_2\text{Ph}_2)_2](\text{BF}_4)_3$  (68%);  $[\text{Au}(\text{NO}_3)(\text{PAnthPh}_2)]$  (95%);  $[\text{Au}(\text{NO}_3)(\text{PAnth}_2\text{Ph})]$  (79%);  $[\text{Au}(\text{NO}_3)(\text{PAnth}_3)]$  (53%);  $[\text{AuCl}(\text{PAnthPh}_2)]$  (91%);  $[\text{AuCl}(\text{PAnth}_2\text{Ph})]$  (93%); and  $[\text{AuCl}(\text{PAnth}_3)]$  (72%).

A luminescent molecular metalla(Au)cyclophane **91**, which was synthesized from the self-assembly of the molecular “clip” **92** and bipyridine, showed a large rectangular cavity of  $7.921(3) \times 16.76(3)$  Å (Scheme 31). The electronic absorption/emission spectroscopy and electrochemistry of **91** were studied. The  $2^{4+}$  ions were self-assembled into a 2D mosaic in the solid state via complementary edge-to-face interactions between phenyl groups.  $^1\text{H}$  NMR titrations ratified the 1:1 complexation of the cations **91** and various aromatic molecules. Comparison of the structures of the inclusion complexes indicated an induced-fit mechanism operating in the binding. The luminescence emission of  $\mathbf{91}^{4+}$  could be quenched upon the guest binding. The binding constants were determined by both  $^1\text{H}$



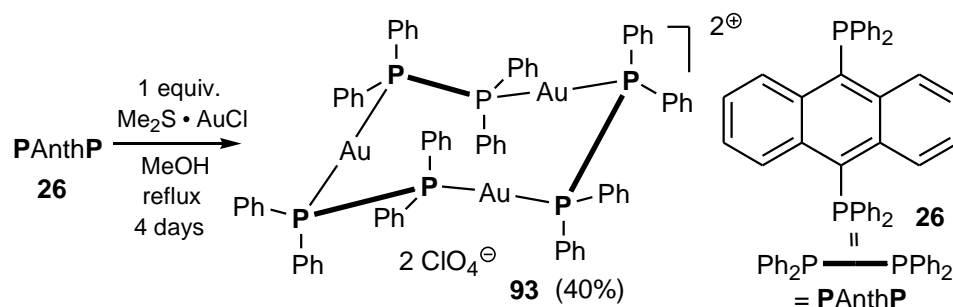
NMR and fluorescence titrations. Solvophobic and ion-dipole effects were shown to be important in stabilizing the inclusion complexes [44].



**Scheme 31.** Synthesis of metalla(Au)cyclophane **91**.

Complexes **92** (X = OTf<sup>−</sup>, ClO<sub>4</sub><sup>−</sup>, PF<sub>6</sub><sup>−</sup>, BF<sub>4</sub><sup>−</sup>), as discrete binuclear, trinuclear, and tetranuclear metallacycles, were isolated and characterized, showing novel puckered-ring and saddles-like structures in the tri- and tetranuclear metallacycles (Scheme 31) [45].

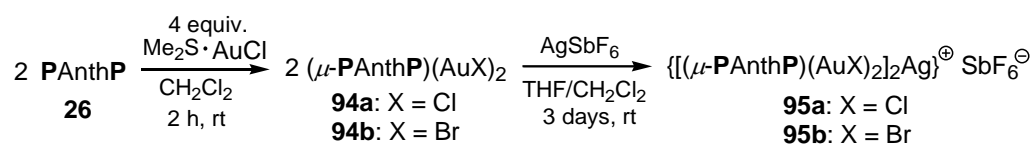
The trinuclear Au(I) complex [Au<sub>3</sub>(PAnthP)<sub>3</sub>][ClO<sub>4</sub>]<sub>3</sub> **93** was synthesized by Yip and co-workers in the reaction of 9,10-bis-(diphenylphino)anthracene (PAnthP) **26** and 1 equiv. of Me<sub>2</sub>S AuCl in methanol at reflux. The authors observed a stable gold ring in the solution and no NMR signals arising from the free ligand (Scheme 32) [40].



**Scheme 32.** The synthesis of the trinuclear Au(I) complex [Au<sub>3</sub>(PAnthP)<sub>3</sub>][ClO<sub>4</sub>]<sub>3</sub> **93**.

The UV/Vis absorption spectra of **26** and its complex **93** showed intense bands at 396 and 424 nm assigned to <sup>1</sup>π-π\* transitions in the anthryl ring. Excitation of CH<sub>3</sub>CN solution of **93** at 400 nm gave an emission at 475 nm with a quantum yield of Φ = 0.05.

The reaction of **26** (PAnthP) with 2 equiv. of Me<sub>2</sub>SAuX in CH<sub>2</sub>Cl<sub>2</sub> led to the new binuclear complexes (μ-PAnthP)(AuCl)<sub>2</sub> **94a** and (μ-PAnthP)(AuBr)<sub>2</sub> **94b** with Au(I)-X-Ag(I) halonium cation (Scheme 33) [46]. The reaction of **94a** and **94b** with 2 equiv. of AgSbF<sub>6</sub> led to spontaneous formation of the [(μ-PAnthP)-Au<sub>2</sub>]<sup>2+</sup> ion, and then, after the addition of AgSbF<sub>6</sub> (0.5 equiv.) in a THF solution, gave crystals of {[(μ-PAnthP)(AuCl)<sub>2</sub>]<sub>2</sub>Ag}<sup>+</sup>SbF<sub>6</sub><sup>−</sup> **95a** and {[(μ-PAnthP)(AuCl)<sub>2</sub>]<sub>2</sub>Ag}<sup>+</sup>SbF<sub>6</sub><sup>−</sup> **95b** as products.



**Scheme 33.** The synthesis of Au/Ag/Sb complexes **94a,b** and **95a,b**.

9,10-Bis(diphenylphosphino)anthracene (PAnthP) **26** with two donor phosphorus atoms has been used as a P-ligand unit for metals. Thus, the double-helicate dinuclear silver(I) complex,  $[\text{Ag}_2(4'\text{-Ph-therpy})_2](\text{SO}_3\text{CF}_3)_2$ , was reacted with **26** to give the corresponding dinuclear complex **96** (4'-Ph-therpy = 4'-phenyl-terpyridine). The latter showed a strong fluorescence in the solid state with an excitation band at 383.5 nm, emission band at 535.5 nm, and lifetime of 4.20 ns, but the derived complexes did not show fluorescent properties (Figure 2) [47].

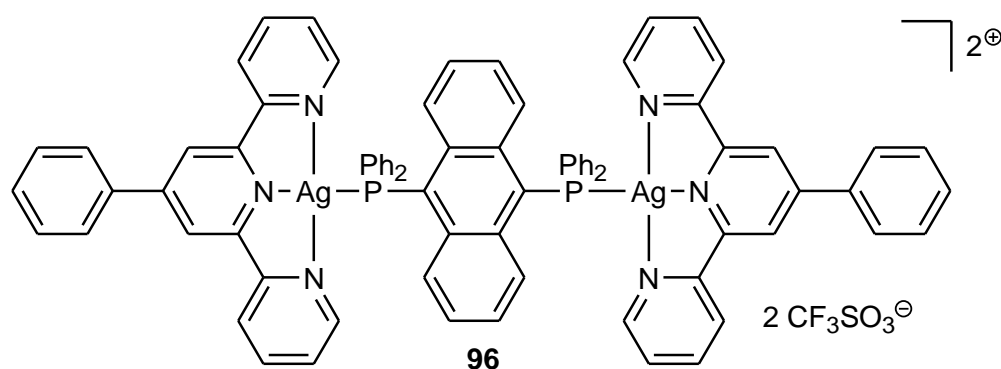
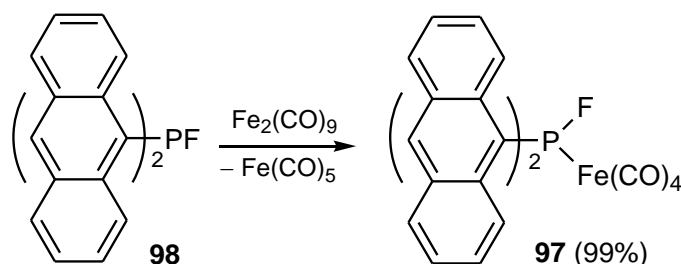


**Figure 2.** The dinuclear silver complex **96** derived from 9,10-bis(diphenylphosphino)anthracene.

An iron(0)tetracarbonyl complex **97** was synthesized from di(9-anthryl)fluorophosphine **98**, which was stable to redox disproportionation (Scheme 34) [48].



**Scheme 34.** The synthesis of the iron(0)tetracarbonyl complex **97**.

Pincer iridium complexes **99** derived from 1,8-bis(diphenylphosphino)anthracene **35** turned out to be suitable platforms for the C–H activation of methyl *tert*-butyl ether (MTBE) (Figure 3) [49].

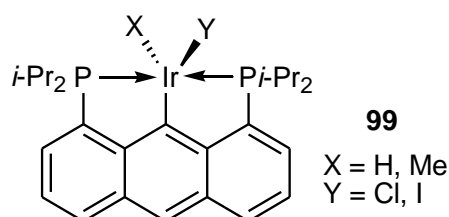
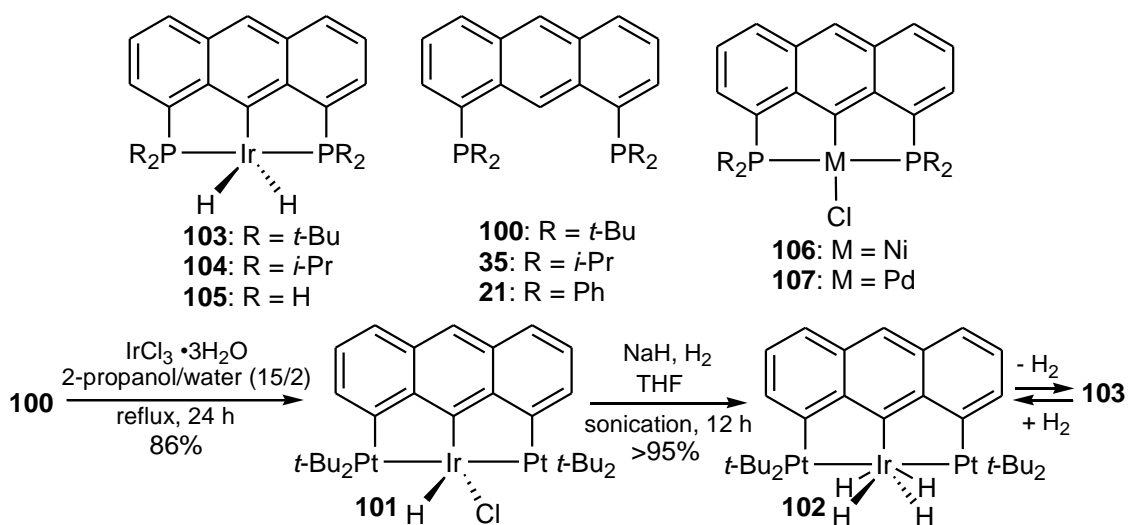


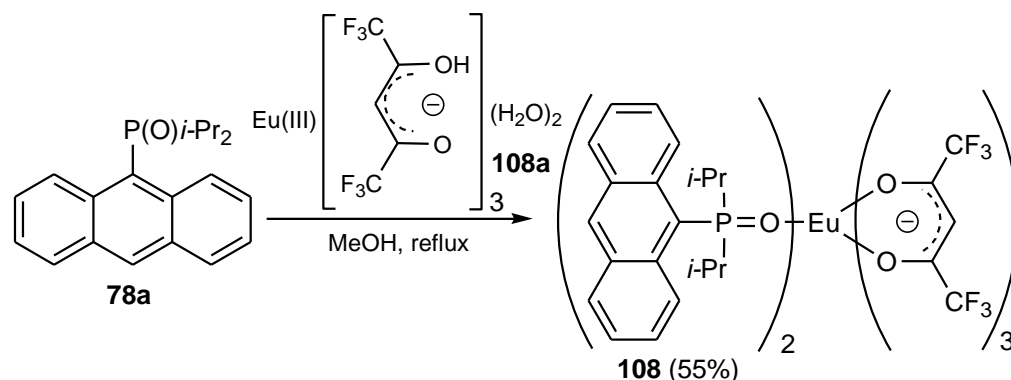
**Figure 3.** Pincer iridium complexes **99**.

A series of thermally stable Ir, Ni, and Pd complexes were obtained from 1,8-bis(dialkyl and diphenylphosphino)anthracenes **100**, **35**, and **21**. The anthracenes **100** and **35** were prepared similarly to **21** by direct nucleophilic substitution of fluorine atoms in 1,8-difluoroanthracene by potassium di-*tert*-butylphosphide or potassium di-*iso*-propylphosphide. The reaction of **100** with  $\text{IrCl}_3 \cdot 3\text{H}_2\text{O}$  in 2-propanol/water afforded the complex **101** as a red crystalline powder in an 86% yield (Scheme 35). The reduction of **101** under a hydrogen atmosphere gave mixtures of the yellow-colored iridium tetrahydride **102** and the red-colored iridium dihydride **103**. By saturating solutions of such mixtures with hydrogen, the equilibrium was shifted towards **102**. Evaporation of the solvent under vacuum resulted in the formation of the analytically pure complex **103** in a >95% yield. The thermally stable complexes **103** and **104** were ideal for homogeneous catalysts in the alkane dehydrogenation above 200 °C. The complex **103** in alkane solution was stable at 250 °C and catalyzed the dehydrogenation reactions at this temperature [50].



**Scheme 35.** The synthesis of thermally stable iridium complexes **103** and **104**.

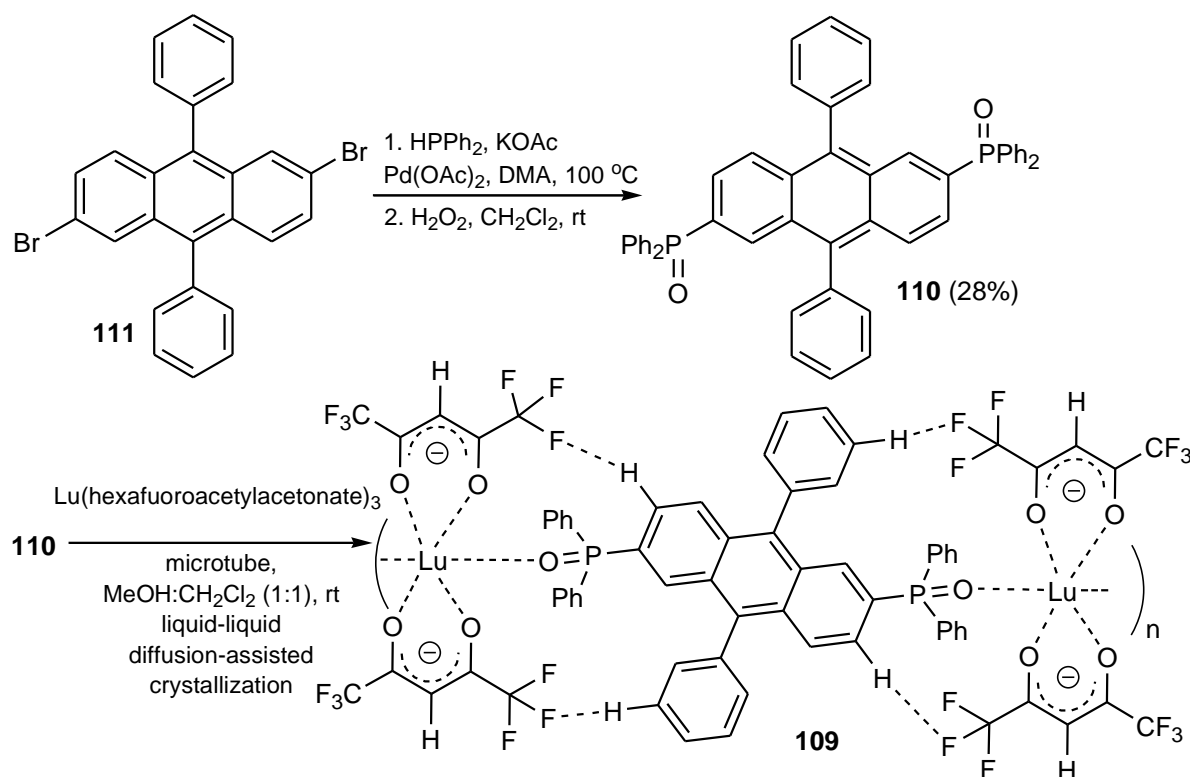
Osawa et al. [51] synthesized bis[(9-diisopropylphosphino)anthracene]-tris(hexafluoroacetylacetonato)europium(III) **108** (Scheme 36). First, the authors prepared 9-(diisopropylphosphino)anthracene **78a** (Scheme 26) according to the Schwab et al. protocol [29], which was next reacted with tris(hexafluoroacetylacetonato)europium(III) **108a** for 8 h in refluxing methanol solution to obtain **108** in a 55% yield after recrystallization.



**Scheme 36.** The preparation of the europium complex **108**.

Osawa and co-workers determined the crystal structure of the Eu(III) complex **108** and studied its intra-complex energy transfer. The studies revealed that laser irradiation of this compound in *n*-hexane gave blue emission, which was ascribed only to the 9-(diisopropylphosphino)anthracene moiety, not to the central Eu(III) ion (Scheme 36).

Kitagawa and co-workers [52] obtained a novel coordination polymer **109** based on 9,10-diphenyl-2,6-bis(diphenylphosphinoyl)anthracene **110** as a core and two molecules of Lu(hexafluoroacetylacetonate)<sub>3</sub> that interacted with the core (Scheme 37).



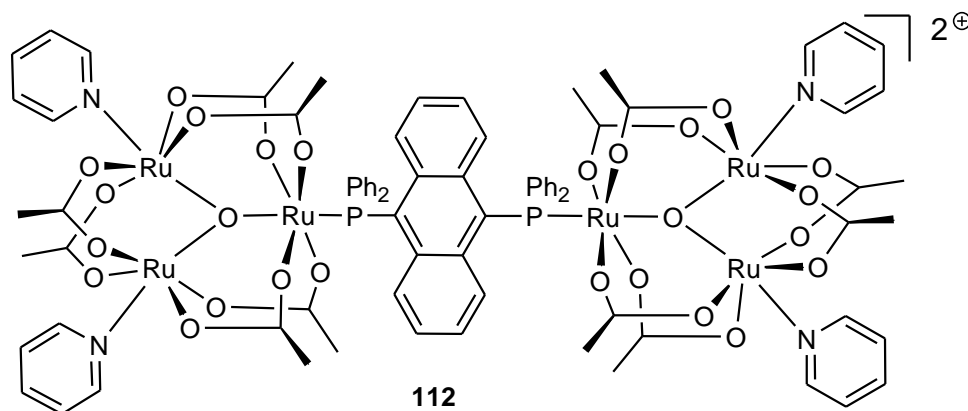
**Scheme 37.** The preparation of the coordination polymer **109**.

First, the anthracene **110** was synthesized from 2,6-dibromo-9,10-diphenylanthracene **111** and diphenylphosphine. The first step of the synthesis was performed in the presence of potassium acetate and palladium acetate, and next the resulting bisphosphine intermediate was oxidized to **110** in a 28% yield. The polymer **109** was prepared in a microtube by the liquid-liquid diffusion-assisted crystallization method. The authors studied the photophysical properties and thermal stability of **109** and its oxide **110**. The luminescence quantum yield was enhanced from 18% up to 25% ( $\lambda_{\text{ex}} = 380 \text{ nm}$ ) due to the introduction of Lu(hexafluoroacetylacetonate)<sub>3</sub> molecules into the phosphine oxide system, as a result of which bright, pure sky-blue emission was observed. In addition, the compound **109** showed a higher temperature of decomposition (340 °C) than **110**.

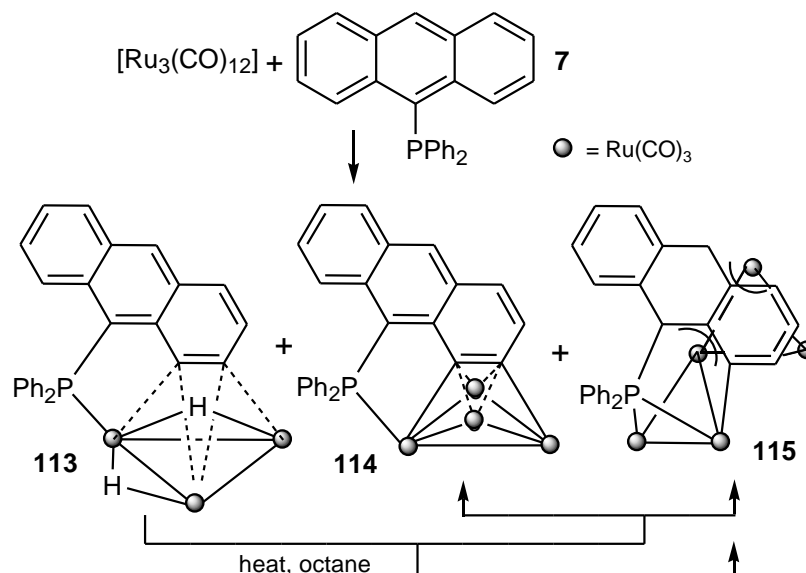
The diphosphine-bridged dimer of the oxo-centered triruthenium–acetate cluster unit  $[\{\text{Ru}_3\text{O}(\text{OAc})_6(\text{py})_2\}_2(\text{dppan})](\text{PF}_6)$  **112** was synthesized by Chen and his co-workers (Scheme 38). The reaction of  $[\text{Ru}_3\text{O}(\text{OAc})_6(\text{py})_2(\text{CH}_3\text{OH})](\text{PF}_6)$  with 9,10-bis(diphenylphosphino)anthracene (dppan) **26** resulted in the formation of **112** in a 67% yield. The redox studies of the complex **112** revealed the presence of electronic communication between two triruthenium units mediated through bridging dppan [53].

A number of tri-, tetra-, and penta-ruthenium clusters **113**–**115** were synthesized by Deeming and co-workers. When a suspension of  $[\text{Ru}_{13}(\text{CO})_{12}]$  and a slight excess of 9-(diphenylphosphino)anthracene **7** in octane were heated to reflux at 125 °C for 4 h, several products were obtained, including the yellow trinuclear cluster  $[\text{Ru}_3(\mu\text{-H})_2(\text{CO})_8(\mu_3\text{-C}_{14}\text{H}_7\text{PPh}_2)]$  **113** and the purple tetra-ruthenium butterfly complex  $[\text{Ru}_4(\text{CO})_{11}(\mu_4\text{-C}_{14}\text{H}_7\text{PPh}_2)]$  **114**. Both anthracene complexes and also the dark purple penta-ruthenium bow-tie cluster,  $[\text{Ru}_5(\text{CO})_{13}(\mu_5\text{-}\eta^1\text{-}\eta^2\text{-}\eta^3\text{-}\eta^3\text{-C}_{14}\text{H}_8\text{-}\eta^1\text{-PPh}_2)]$  **115** were obtained via the double metallation from one of the unsubstituted rings (Scheme 39). Furthermore, treatment of the trinuclear species **113** with 1 equivalent of  $[\text{Ru}_3(\text{CO})_{12}]$  in refluxing octane resulted in a cluster build-up, with the formation

of the tetra- and penta-ruthenium species **114** and **115**. Likewise, the thermolysis reaction of **114** with  $[\text{Ru}_3(\text{CO})_{12}]$  also led to **115**. The crystal structure of **3** revealed a unique  $\mu_5$ -interaction of the ligand with the ruthenium cluster [54].

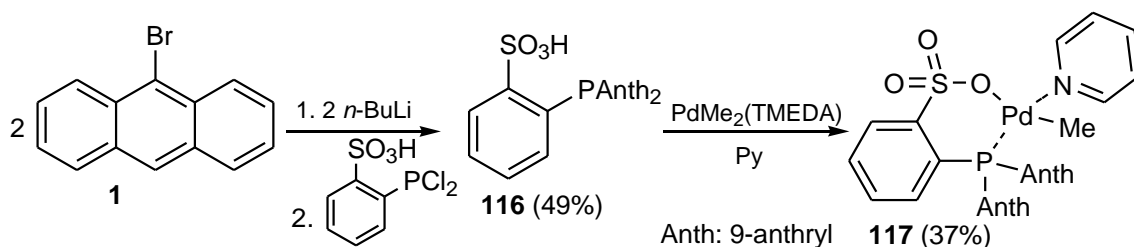


Scheme 38. The synthesis of the Ru-diphosphine-bridged complex **112**.



Scheme 39. The synthesis of tri-, tetra-, and penta-ruthenium clusters **113**, **114**, and **115**.

The bulky phosphine ligand **116** was prepared by Claverie et al. and used to generate the phosphine palladium complex **117**. The complex catalyzed ethene polymerization to yield linear polyethene; however, its catalytic activity was smaller compared to complexes with phenyl, naphthyl or phenanthryl substituents, which corresponded to increasing cone angles and decreasing basicity (Scheme 40) [55].



Scheme 40. The synthesis of the phosphine palladium complex **117**.

Yamamoto and Shimizu synthesized 9-(diphenylphosphino)anthracene-based palladacycles **118a** and **118b** that catalyzed conjugate addition of arylboronic acids to electron-deficient alkenes, such as  $\alpha,\beta$ -unsaturated ketones, esters, nitriles, and nitroalkenes. The monomeric catalysts, which were synthesized from  $K_2PdCl_4$ , 9-(diphenylphosphino)anthracene, and trialkyl phosphites, exhibited turnover numbers of up to 700 (Figure 4) [56].

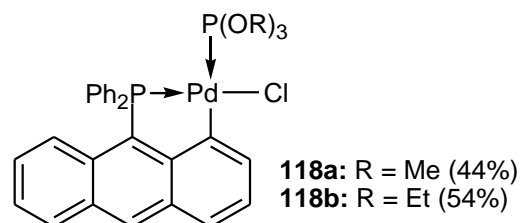
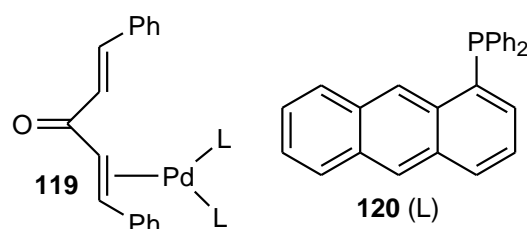


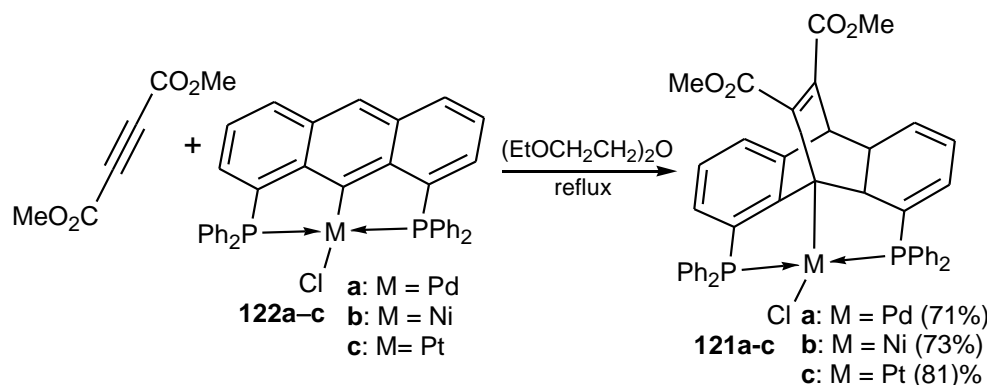
Figure 4. Structures of phosphapalladacycles **118a** and **118b**.

Mingos and co-workers reported the synthesis and structural characterization of the Pd complex  $[Pd(dba)L_2]$  **119** (where L = **120** and dba = dibenzylideneacetone) obtained from  $[Pd_2(dba)_3]$  and the corresponding 1-(diphenylphosphino)anthracene **120** (L) (Scheme 41). The single-crystal X-ray structural analyses confirmed that these complexes adopted a trigonal planar structure, with the dba ligand coordinated by a double bond [57].



Scheme 41. The synthesis of the palladium complex **119** with 1-(diphenylphosphino)anthracene **120** (L) as a ligand.

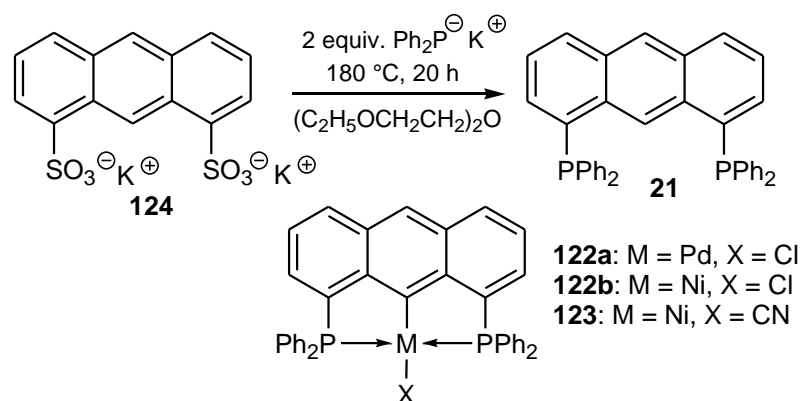
Dibenzobarrelene-based  $C(sp^3)$ -metallated pincer complexes **121a**, **121b**, and **121c** were synthesized by the Diels–Alder [4 + 2] cycloaddition reaction of organometallic anthracene dienes **122a**, **122b**, and **122c** with dimethyl acetylenedicarboxylate as a dienophile (Scheme 42). This straightforward approach has an advantage over traditional synthetic routes, such as either C–H activation or oxidative insertion of a coordinated transition metal into the C–X bond of the halogenated spacer [58].



Scheme 42. The synthesis of (Pd, Ni, Pt)-complexes **121a-c** via the Diels–Alder approach.

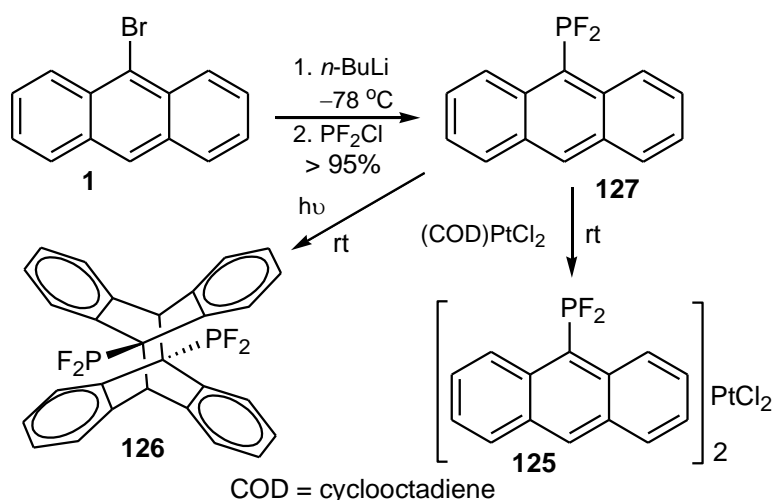
A number of metal complexes **122a**, **122b**, and **123** have been synthesized using 1,8-bis(diphenylphosphino)anthracene **21** as a ligand (Scheme 43). The latter was synthesized from dipotassium 1,8-anthracenedisulfonate **124** and potassium diphenylphosphide

(Ph<sub>2</sub>PK). The reaction of **21** with nickel(II) chloride or bis-(benzotriple)palladium(II) chloride led to cyclometallation of the anthracene C-H bond at 9-position and resulted in the formation of square-planar chelate complexes **122b** or **122a**, respectively. Treating the complex **122b** with aqueous potassium cyanide did not remove nickel from **122b** but converted **122b** into **123** by substituting chloride with cyanide, confirming the high stability of these cyclometallated chelate complexes. The strong metal bonding in **122b** made it an ideal ligand for the development of new catalysts. Like the anthracene unit in **21**, other polycyclic acenes or heteroarenes might also be useful as a rigid backbone for bidentate phosphines [59].



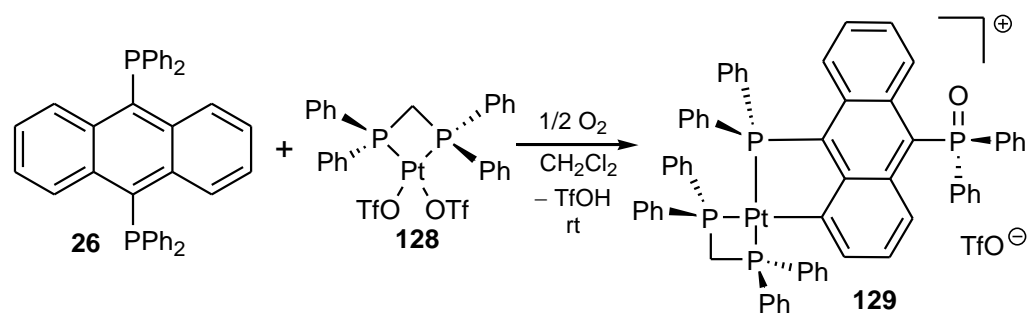
**Scheme 43.** The synthesis of the 1,8-bis(diphenylphosphino)anthracene ligand **21** and metal complexes **122a**, **122b**, and **123**.

The platinum (II) complex **125** and photochemically dimerized product **126** were synthesized from 9-(difluorophosphino)anthracene **127** (Scheme 44), obtained in the reaction of anthryllithium with chlorodifluorophosphine, with the former being synthesized in the reaction of *n*-butyllithium with 9-bromoanthracene **1**. The dimer **126** constituted one of the six possible rotational isomers. A rotation of the PF<sub>2</sub> group was hindered by strong F-H interactions at temperatures up to at least 105 °C [60].



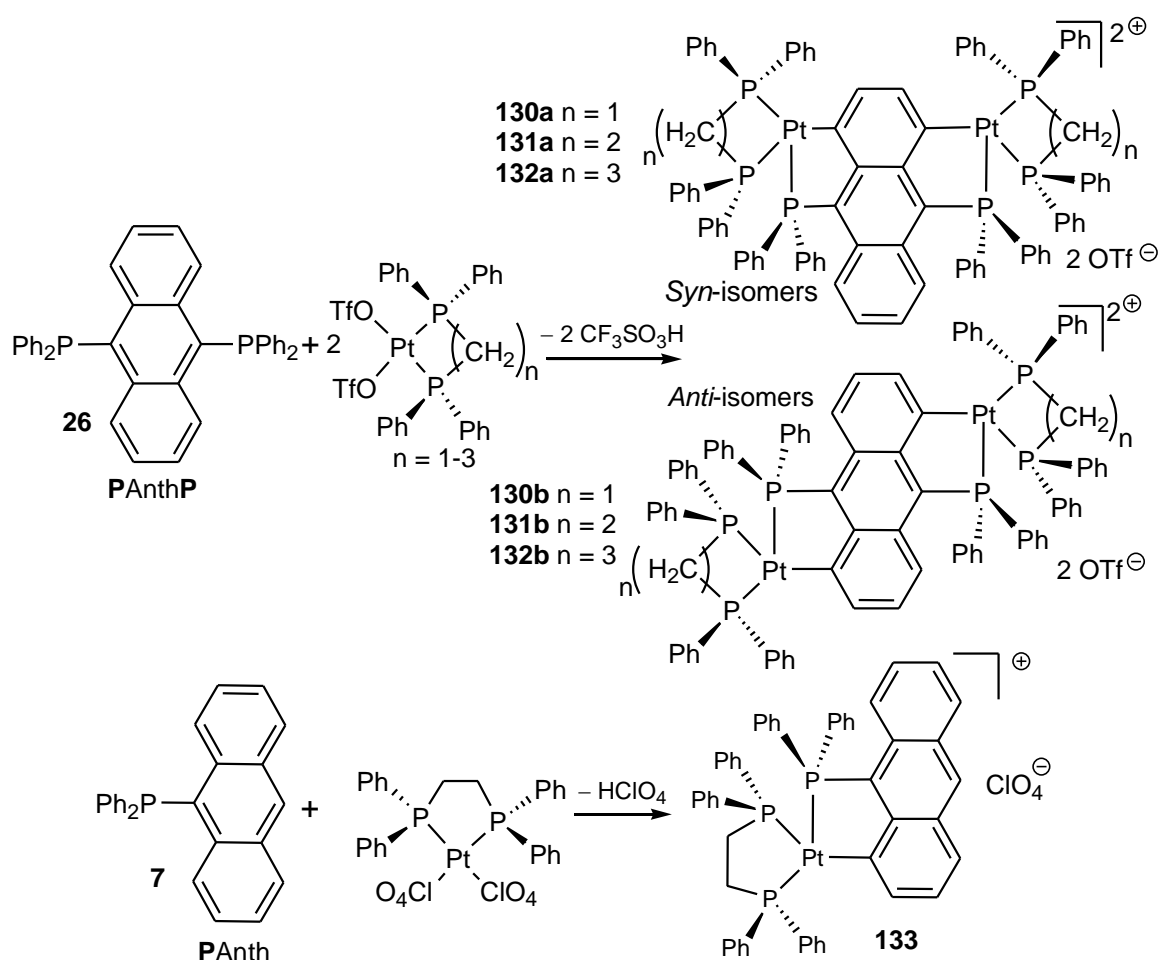
**Scheme 44.** The synthesis of the Pt(II) complex **125** and the dimer **126**.

Hu et al. [61] described the cycloplatination reaction of 9,10-bis(diphenylphosphino)anthracene **26** with Pt(bis(diphenylphosphino)methane)(OTf)<sub>2</sub> **128** to give [Pt(bis(diphenylphosphino)methane)(9-(diphenylphosphino)anthracene)PO-H]OTf **129**. The uncoordinated P atom in the complex was oxidized when exposed to air (Scheme 45).



**Scheme 45.** The preparation of the platinum complex **129**.

The same authors also studied the influence of the reaction conditions on the regioselectivity of the double cyclometallation process (Scheme 46) [62].



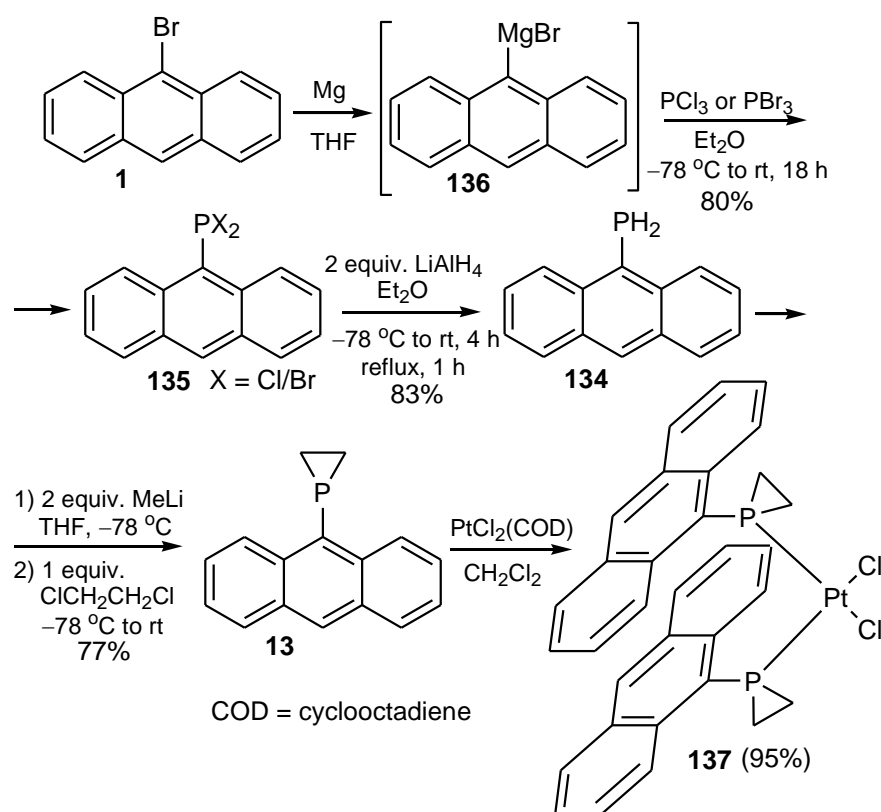
**Scheme 46.** The synthesis of the dicyclopalladated complexes **130–132** (*syn* and *anti*) and the monocyclopalladated complex **133**.

Other dicyclopalladated complexes *syn*- and *anti*-[Pt<sub>2</sub>(L)<sub>2</sub>(PAnthP-H<sub>2</sub>)](OTf)<sub>2</sub>(Pt<sub>2</sub>) (Anth = anthrylene) **130–132** have been synthesized in reactions of **26** (PAnthP) with Pt(L)(OTf)<sub>2</sub> (L = diphosphine, OTf) (Scheme 46). To understand the effect of the number of Pt ions on the extent of perturbation, a mononuclear analog **133** was also prepared. The UV–vis absorption spectra of **133** and PAnth displayed moderately intense vibronic bands at around 320–440 nm. The spectra of the binuclear complexes **130–132** were different from that of **133**. The spectra of the *syn*-isomers **130a**, **131a**, and **132a** displayed two intense overlapping absorption bands at 320–520 nm. The *anti*-isomers **130b** and **132b** also displayed two intense



bands in a similar spectral range (300–500 nm). The emission energies in degassed DCM at room temperature followed the order **133** > **131b**, **132b** > **130a**, **131a**, and **132a** [62].

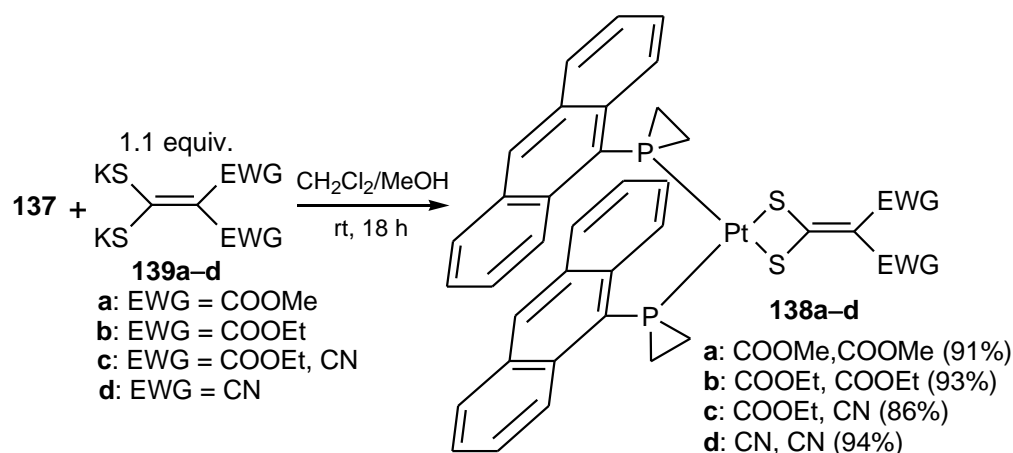
9-(Dihydrophosphino)anthracene **134** was prepared in two steps starting from 9-bromoanthracene **1**, which was next converted to 9-(dihalophosphino)anthracenes **135** (X = Cl, Br) via the Grignard reagent **136**, which reacted with PCl<sub>3</sub> or PBr<sub>3</sub>, respectively. Next, reduction of the latter with 2 equiv. of LiAlH<sub>4</sub> in diethyl ether at –78 °C and then reflux for 1 h delivered **134**. In the reaction of the dilithium derivative of **134** with 1,2-dichloroethane, Kubiak and co-workers obtained 9-(1-phosphirano)anthracene **13**. Then, the reaction of **13** with 0.5 equiv. of PtCl<sub>2</sub>(1,5-cyclooctadiene) gave the platinum complex, *cis*-dichlorobis[1-(9-anthracene)phosphirano]platinum(II) **137** (Scheme 47) [63]. The complex **137** displayed novel intramolecular  $\pi$ -stacking interactions between the anthracene ring systems.



**Scheme 47.** The synthesis of 9-(1-phosphirano)anthracene **13** and its platinum complex **137**.

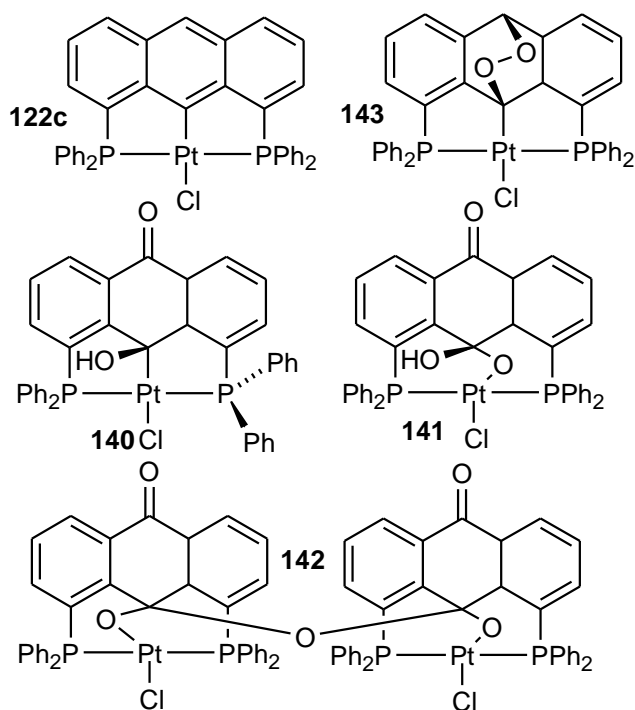
The same research group synthesized other platinum complexes, such as bis[1-(9-anthracene)phosphirano]dithiolateplatinum complexes **138a–d**, in the reaction of **137** with appropriate potassium-ethylene-2,2-dithiolates **139a–d** containing two electron-withdrawing groups (EWGs) in positions 1, such as methoxycarbonyl, ethoxycarbonyl and cyano groups. The final products **138a–d** were obtained in CH<sub>2</sub>Cl<sub>2</sub>/MeOH mixture after 18 h at room temperature in high yields. X-ray studies of the complexes displayed the intra- or intermolecular anthracene ring of the *cis*-bis{1-(9-anthracene)phosphirane} stacked structures (Scheme 48) [64].

All of the platinum complexes **138a–d** reported emitted light at low temperatures in the solid state. Complexes **138a–d** exhibited a strong green fluorescence at 530 nm at low temperatures in the solid state. Moreover, the complex **138d** strongly emitted blue light in the THF or benzene solution at 450 nm after excitation at 420 nm. The blue emission of the complex **138d** with two cyano groups and a very small Stokes shift was similar to that observed for free 9-(1-phosphirano)anthracene and anthracene rings.



**Scheme 48.** The synthesis of bis[1-(9-anthracene)phosphirano]dithiolatoplatinum(II) complexes **138a-d**.

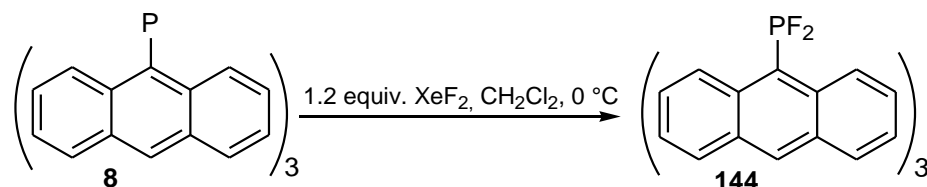
The pincer complexes **140**, **141**, and **142** were synthesized by irradiating the cyclometalated complex **122c** in the presence of  $\text{O}_2$ , which led to oxidations of the anthryl ring (Scheme 49). The first photoproduct, a Pt(II)-9,10-endoperoxide complex **143**, was converted photochemically to the Pt(II)-9-hydroxyanthrone complex **140**, which was further oxygenated to the Pt(II)-hemiketal **141**. The oxidation of **140**, which could be accelerated by light irradiation, probably involved a Pt(II)-anthraquinone intermediate. The Pt(II)-hemiketal **141** underwent acid-catalyzed ketalization to form a binuclear Pt(II) 2-diketal **142**. The structures were characterized by NMR and single-crystal X-ray diffraction. All complexes possessed similar absorption spectra, showing a moderately intense vibronic band at 390–480 nm ( $\lambda_{\text{max}} = 454 \text{ nm}$ ,  $\epsilon_{\text{max}} = 7.6\text{--}9.2 \times 10^3 \text{ M}^{-1} \text{ cm}^{-1}$ ) and a very intense band at 280 nm ( $\epsilon_{\text{max}} = 5.2\text{--}5.9 \times 10^4 \text{ M}^{-1} \text{ cm}^{-1}$ ). The Pt complexes were also luminescent in solution and in the solid state at room temperature. Irradiating degassed  $\text{CH}_2\text{Cl}_2$  solutions of the complexes at 390 nm resulted in an emission band at  $\lambda_{\text{max}} = 474 \text{ nm}$  with a vibronic shoulder at 520 nm [65].



**Scheme 49.** The synthesis of the Pt(II) pincer complex **50** and its sequential oxygenated products **140**, **141**, and **142**.

#### 2.4. Phosphoranes ( $\text{AnthPR}_2\text{X}_2$ ) ( $\text{X} = \text{F}$ )

Yamaguchi et al. [26] reported the synthesis and photochemical characterization of tri(9-anthryl)difluorophosphorane **144** obtained from the reaction of xenon difluoride with tri(9-anthryl)phosphine **8**. The synthesis of **144** is presented in Scheme 50.

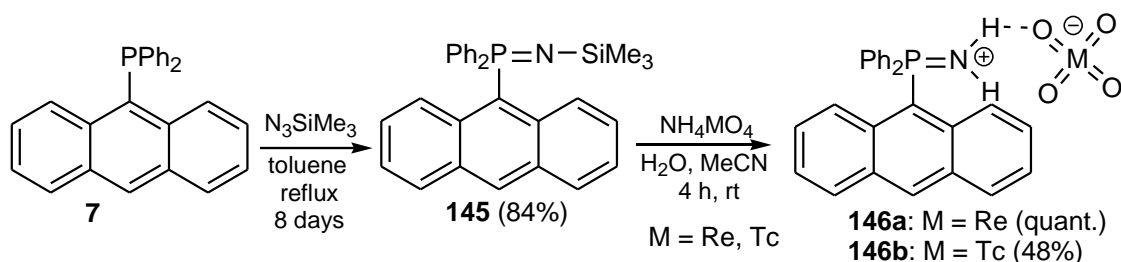


**Scheme 50.** The synthesis of tri(9-anthryl)difluorophosphorane **144**.

The authors proved that the fluorescence intensity is attributed to the coordination number of phosphorus. The tri-coordinated **8** exhibited a weak fluorescence while pentacoordinated **18** showed a significant fluorescence.

#### 2.5. Phospinimines ( $\text{AnthR}_2\text{P} = \text{N-R}^1$ ) and Phospiniminium Derivatives ( $\text{AnthR}_2\text{P} = \text{NH}_2^+$ )

Jurisson and co-workers synthesized the *N*-protected phosphinimine **145** and its phosphiniminium ion pairs **146a** and **146b** with  $[\text{ReO}_4^-]$  and  $[\text{TcO}_4^-]$  anions. The phosphinimine **145** was fluorescent but the addition of  $[\text{TcO}_4^-]$  or  $[\text{ReO}_4^-]$  anions to **145** did not change the original spectrum in terms of the overall spectral features or intensity. In addition, the anthracene molecule scintillated in the presence of  $[\text{TcO}_4^-]$ , making it a possible reporter group for a scintillation sensor using this molecule (Scheme 51) [66].

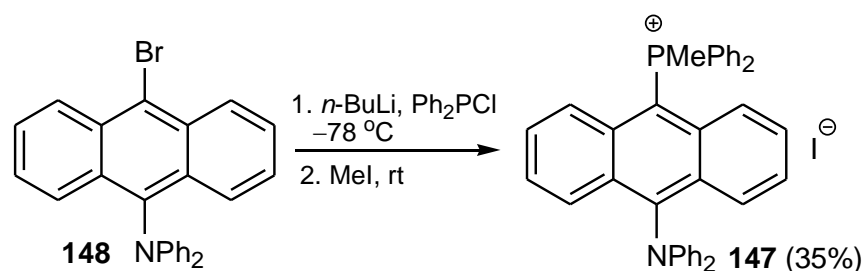


**Scheme 51.** The synthesis of *N*-trimethylsilyl-protected phosphinimine **1** and phosphiniminium salts **146a** and **146b**.

#### 2.6. Phosphonium Salts ( $\text{AnthPR}_3^+$ )

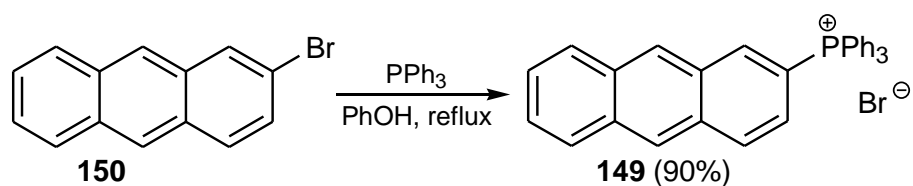
Usually, phosphonium salts are obtained from phosphines by quaternization of a tricoordinated phosphorus atom with a free electron pair.

The D- $\pi$ -A type of phosphonium salts, in which electron acceptor ( $\text{A} = \text{PR}_3^+$ ) and donor ( $\text{D} = \text{NPh}_2$ ) groups were linked by polarizable  $\pi$ -conjugated spacers, showed an intense fluorescence classically ascribed to the excited state intramolecular charge transfer (ICT). Therefore, a series of such phosphonium salts with different lengths of spacers and counterions were synthesized and characterized. The salt **147** was synthesized by the two-step approach involving the preparation of tertiary aryl phosphine from **158** followed by methylation with methyl iodide. The peak wavelengths ( $\lambda_{\text{abs}}$ ) were gradually red-shifted along with the extension of the  $\pi$ -spacer:  $\pi = \text{phenylene}$  (333 nm) <  $\pi = \text{biphenylene}$  (387 nm) <  $\pi = \text{naphthylene}$  (407 nm) <  $\pi = \text{anthrylene}$  (**147**, 519 nm). The extension of the  $\pi$ -system from phenylene to the polycyclic naphthalene and anthracene motifs in **147** caused a gradual growth of  $\lambda_{\text{em}}$  to 560 and 679 nm for **147** in DCM, which was, however, accompanied by a drop in the quantum yield (Scheme 52) [67].



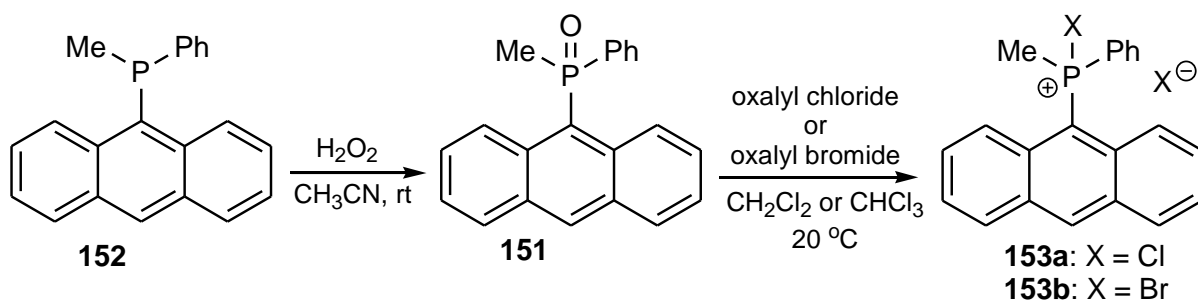
**Scheme 52.** The synthesis of the phosphonium salt **147**.

A metal-free synthesis of 2-anthryl phosphonium bromide **149** by the reaction of triphenylphosphine with 2-bromoanthracene **150** in refluxing phenol was developed by Huang et al. Examination of other solvents with a boiling point of around 200 °C showed that tetralin, PhCN, ethoxybenzene, or 2-chlorophenol could also produce phosphonium salts, although in lower yields (5–44%). A two-step addition-elimination mechanism was proposed, in which the second step of the bromide elimination was fast, as indicated by the deuterium experiment. The authors suggested that phenol could form a hydrogen bond with bromide, facilitating the addition of triphenylphosphine and elimination of bromide by polarizing the carbon–bromide bond, and making phenol the optimal solvent among the solvents tested (Scheme 53) [68].



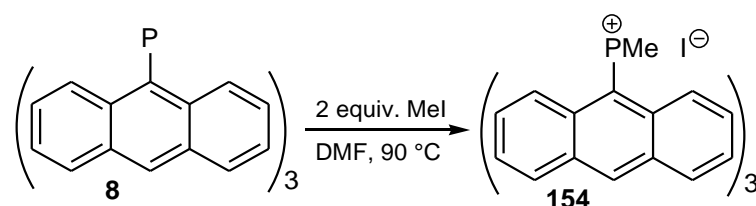
**Scheme 53.** The synthesis of the phosphonium bromide **149**.

Nikitin and co-workers [69] synthesized 9-(methylphenylphosphinoyl)anthracene **151** by the oxidation of 9-(methylphenylphosphino)anthracene **152** with hydrogen peroxide in acetonitrile solution (Scheme 54). The compound **151** was then converted into the corresponding phosphonium chloride **153a** and bromide **153b** using oxalyl chloride and bromide, respectively. The authors measured the exchange barriers of self- and cross-exchange of halides in phosphonium salts using the 2D EXSY NMR technique to visualize the processes.



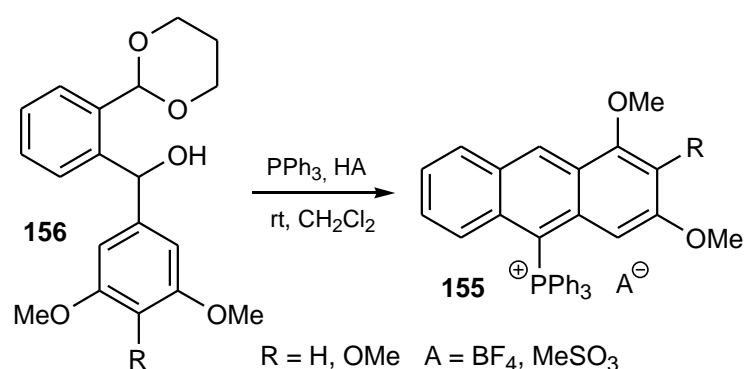
**Scheme 54.** The synthesis of the phosphonium chloride **153a** and the phosphonium bromide **153b**.

Tri(9-anthryl)(methyl)phosphonium iodide **154** was synthesized by Yamaguchi et al. in the quaternization reaction of the phosphine **8** with methyl iodide. The tri-coordinated **8** and tetra-coordinated derivatives **154** exhibited a weak fluorescence (Scheme 55) [26].



**Scheme 55.** The synthesis of tri(9-anthryl)methylphosphonium iodide **154**.

Bałczewski et al. [70,71] recently presented a novel, one-pot *phospho*-Friedel–Crafts–Bradsher cyclization, which led to higher-substituted phosphonium salts **155**. In the new reaction, (*o*-diacetoalaryl)arylmethanols **156**, as the starting materials, in the presence of triphenylphosphine and acids HA, spontaneously cyclized directly to **155** under very mild reaction conditions (Scheme 56).



**Scheme 56.** The synthesis of anthryl phosphonium salts **155** from diarylmethanols **156**.

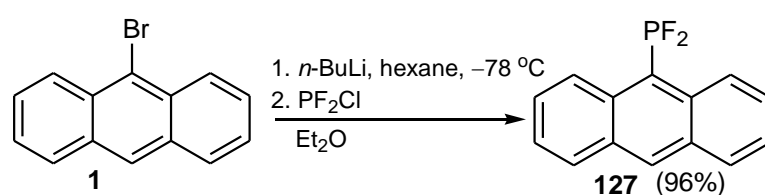
### 3. Synthesis and Reactions of P<sup>III</sup> Acids, Their P<sup>IV</sup> Tautomers, and Derivatives

This section covers P<sup>III</sup> acids derivatives containing at least one anthracene moiety linked either directly to the phosphorus atom via the P-Csp<sup>2</sup> (Anth) bond (Sections 3.1 and 3.2) or indirectly via the P-O-Csp<sup>2</sup> (Anth) bond (Section 3.3). The phosphonous RP(OH)<sub>2</sub>, phosphinous R<sub>2</sub>POH, and phosphorous P(OH)<sub>3</sub> free acids are the organophosphorus members of the group of substances known as the lower acids of phosphorus. These P<sup>III</sup> trivalent species exist as minor tautomers in equilibrium with major P<sup>IV</sup> tetravalent forms, which exhibit one less acidic function than might be expected [8]. Derivatives of P<sup>III</sup> acids, such as halides, amides, and esters, may exist in stable, trivalent forms and they will be described separately in Sections 3.1–3.3. The P<sup>IV</sup> tautomers are discussed in Sections 3.4 and 3.5.

#### 3.1. Phosphonous Acid Dihalides and Phosphinous Acid Halides (Halophosphines) (AnthPX<sub>2</sub>) and (Anth<sub>2</sub>PX) (X = F, Cl, Br)

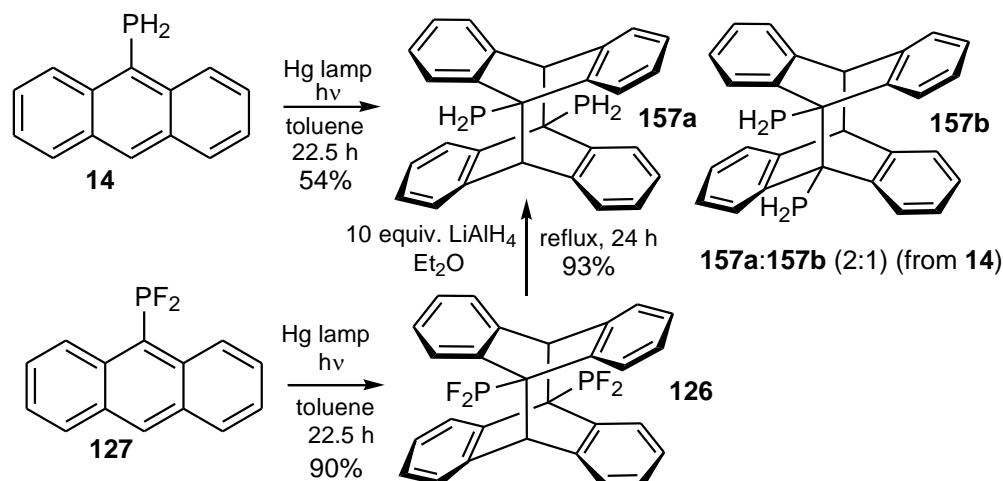
Halo- and dihaloanthracenes of the formula AnthPX<sub>2</sub> and Anth<sub>2</sub>PX (X = F, Cl, Br), which contain at least one P-C bond and one or two halogen atoms, are classified as halides of the corresponding lower P<sup>III</sup> acids. Syntheses of 9-(difluoro, dichloro, dibromo)anthracenes are also described in Section 2.3.

9-Difluoroanthracene **127** was synthesized by Schmutzler et al. starting from 9-bromoanthracene **1** and chlorodifluorophosphine in a 96% yield (Scheme 57) [10].



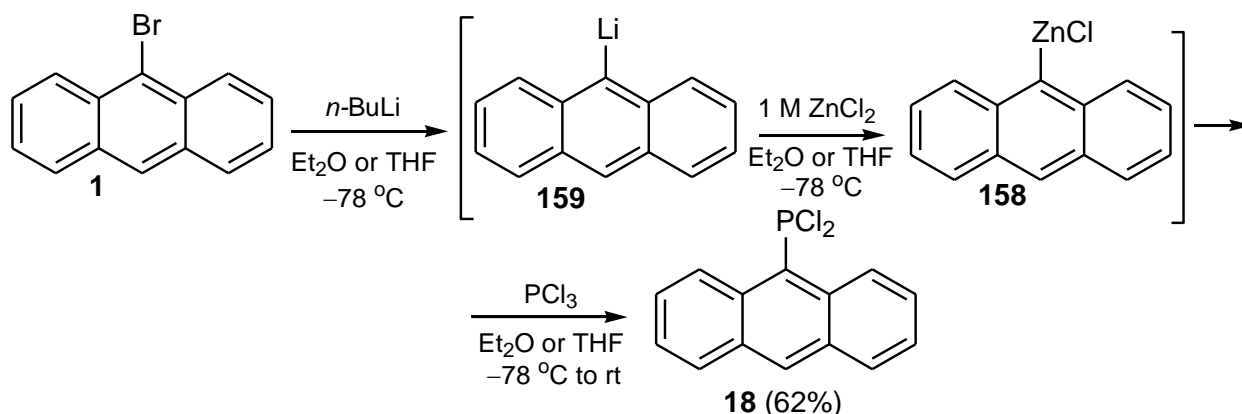
**Scheme 57.** The synthesis of 9-difluoroanthracene **127**.

9-(Difluorophosphino)anthracene **127** was also employed by the group of Schmutzler in further investigations. They used 9-(dihydrophosphino)anthracene **14** and irradiated it with a mercury lamp in toluene for 22.5 h to obtain two isomeric dimers **157a** and **157b** in a 2:1 ratio, which could be observed in  $^{31}\text{P}$  NMR. Irradiation of 9-(difluorophosphino)anthracene **127** under the same conditions gave only one dimeric isomer **126**. Hydrogenation reaction of the latter with 10 equiv. of  $\text{LiAlH}_4$  in diethyl ether at reflux for 24 h delivered a single isomer **157a** in a 93% yield (Scheme 58) [10].



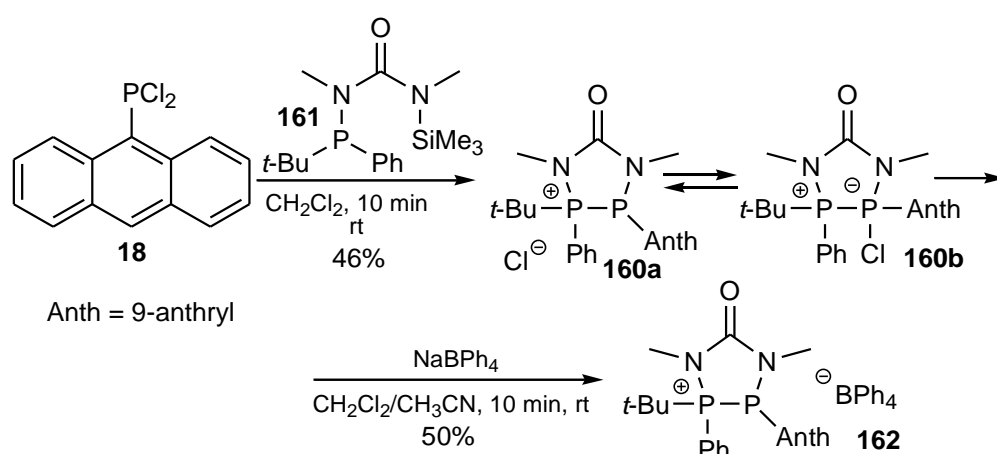
**Scheme 58.** The photodimerization of **14** and **127** and the reduction reaction of the dimer **126** to **157a**.

Kirst and et al. [72] synthesized 9-(dichlorophosphino)anthracene **18** by the reaction of  $\text{PCl}_3$  with the organozinc compound **158**. The latter was obtained from 9-bromoanthracene **1**, which was first lithiated with *n*-butyllithium to obtain **159** and then submitted to the Li/Zn transmetalation with dry  $\text{ZnCl}_2$  (Scheme 59).



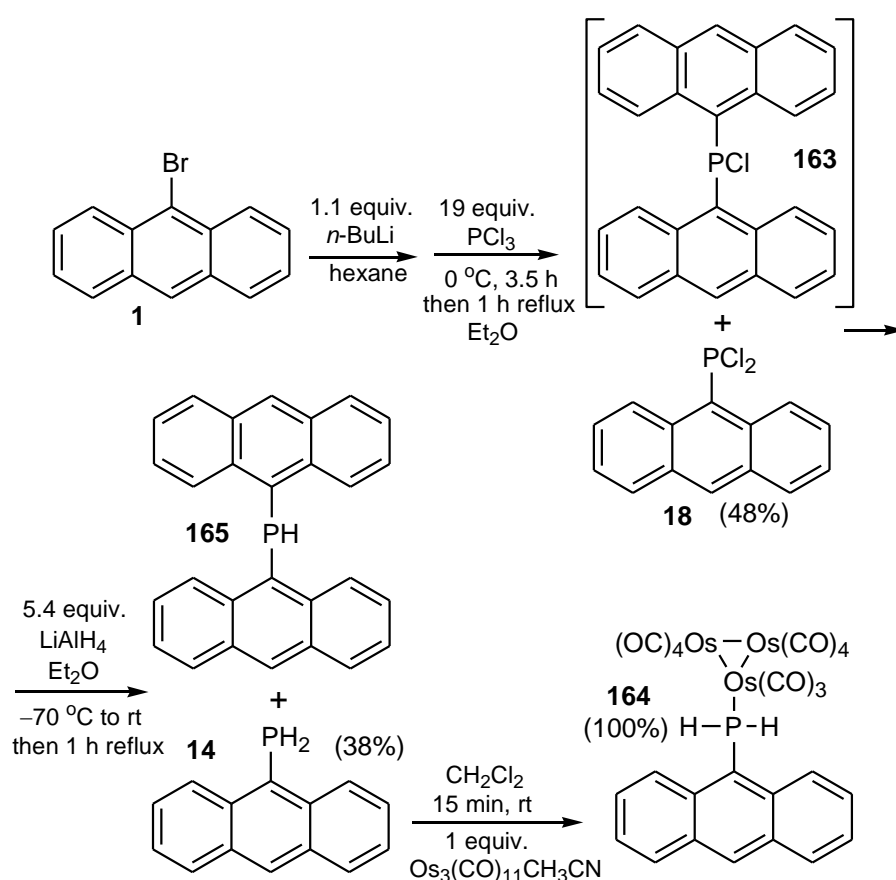
**Scheme 59.** The synthesis of 9-(dichlorophosphino)anthracene **18**.

9-(Dichlorophosphino)anthracene **18** was further utilized by the group of Schmutzler in the preparation of cyclic (*P*-anthrylphosphino)phosphonium chloride remaining in equilibrium **160a/160b** in the reaction of 9-(dichlorophosphino)anthracene **18** and *N*-[*tert*-butyl(phenyl)phosphino]-*N,N*-dimethyl-*N*-(trimethylsilyl)urea **161** in  $\text{CH}_2\text{Cl}_2$  at room temperature in a 46% yield. The existence in solution of the equilibrium between the ionic structure **160a** and the covalent form **160b** was observed. Next, the chloride **160a/160b** was converted into the corresponding phosphonium tetraphenylborate **162** by treatment of  $\text{NaBPh}_4$  in  $\text{CH}_2\text{Cl}_2/\text{CH}_3\text{CN}$  in a 50% yield (Scheme 60) [73].



**Scheme 60.** The synthesis of (*P*-anthrylphosphino)phosphonium chloride **160a**/**160b** and the tetraphenylborate **162**.

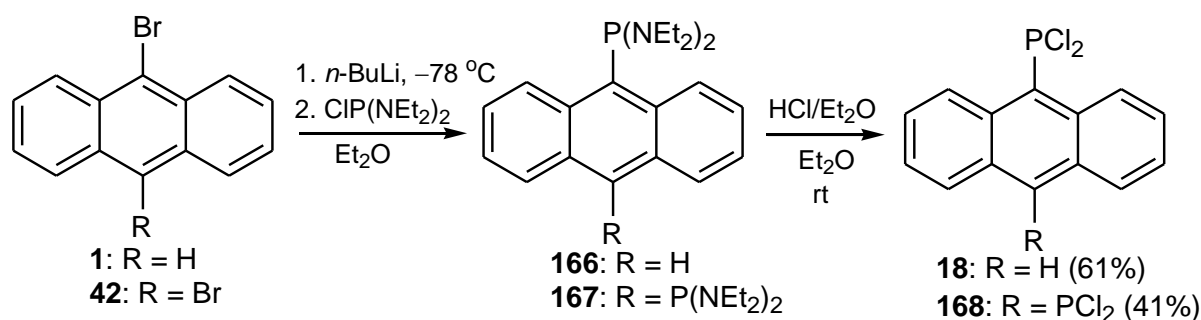
Schmutzler and co-workers presented a synthesis of 9-(dichlorophosphino)anthracene **18** and 9-(anthrylchlorophosphino)anthracene **163** from 9-bromoanthracene **1** using a large excess of  $\text{PCl}_3$  (19 equiv.) in a 48% yield. The resulting mixture of **18** and **163** was reduced with 5.4 equiv. of  $\text{LiAlH}_4$  in diethyl ether at reflux to obtain 9-(dihydrophosphino)anthracene **14** and (anthrylhydrophosphino)anthracene **165**. Next, pure **14** was reacted with 1 equiv. of  $\text{Os}_3(\text{CO})_{11}(\text{CH}_3\text{CN})$  in  $\text{CH}_2\text{Cl}_2$  at room temperature to give triosmiumdodecacarbonyl cluster **164** quantitatively (Scheme 61) [10].



**Scheme 61.** The synthesis of 9-(chlorophosphino)anthracenes **18**, **163**, 9-(hydrophosphino)anthracenes **14**, **165**, and the osmium complex **164**.

### 3.2. Phosphonous Acid Diamides ( $\text{AnthP}(\text{NR}_2)_2$ )

9-[Bis(diethylamino)phosphino]anthracene **166** and 9,10-bis[bis(diethylamino)phosphino]anthracene **167** were prepared by Tokitoh and co-workers starting from 9-bromoanthracenes **1** and **42**, which were first lithiated with *n*-butyllithium and then reacted with bis(diethylamino)chlorophosphine. The resulting anthracenes **166** and **167** were transformed to 9-(dichlorophosphino)anthracene **18** and 9,10-bis(dichlorophosphino)anthracene **168** using hydrogen chloride in diethyl ether (Scheme 62) [74].



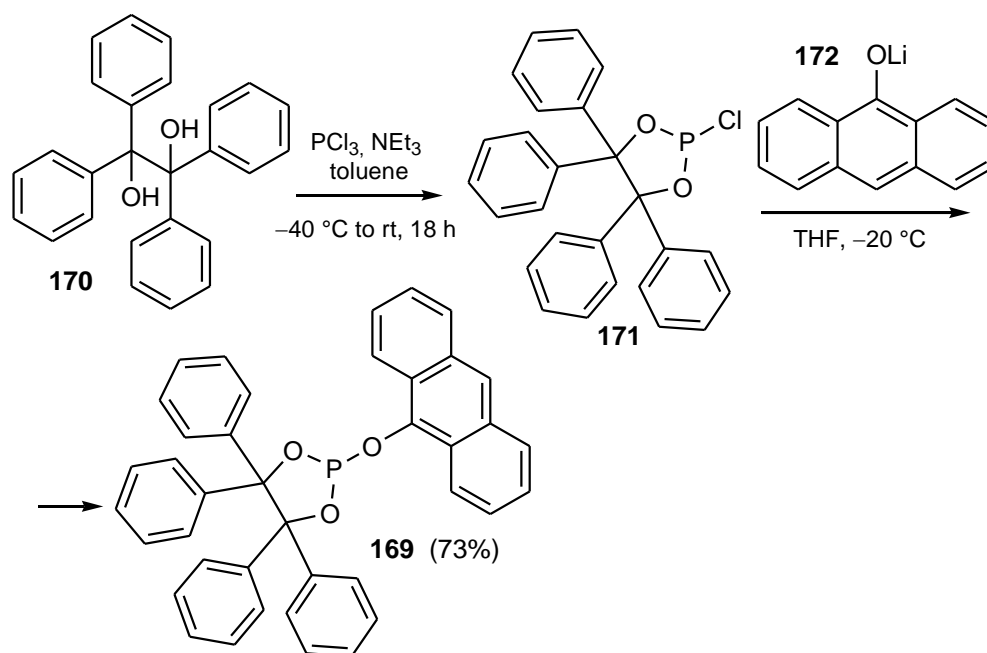
**Scheme 62.** The synthesis and transformation of bis(diethylamino)phosphinoanthracenes **166** and **167**.

### 3.3. Phosphorous Acid Esters (Phosphites) ( $\text{AnthOP}(\text{OR})_2$ )

This subsection covers P<sup>III</sup> acids derivatives containing one anthracene moiety linked indirectly to the phosphorus atom via the P–O–Csp<sup>2</sup> (Anth) bond.

Kloß et al. conducted a study of numerous phosphite-based ligands for rhodium catalysts, which were used in hydroformylation reactions [3]. The authors revealed that anthryl phosphites were susceptible to hydrolysis, which limits their use for the synthesis of catalysts. Therefore, they synthesized relatively stable phosphites, one of which was the phosphite **169**.

The latter, as a solid, was synthesized by a procedure involving the treatment of benzopinacol **170** with phosphorus trichloride to give chlorophosphite **171**, followed by the addition of lithium anthr-9-olate **172** (Scheme 63).



**Scheme 63.** The synthesis of the phosphite **169** from PCl<sub>3</sub> and the dialcohol **170**.

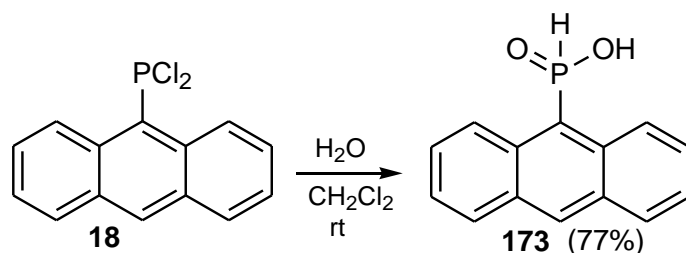


Implemented in a rhodium catalyst, it exhibited high activity towards hydroformylation. The ligand turned out to be relatively stable under hydrolysis conditions.

### 3.4. Phosphonous Acid $P^{IV}$ Tautomers (*H*-phosphinic Acids) (*AnthP(O)H(OH)*)

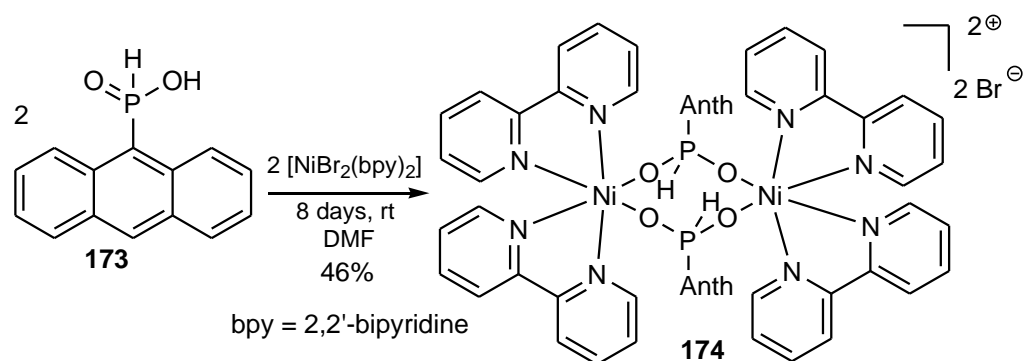
The synthesis of the ester of the  $P^{III}$  tautomeric form of phosphonous acid, i.e., diphenyl 9-anthrylphosphonite **2**, is mentioned in Section 2.

Schmutzler and co-workers presented the hydrolysis of 9-(dichlorophosphino)anthracene **18** in  $CH_2Cl_2$  with water at room temperature, which gave anthryl-*H*-phosphinic acid **173** in a 77% yield (Scheme 64) [10].



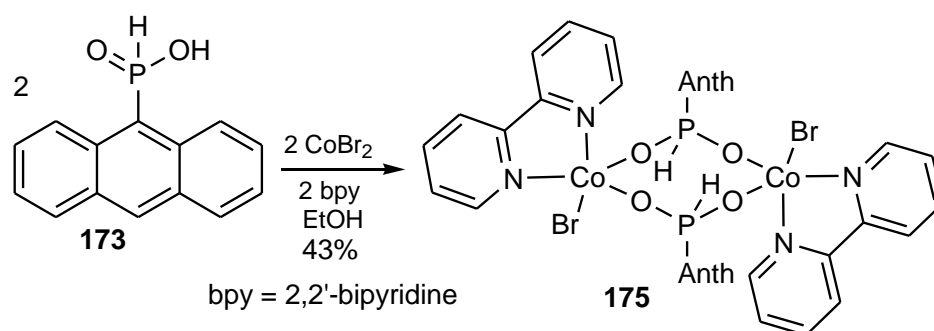
**Scheme 64.** The synthesis of anthrylphosphinic acid **173**.

Yakhvarov et al. reported the synthesis of the first example of dinuclear nickel complex **20** with the bridging anthr-9-yl- $P(H)O_2$  ligands. Anthr-9-yl-phosphinic acid **173** in the reaction with  $NiBr_2(bpy)_2$  in dimethylformamide after 8 days at room temperature gave the nickel complex **174** in a 46% yield (Scheme 65) [75].



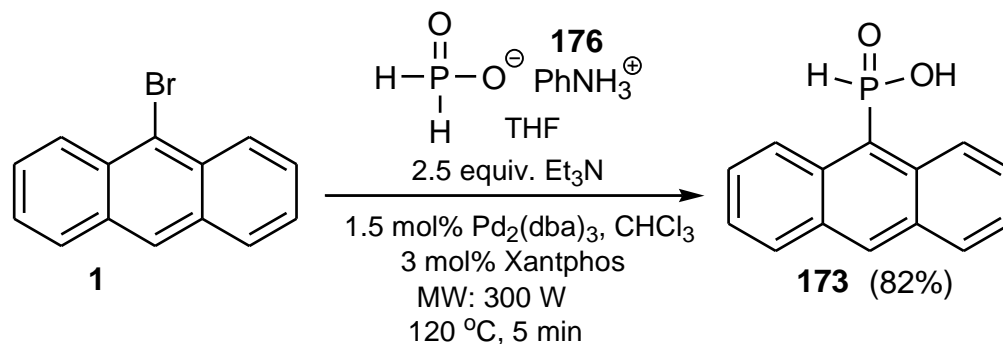
**Scheme 65.** The synthesis of the binuclear nickel complex **174** with the  $AnthP(H)O_2$  ligand.

The same authors reported the formation of the first example of a neutral dinuclear cobalt complex **175** formed in the reaction of cobalt dibromide with 2,2'-bipyridine (bpy) and 9-anthrylphosphinic acid **173** (Scheme 66) [76].



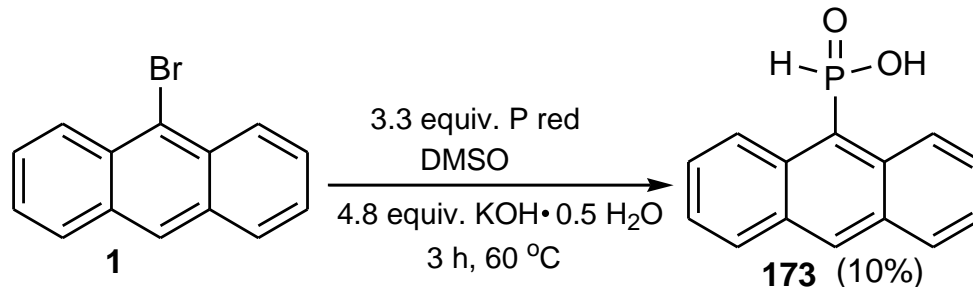
**Scheme 66.** The synthesis of the dinuclear cobalt complex **175** with the 9-anthrylphosphinic acid ligand.

Stawinski and co-workers reported a microwave-assisted (MW) synthesis of a series monoaryl-*H*-phosphinic acids, including anthr-9-yl-*H*-phosphinic acid **173** [77]. The microwave-assisted cross-coupling of 9-bromoanthracene **1** and anilinium *H*-phosphinate **176** was catalyzed by 3 mol% Pd<sub>2</sub>(dba)<sub>3</sub> CHCl<sub>3</sub>/Xantphos<sup>®</sup> as a supporting ligand and was carried out in the presence of 2.5 equiv. of triethylamine. Irradiation of the mixture with a microwave (MW) for 5 min at 120 °C produced *H*-phosphinic acid **173** in an 82% yield (Scheme 67).



**Scheme 67.** The synthesis of anthr-9-yl-*H*-phosphinic acid **173** from 9-bromoanthracene **1**.

Trofimov and co-workers reported another synthesis of anthr-9-yl-phosphinic acid **173** in the reaction of 9-bromoanthracene **1** with elemental phosphorus in a superbasic medium [78]. The authors treated **1** with 3.3 equiv. of phosphorus red in DMSO and the mixture of 4.8 equiv. of KOH and H<sub>2</sub>O as a superbase at 60 °C for 3 h (Scheme 68). In this case, the yield of **173** was only 10%.

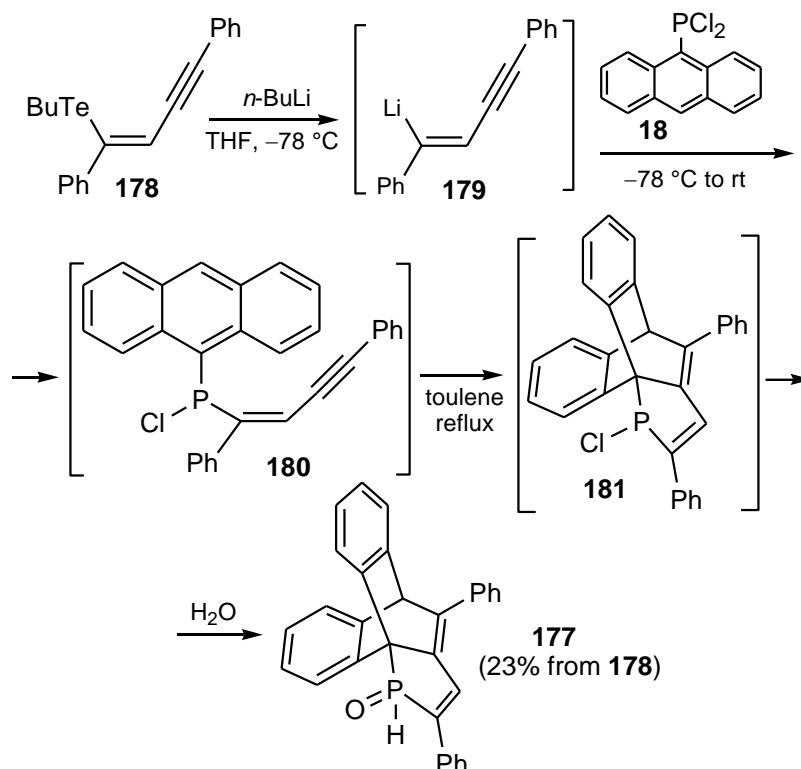


**Scheme 68.** The reaction of 9-bromoanthracene **1** with red phosphorus.

### 3.5. Phosphinous Acid P<sup>IV</sup> Tautomers (*H*-phosphine Oxides) (Anth<sub>2</sub>P(O)H)

The synthesis of esters of the P<sup>III</sup> tautomeric form of phosphinous acid, i.e., phenyl 9-anthryl(1-naphthyl)phosphinite **3** and phenyl dianthrylphosphinite **6**, is mentioned in Section 2.

The 1-(phosphino)-1,4-diphenyl-1,3-butadiene moiety, incorporated with a dibenzobarrelene skeleton in **177**, was synthesized by Ishii and co-workers [79]. They started the synthesis from lithiation of the starting reagent **178** with *n*-butyllithium to obtain the organolithium intermediate **179** followed by treatment of the latter with 9-dichlorophosphinoanthracene **18** to obtain the key precursor (*Z*)-1-(9-anthrylchlorophosphino)butenyne **180**. Then, the dibenzobarrelene structure **181** was obtained by an intramolecular [4+2] cycloaddition reaction of **180** (Scheme 69). Further hydrolysis of **181** gave the secondary phosphine oxide **177**, which exhibited a long-wavelength absorption ( $\lambda_{\text{abs}} = 355 \text{ nm}$ ) and emission ( $\lambda_{\text{em}} = 442 \text{ nm}$ ).

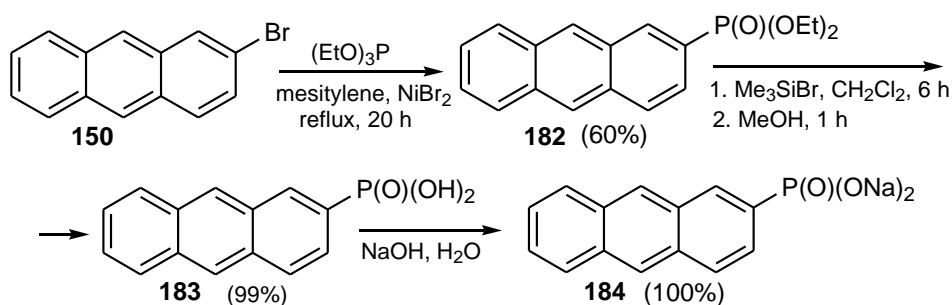


**Scheme 69.** The synthesis of the secondary phosphine oxide **177** from (*n*-butyltelluro)butenyne **178**.

#### 4. Synthesis and Reactions of Phosphonic Acids (AnthP(O)(OH)<sub>2</sub>) and Phosphonates (AnthP(O)(OR)<sub>2</sub>) (Anth = Anthryl)

In this section, P<sup>IV</sup> organophosphorus-substituted acenes with one P-Csp<sup>2</sup> (Anth) bond, two P-O, and one P=O bonds are reviewed. Hence, this section includes phosphonic acids and their esters. Interestingly, no thio- and seleno phosphonic acids AnthP(X)(YH)<sub>2</sub> and the corresponding hetero-phosphonates AnthP(X)(YR)<sub>2</sub> (Anth = anthryl), (X, Y = S, Se) were reported in the review period.

The synthesis of a series of anthracenes substituted in position 2 with diethoxyphosphoryl groups was described by French and coworkers (Scheme 70) [80]. The Arbuzov reaction of 2-bromo-anthracene **150** with triethylphosphite, catalyzed by nickel bromide, proceeded in refluxing mesitylene for 20 h and led to 2-(diethoxyphosphoryl)anthracene **182**. Then, the latter was transformed into the disilyl diester by treatment with bromotrimethylsilane in dichloromethane and next hydrolyzed to the free acid **183** with methanol. Dissolving **183** in an aqueous solution of a stoichiometric amount of sodium hydroxide gave the sodium salt **184** quantitatively.

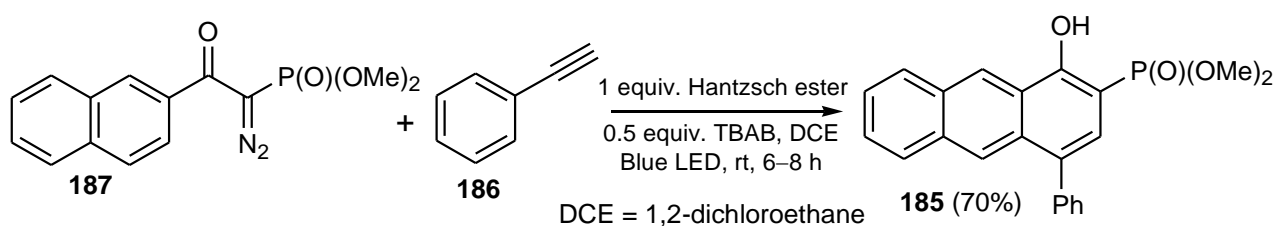


**Scheme 70.** The synthesis of 2-(dihydroxyphosphoryl)anthracene **183**.

Then, the authors investigated the spectroscopic properties of the obtained compounds, including the absorbance, fluorescence, and quantum yields  $\Phi$  [80]. A slight blue shift was

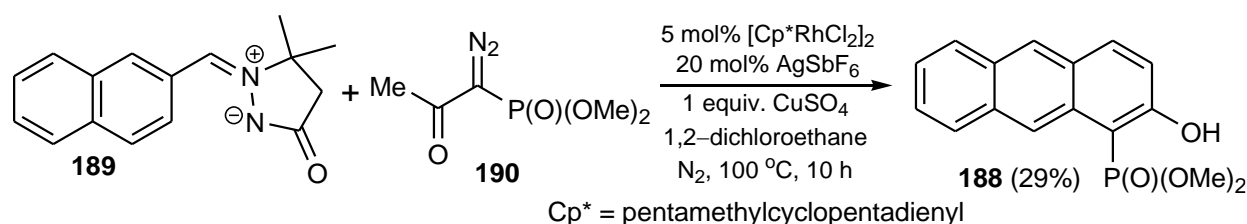
observed after the conversion of phosphonate ester into phosphonic acid and also when the phosphonic acid was converted to the corresponding sodium salt. Shifts of 53, 53, and 49 nm were observed for **182**, **183**, and **184**, respectively. Compounds **182**, **183**, and **184** showed quantum yields of fluorescence  $\Phi = 33\%$ ,  $40\%$ , and  $0\%$ , respectively. Additionally, compounds **182**, **183**, and **184** formed micelles in water.

Nagode and co-workers [81] synthesized 1-hydroxy-4-phenyl-2-(dimethoxyphosphoryl)anthracene **185** using  $\alpha$ -diazophosphonate **186**, phenylacetylene **187**, Hantzsch ester, and tetrabutylammonium bromide (TBAB) in dichloroethane under blue LED irradiation. This reaction was conducted at room temperature for 6–8 h and the product **185** was obtained in a 70% yield (Scheme 71).



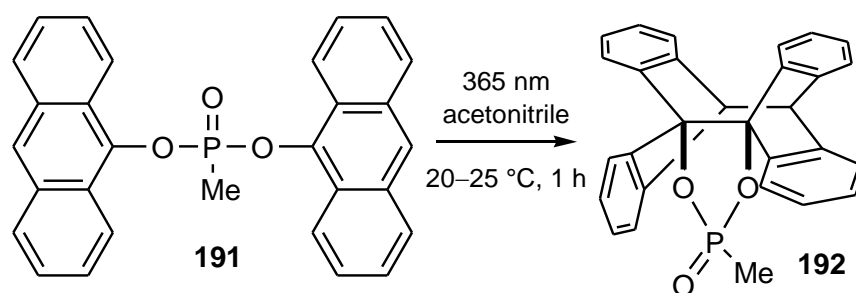
**Scheme 71.** The synthesis of 1-hydroxy-4-phenyl-2-(dimethoxyphosphoryl)anthracene **185**.

Shu et al. [82] described a new synthetic method for the preparation of 2-hydroxy-1-(dimethoxyphosphoryl)anthracene **188** in the reaction of an imine derivative of azomethine **189** and dimethyl diazophosphonate **190** in the presence of inorganic additives (Scheme 72). The reaction was carried out at 100 °C and the compound **188** was obtained in a 29% yield.



**Scheme 72.** The synthesis of 2-hydroxy-1-(dimethoxyphosphoryl)anthracene **188**.

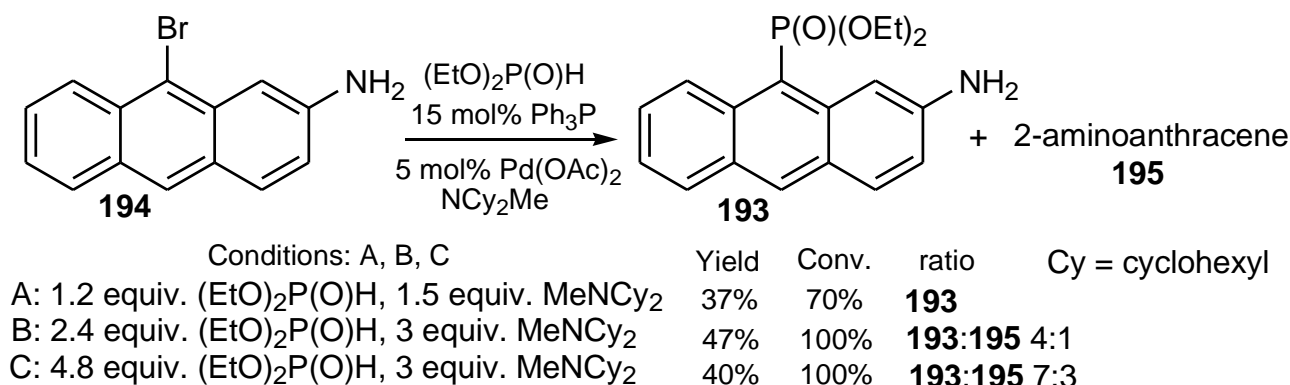
Nakamura and co-workers [83] studied the photolysis reactions of di(anthr-9-yl) methylphosphonate **191**. The authors demonstrated that upon irradiation with monochromatic light at 365 nm, **191** underwent cyclization to **192** (Scheme 73), similarly to the compound **230** (see below Scheme 87).



**Scheme 73.** The cyclization of **191** to **192** upon irradiation with 365 nm monochromatic light.

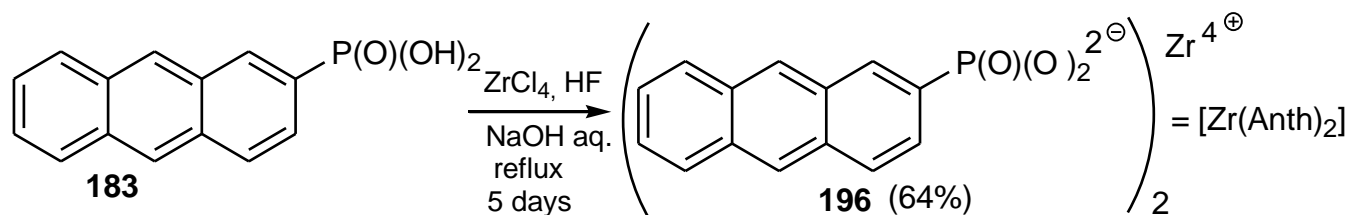
Bessmertnykh and co-authors presented a direct synthesis of 9-(diethoxyphosphoryl)anthracene **193** bearing an amino group on the aromatic ring at the position 2 in a Hirao reaction. The authors carried out a reaction of 2-amino-9-bromoanthracene **194** with diethyl phosphite in the presence of *N,N*-dicyclohexylmethylamine in refluxing ethanol for 48 h and

using catalytic amounts of palladium acetate (5 mol %) and triphenylphosphine (15 mol %). The outcome of this reaction depended on the stoichiometry used (Scheme 74) [84].



**Scheme 74.** The synthesis of diethyl 2-amino-9-anthrylphosphonate **193**.

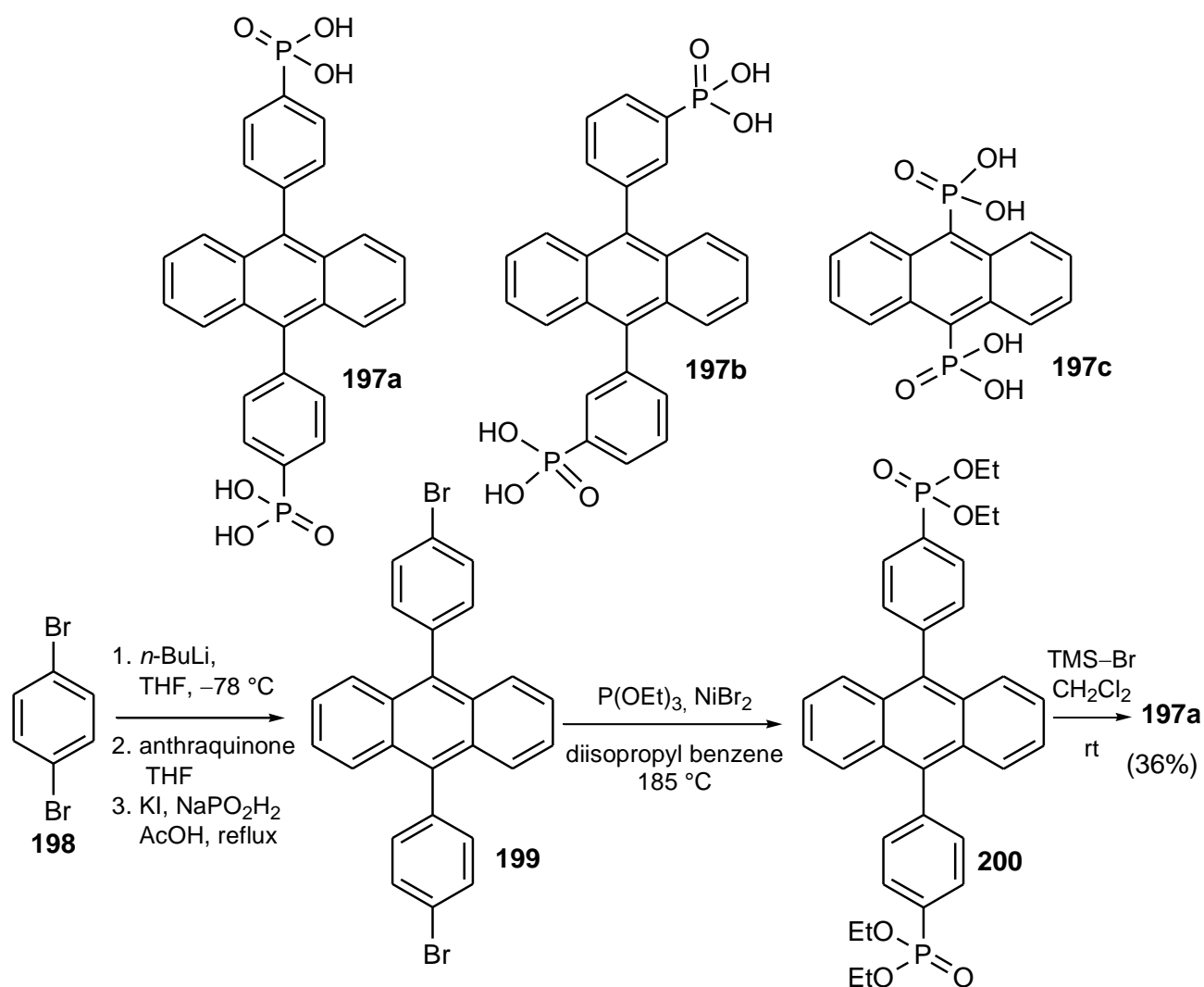
Leenstra and co-workers synthesized zirconium bis-(2-anthrylphosphonate) [Zr(Anth)<sub>2</sub>] **196** by mixing zirconyl chloride with hydrofluoric acid, sodium hydroxide, and 2-naphthylphosphonic acid **183** in water for 5 days at reflux (Scheme 75) [85].



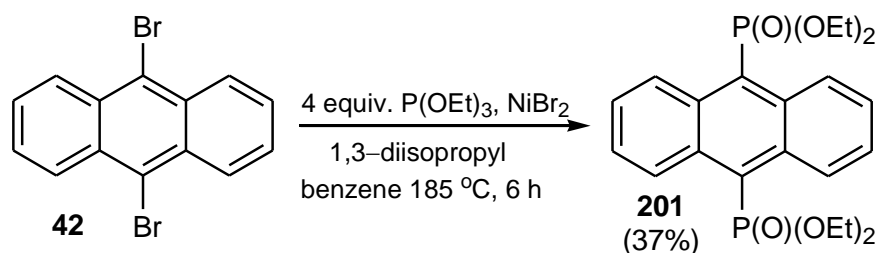
**Scheme 75.** The synthesis of zirconium bis(2-anthrylphosphonate) **196**.

The same authors showed the readily excimer formation of zirconium bis-(2-anthrylphosphonate) [Zr(Anth)<sub>2</sub>] **196** as a powdered solid in glycerol and its precursor, 2-anthrylphosphonic acid **183**, in methanol solution (Scheme 75) [86]. The fluorescence spectrum of **196** [Zr(Anth)<sub>2</sub>] had a broad emission band with a maximum at 448 nm in the solid. Additionally, the authors observed that [Zr(Anth)<sub>2</sub>] **196** did not display a time-dependent quenching of the fluorescence emission, suggesting that the photodimerization reaction of the anthracene group to bianthryl did not exist in the solid state.

Zhou and coworkers [6] investigated five anthracene-based bis(phosphonic acids), of which three **197a**, **197b**, and **197c** possessed the direct P-C<sub>sp</sub><sup>2</sup> bonding. They were prepared according to the literature procedures cited there (Scheme 76). Thus, 4,4'-(anthracene-9,10-diyl)bis(4,1-phenylene) bis(phosphonic acid) **197a** was synthesized by treatment of 1,4-dibromobenzene **198** with *n*-butyllithium, followed by the addition of the resulting 4-bromo-1-lithiobenzene to anthraquinone and subsequent reduction of the resulting anthryl dialcohol to give **199**. Then, the Arbuzov-type reaction followed by hydrolysis with trimethylsilyl bromide (TMS-Br) of the obtained bis(phosphonate) **200** gave the bis(phosphonic acid) **197a** in a 36 % yield (Scheme 76) [87]. Using this procedure and 1,3-dibromobenzene as the starting material, the authors obtained the corresponding regioisomeric 4,4'-(anthracene-9,10-diyl)bis(3,1-phenylene)bis(phosphonic acid) **197b** [88]. Anthracene-9,10-bis(phosphonic acid) **197c** was prepared analogously, based on the procedure by Pramanik et al. of the synthesis of the corresponding tetraethyl ester **201** (Scheme 77) [7], which was next hydrolyzed in this work with TMS-Br to give **197c**. Compounds **197a** and **197c** exhibited red-shift fluorescence. They were deposited on a zirconium dioxide layer as triplet-triplet annihilation acceptors.



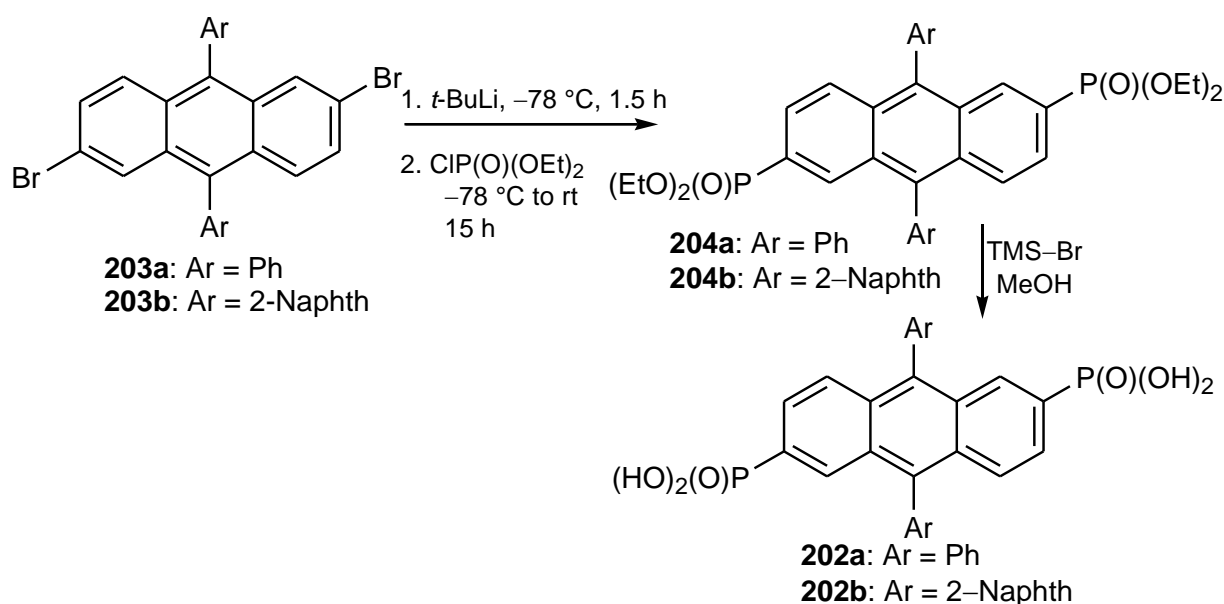
**Scheme 76.** The synthesis of the bis(phosphonic acid) **197a** from 1,4-dibromobenzene **198**.



**Scheme 77.** The synthesis of 9,10-bis(diethoxyphosphoryl)anthracene **201**.

M. Pramanik et al. [7] synthesized **201** from 9,10-dibromoanthracene **42** in a 37% yield, at high temperature, using an excess of triethyl phosphite and  $\text{NiBr}_2$  in 1,3-diisopropylbenzene (Scheme 77). The compound **201**, in the form of fluorescent organic nanoparticles, was explored as a selective anticancer candidate by apoptosis-mediated cancer therapy towards U937 cells.

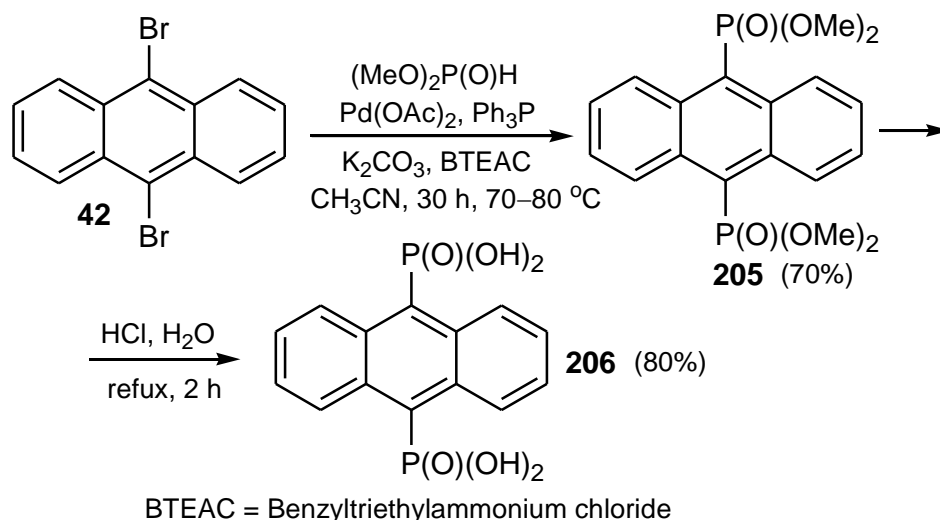
In another study, Yazji et al. [89] obtained 9,10-diphenyl-2,6-bis(phosphonic acids) **202a** and **202b** (Scheme 78) from 9,10-diaryl-2,6-dibromoanthracenes **203a** and **203b** which next were transformed to the corresponding 2,6-dilitio derivatives with *t*-butyllithium, and then reacted with diethyl phosphorochloridate to give bis(phosphonates) **204a** and **204b**, which were finally converted, by the hydrolysis of the diester, to the corresponding bis(phosphonic acids) **202a** and **202b** (Scheme 78).



**Scheme 78.** The synthesis of bis(phosphonic acids) **202a** and **202b** from 9,10-diaryl-2,6-dibromoanthracenes **203a** and **203b**.

The authors investigated the use of these compounds in thin films deposited on a silicon dioxide surface, acting as nucleation sites for pentacene crystallization. This study suggested that high optical anisotropy of pentacene, crystallized on such films, indicated that compounds **202a** and **202b** changed the silicon dioxide surface into a lattice, which induced the nucleation of pentacene. A similar study involving **202a** and **202b** was also conducted by Cattani-Scholz and co-workers [90], who synthesized these compounds in the same manner as the group of Yazji et al.

Kabachnik and coworkers demonstrated a synthesis of tetramethyl bis(phosphonate) **205** starting from 9,10-dibromo-anthracene **42** and dimethyl phosphite (Scheme 79) [91]. This reaction was catalyzed by palladium acetate/triphenylphosphine and was carried out under bi-phasic conditions for 30 h at 70–80 °C in acetonitrile in the presence of  $K_2CO_3$  as a base and benzyltriethylammonium chloride (BTEAC) as a phase-transfer catalyst (PTC) to give the desired product **205** in a 70% yield.



**Scheme 79.** The synthesis of 9,10-bis(phosphonic acid) **206** from 9,10-dibromoanthracene **42**.

Next, the authors transformed both phosphonate ester groups in **205** to the corresponding bis(phosphonic acid) **206** by refluxing it in an aqueous solution of hydrochloric acid for 2 h in an 80% yield (Scheme 79) [91].

Organic thin-film transistors based on pentacene as a semiconductor were fabricated on silicon. A self-assembled monolayer derived from the phosphonate (SAMP) **207a** showed an improvement over monolayers using octadecylsilane and other phosphonates (Figure 5). These devices had substantially reduced trap states, on/off ratios of  $10^8$ , sub-threshold slopes of 0.2 V/decade, and substantially uniform threshold voltages of  $-4.5$  V across a large number of devices [92].

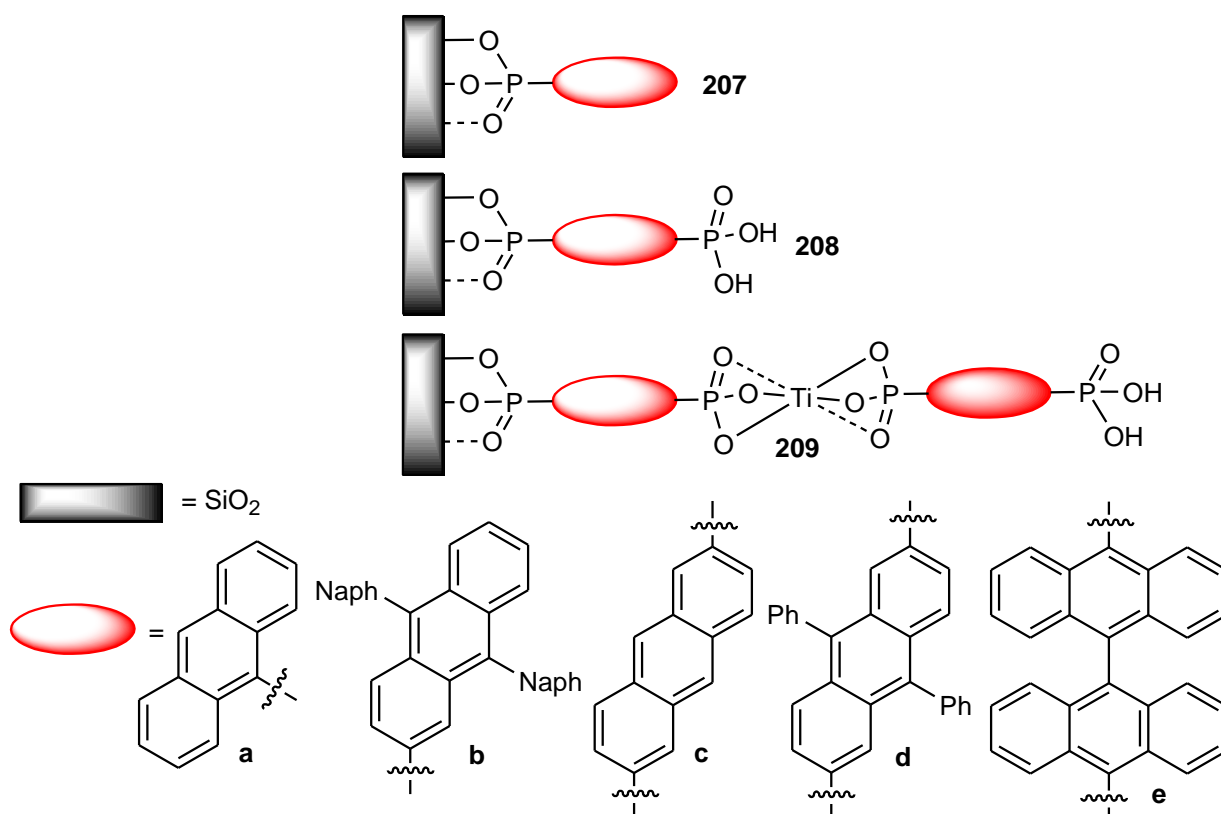


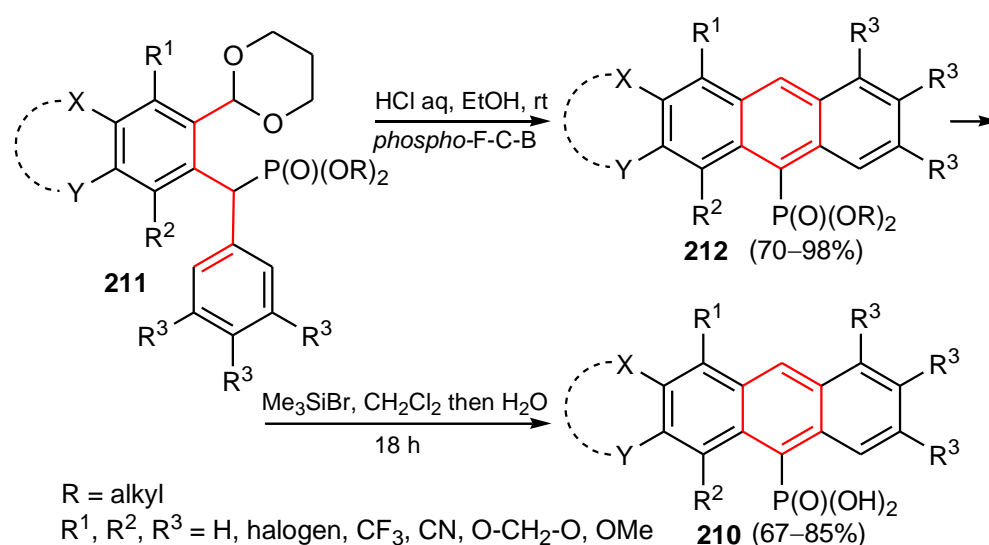
**Figure 5.** General structures of SAMPs **207**, **208**, and duplexes **209**.

Good device characteristics were also measured for the monolayer **207b**, in which the calculated molecular spacings were about 0.7 nm. This created channels that were on the order of the “thickness” of an aromatic  $\pi$  system, and which could allow intercalation of pentacene units, favoring a  $\pi$ -stacking motif for this first pentacene layer [93].

Tornow and co-workers synthesized SAMPs **208c–e** and self-assembled organophosphonate duplexes **209c,d** ensemble on nanometer-thick  $\text{SiO}_2$ -coated, highly doped silicon electrodes (Figure 5) [5].

Most of the reviewed papers in the previous sections discussed organophosphorus-substituted anthracenes that did not contain other substituents or anthracenes with a very low degree of substitution. This problem also concerns a group of phosphonates and phosphonic acids. Bałczewski et al. [70,71] recently presented a new *phospho*-Friedel–Crafts–Bradsher cyclization, which enabled the synthesis of highly substituted anthracenes **210**. In this new reaction, (*o*-diacetoaryl)arylmethylphosphonates **211** were cyclized under very mild conditions at room temperature to give 10-(dialkoxyphosphorylanthracenes **212** in a 70–98% yield. The latter were hydrolyzed to the corresponding phosphonic acids **210** in a 67–85% yield (Scheme 80).



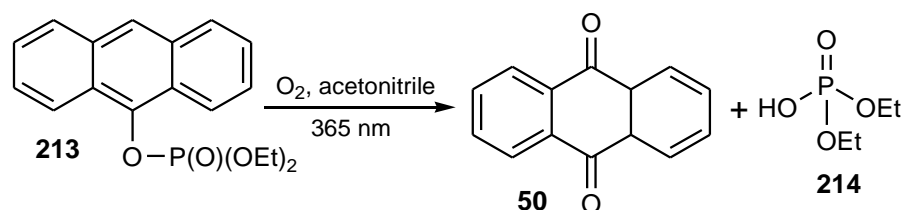


**Scheme 80.** The *phospho*-Friedel-Crafts-Bradsher cyclization of phosphonates **211** to sterically hindered anthracenes **212**.

### 5. Synthesis and Reactions of Phosphoric Acids and Phosphates (AnthOP(=O)(OR)<sub>2</sub>) (R = H, alkyl, aryl)

Unlike previous sections (except Section 3.3), which reviewed the synthesis and reactions of compounds containing a phosphorus atom linked to the anthracene moiety directly by the P-Csp<sup>2</sup> (Anth) bond, this section and Section 3.3 cover anthracenes that are bonded to the phosphorus atom indirectly via an oxygen atom by the P-O-Csp<sup>2</sup> (Anth) bond. Interestingly, no hetero-analogs of phosphates were reported in the reviewed period.

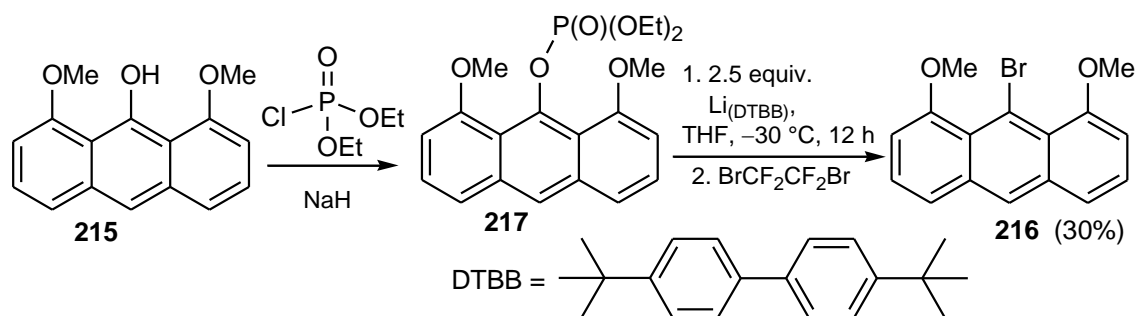
Buckland and Davidson [94] investigated the photo-oxidation of 10-diethoxyphosphoryloxyanthracene **213**, which represents a group of acenyl phosphates. The authors showed that in the presence of oxygen, the photochemically labile phosphate **213**, dissolved in acetonitrile, could be oxidized to anthraquinone **50** and diethyl hydrogen phosphate **214** upon irradiation with a 365 nm monochromatic light (Scheme 81).



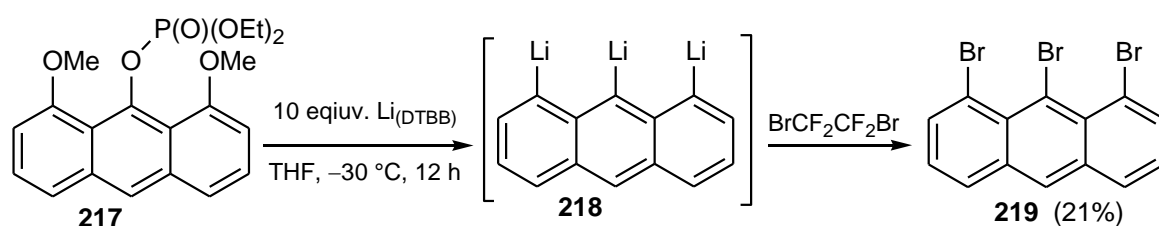
**Scheme 81.** The aerobic photochemical oxidation of the phosphate **213**.

Yamashita et al. [95] conducted a study in which 1,8-dimethoxyanthr-9-ol **215** was used for the synthesis of 9-bromo-1,8-dimethoxyanthracene **216**. The former was treated with diethyl phosphorochloridate in the presence of sodium hydride, yielding 9-diethoxyphosphoryloxy-1,8-dimethoxy-anthracene **217**. Then, the phosphate/lithium exchange with Li<sub>(DTBB)</sub> (DTBB = 4,4'-di-tert-butylbiphenyl) followed by bromination with 1,2-dibromo-1,1,2,2-tetrafluoroethane gave **216** as a pale-yellow solid in a 30 % yield (Scheme 82).

Another study, carried out by the group of Yamashita and co-workers [96], showed further application of the Li<sub>(DTBB)</sub> system towards the substrate **217**. When 2.5 equiv. of Li<sub>(DTBB)</sub> was used, the reaction followed the path from Scheme 82. However, when an excess (10 equiv.) of the Li<sub>(DTBB)</sub> reagent was used, the phosphate **217** was transformed to 1,8,9-trilithioanthracene **218**, which then underwent bromination with 1,2-dibromo-1,1,2,2-tetrafluoroethane to give 1,8,9-tribromoanthracene **219** (Scheme 83).

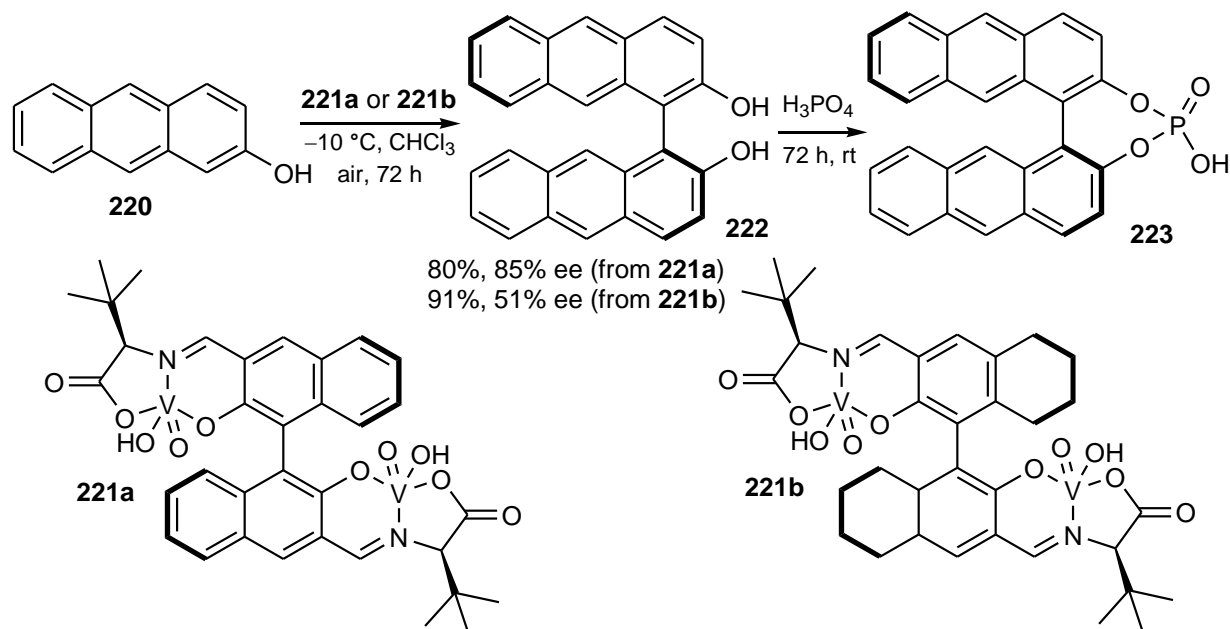


**Scheme 82.** The synthesis of 9-bromo-1,8-dimethoxyanthracene **216** via 9-diethoxyphosphoryloxy-1,8-dimethoxy-anthracene **217** as the intermediate.



**Scheme 83.** The conversion of the phosphate **217** to 1,8,9-tribromoanthracene **219**.

Takizawa et. al. [4] discovered an enantioselective, oxidative-coupling reaction of anthr-2-ol **220** with the chiral vanadium complexes **221a** and **221b** to deliver bianthrol **222**, which was then esterified with phosphoric acid to give 4,4'-bianthryl phosphoric acid **223** (Scheme 84).

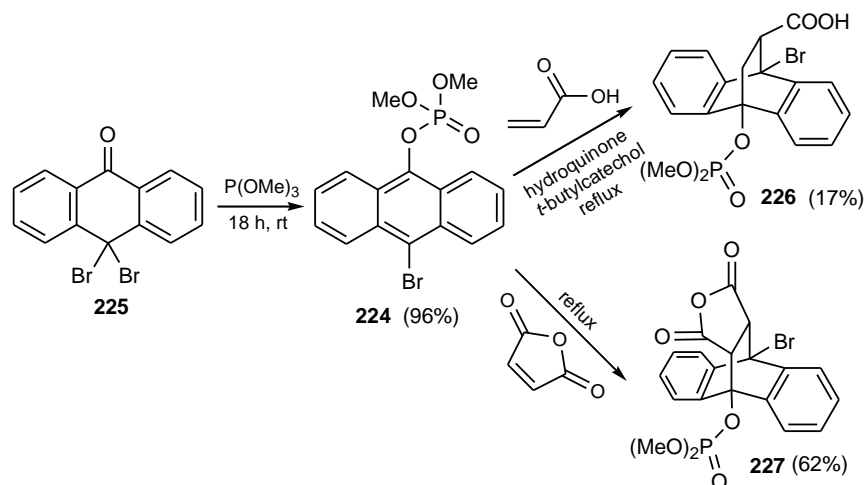


**Scheme 84.** The synthesis of 4,4'-bianthryl phosphoric acid **223** from anthr-2-ol **220** using the vanadium complexes **221a** and **221b**.

The authors investigated the catalytic properties of **223** in the Diels–Alder reaction of 2-cyclohexenone with aldimines; however, it gave only racemic mixtures.

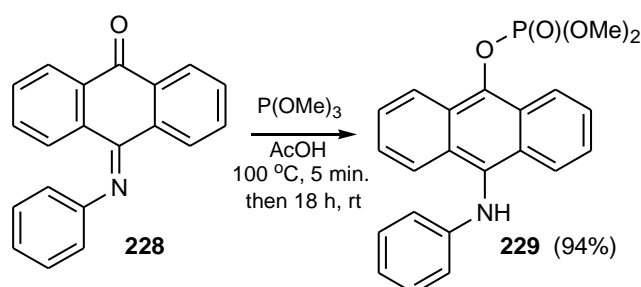
Another application of anthryl phosphates in the Diels–Alder reaction was performed by Meek and Koh [97], who described the synthesis of 10-bromo-9-(dimethoxyphosphoryloxy)

anthracene **224** obtained from 10,10-dibromoanthrone **225** and trimethyl phosphite. Next, they applied **224** as a diene in the Diels–Alder reaction with acrylic acid and maleic anhydride, which delivered adducts **226** and **227**, respectively (Scheme 85).



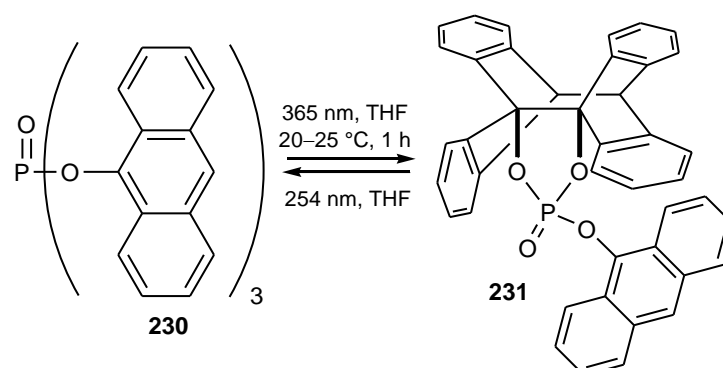
**Scheme 85.** The synthesis of **224** and its application in the Diels–Alder reaction with maleic anhydride and acrylic acid.

Then, the authors [97] described the reaction of anthraquinone anil **228** with trimethyl phosphite, yielding 9-(dimethoxyphosphoryloxy)-10-(phenylamino)anthracene **229** as yellow needles (Scheme 86).



**Scheme 86.** The synthesis of 9-(dimethoxyphosphoryloxy)-10-(phenylamino)anthracene **229** from anthraquinone anil **228**.

Nakamura and co-workers [83] studied the photolysis reactions of tri(anthr-9-yl)phosphate **230**. The authors demonstrated that upon irradiation with a 365 nm monochromatic light, **230** underwent cyclization to **231** (Scheme 87). Interestingly, the product **231** could be transformed back to **230** upon irradiation with a 254 nm monochromatic light.

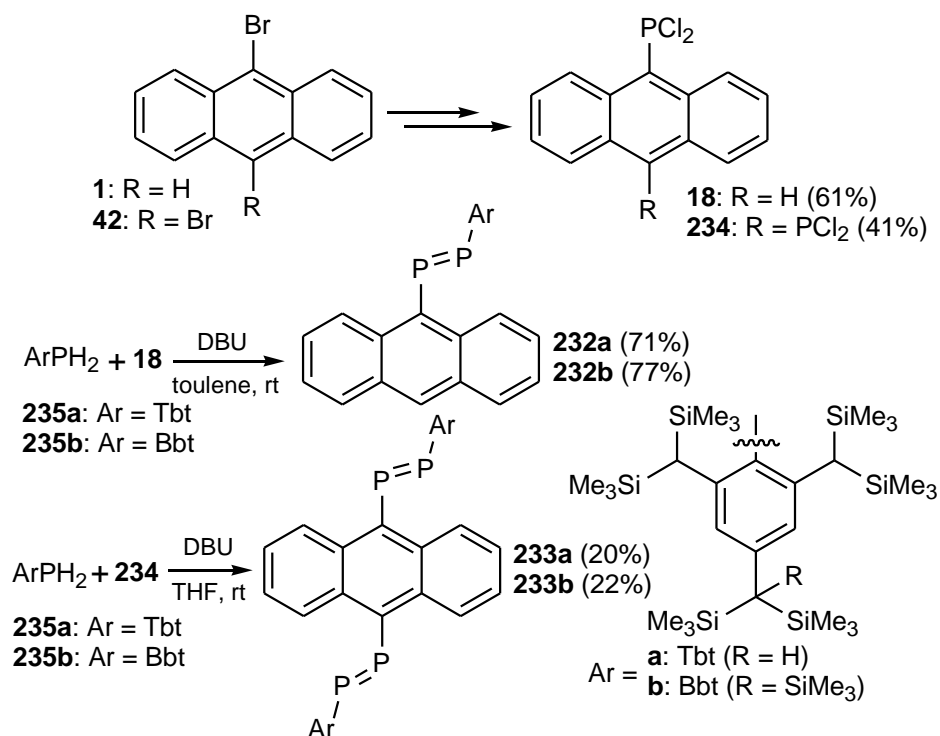


**Scheme 87.** The cyclization of **230** to **231** upon irradiation with a 365 nm monochromatic light.

## 6. Synthesis and Reactions of Diphosphenes (Anth(P=PR)) and Derivatives

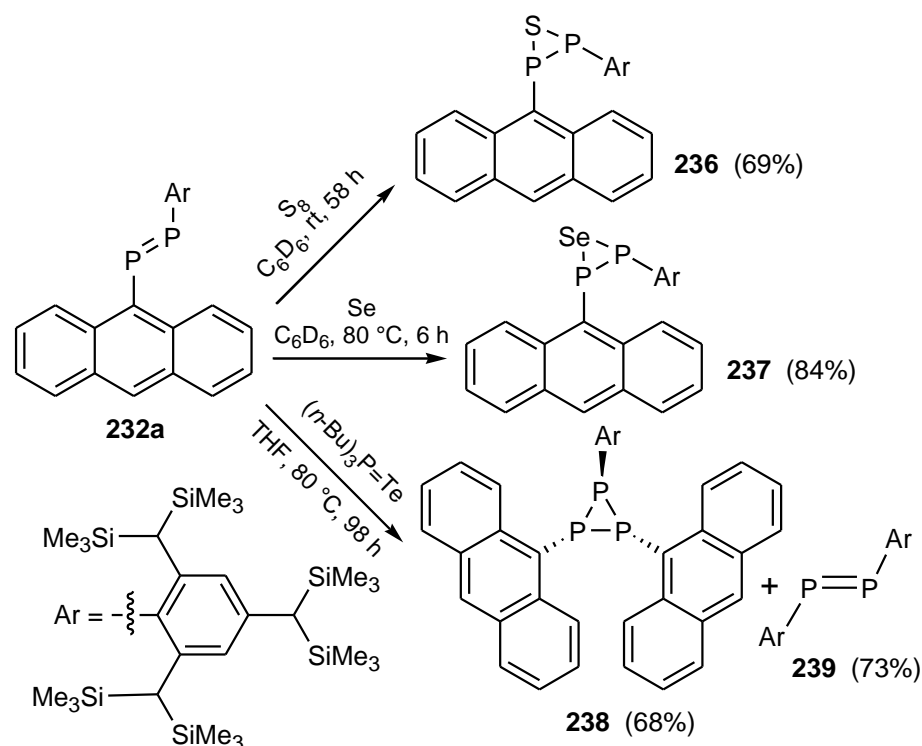
In addition to anthracenes substituted by one, two, or three organophosphorus groups with one phosphorus atom in each group, which have been described in previous sections, this section reviews anthracenes substituted by organophosphorus groups containing two or three phosphorus atoms.

9-(Diphosphenopheno)anthracenes **232** and 9,10-bis(diphosphenopheno)anthracenes **233**, presumably the first stable (diphosphenopheno)anthracenes, were synthesized by Tokitoh and co-workers [74,98]. The 2,4,6-tris[bis(trimethylsilyl)methyl]phenyl (Tbt) and 2,6-bis[bis(trimethylsilyl)methyl]-4-[tris(trimethylsilyl)methyl]phenyl (Bbt) groups, reported by Yoshifuji and co-workers, were employed for stabilization of these molecules [99]. First, 9-dichlorophosphinoanthracene **18** and 9,10-bis(dichlorophosphino)anthracene **234** were readily prepared in moderate yields from 9-bromoanthracenes **1** and **42**. Next, the condensation reaction of TbtPH<sub>2</sub> **235a** and BbtPH<sub>2</sub> **235b** with 9-dichlorophosphinoanthracene **18** in the presence of DBU (DBU = 1,8-diazabicyclo[5.4.0]undec-7-ene) as a base afforded 9-diphosphenophenoanthracenes **232a** and **232b** as stable red crystals in 71 and 77% yields, respectively (Scheme 88). 9,10-Bis(diphosphenopheno)anthracenes **233a** and **233b** were synthesized in a ca. 20% yield in a manner similar to the synthesis of 9-diphosphenophenoanthracenes **232a** and **232b** using 9,10-bis(dichlorophosphino)anthracene **234** instead of 9-(dichlorophosphino)anthracene **18**. The UV-vis spectra of **232** and **233** revealed the electronic communication between the anthryl and P=P units, which was also supported by the TD-DFT calculations. The monodiphosphene derivative **232a** exhibited a weak fluorescence in hexane solution, whereas the bis(diphosphene) derivatives **233** displayed no appreciable luminescence under the same conditions. The compounds **232a,b** and **233a,b** showed absorption maxima at 380–400, 380–400, 403–426, and 404–427 nm, accordingly.



**Scheme 88.** The synthesis of 9-diphosphenopheno- **232** and 9,10-bis(diphosphenopheno)anthracenes **233**.

The same research group also examined the specific reactions of the 9-(diphosphenopheno)anthracene **232a**, including sulfonation, selenation, and attempted telluration with tributylphosphine telluride (Scheme 89) [74,100].



**Scheme 89.** Sulfonation, selenation, and attempted telluration of **232a**.

Thus, sulfonation of **232a** gave thiadiphosphirane **236** while selenation delivered selenadiphosphirane **237** in good yields.

Surprisingly, treatment of **232a** with tributylphosphine telluride did not result in telluration via the tellurium transfer. Instead, the reaction yielded triphosphirane **238** as yellow crystals and the diphosphene derivative **239** as red crystals.

## 7. Conclusions

In this review, covering the period 1968–2022, the synthetic methods, reactions, and applications of acenes were discussed. This review revealed that phosphorus-substituted acenes with a number of benzene rings greater than three remain unknown. This opens the way for the development of new syntheses of longer acenes and insights into the properties and novel applications of such materials. Based on the current knowledge of the properties of multi-ring fused aromatics, it can be predicted that such acenes, especially electron-tunable ( $\text{P}^{\text{III}}$ ,  $\text{P}^{\text{IV}}$ ,  $\text{P}^{\text{V}}$ ) phosphorus-substituted tetracenes and pentacenes, will find more effective applications than lower analogs, mainly in optoelectronics. In particular, solid-anchored phosphonic acids that form monolayers may provide an example of such an application [5,92,93].

The second characteristic of the reviewed compounds was the low degree of substitution of aromatic rings by other substituents than organophosphorus groups and, in particular, most of anthracene moieties were unsubstituted. Apart from our preliminary work [70,71], this review showed, practically, a lack of works devoted to the highly substituted acene systems. It is noteworthy that highly substituted acenes containing thioorganic substituents showed extremely high thermal and photochemical stabilities, properties that would be interesting to verify for acenes with organophosphorus substituents [101,102]. Furthermore, the absence of hetero(S, Se)-analogs of phosphonates and phosphates was recorded during the reviewed period, which additionally opens the way for further research in this area.

**Funding:** This research was funded by the National Science Center (Poland), grant number 2019/33/B/ST4/02843 (2019–2022).

**Acknowledgments:** We thank the Bio-Med-Chem Doctoral School at the University of Łódź and Łódź Institutes of the Polish Academy of Sciences (Ł. K. and V. V) as well as the Faculty of Chemistry, University of Łódź (A. R) for the administrative support.

**Conflicts of Interest:** The authors declare no conflict of interest.

## References

1. Zhao, Y.; Duan, L.; Zhang, X.; Zhang, D.; Qiao, J.; Dong, G.; Wang, L.; Qiu, Y. White Light Emission from an Exciplex Based on a Phosphine Oxide Type Electron Transport Compound in a Bilayer Device Structure. *RSC Adv.* **2013**, *3*, 21453–21460. [[CrossRef](#)]
2. Wu, C.L.; Chang, C.H.; Chang, Y.T.; Chen, C.T.; Su, C.J. High Efficiency Non-Dopant Blue Organic Light-Emitting Diodes Based on Anthracene-Based Fluorophores with Molecular Design of Charge Transport and Red-Shifted Emission Proof. *J. Mater. Chem. C* **2014**, *2*, 7188–7200. [[CrossRef](#)]
3. Kloß, S.; Selent, D.; Spannenberg, A.; Franke, R.; Börner, A.; Sharif, M. Effects of Substitution Pattern in Phosphite Ligands Used in Rhodium-Catalyzed Hydroformylation on Reactivity and Hydrolysis Stability. *Catalysts* **2019**, *9*, 1036. [[CrossRef](#)]
4. Takizawa, S.; Kodera, J.; Yoshida, Y.; Sako, M.; Breukers, S.; Enders, D.; Sasai, H. Enantioselective Oxidative-Coupling of Polycyclic Phenols. *Tetrahedron* **2014**, *70*, 1786–1793. [[CrossRef](#)]
5. Cattani-Scholz, A.; Liao, K.-C.; Bora, A.; Pathak, A.; Hundschell, C.; Nickel, B.; Schwartz, J.; Abstreiter, G.; Tornow, M. Molecular Architecture: Construction of Self-Assembled Organophosphonate Duplexes and Their Electrochemical Characterization. *Langmuir* **2012**, *28*, 7889–7896. [[CrossRef](#)]
6. Zhou, Y.; Ayad, S.; Ruchlin, C.; Posey, V.; Hill, S.P.; Wu, Q.; Hanson, K. Examining the role of acceptor molecule structure in self-assembled bilayers: Surface loading, stability, energy transfer, and upconverted emission. *Phys. Chem. Chem. Phys.* **2018**, *20*, 20513–20524. [[CrossRef](#)]
7. Pramanik, M.; Chatterjee, N.; Das, S.; Saha, K.D.; Bhaumik, A. Anthracene-bisphosphonate based novel fluorescent organic nanoparticles explored as apoptosis inducers of cancer cells. *Chem. Commun.* **2013**, *49*, 9461–9463. [[CrossRef](#)]
8. Frank, A.W. The Phosphonous Acids and Their Derivatives. *Chem. Rev.* **1961**, *61*, 389–424. [[CrossRef](#)]
9. Keller, J.; Schlierf, C.; Nolte, C.; Mayer, P.; Straub, B.F. One-pot syntheses of sterically shielded phosphorus ligands by selective stepwise nucleophilic substitution at triphenyl phosphite. *Synthesis* **2006**, *2*, 354–365. [[CrossRef](#)]
10. Wesemann, J.; Jones, P.G.; Schomburg, D.; Heuer, L.; Schmutzler, R. Phosphorus derivatives of anthracene and their dimers. *Chem. Ber.* **1992**, *125*, 2187–2197. [[CrossRef](#)]
11. Wang, Y.; Lai, C.W.; Kwong, F.Y.; Jia, W.; Chan, K.S. Synthesis of aryl phosphines via phosphination with triphenylphosphine by supported palladium catalysts. *Tetrahedron* **2004**, *60*, 9433–9439. [[CrossRef](#)]
12. Misochko, E.Y.; Akimov, A.V.; Korchagin, D.V.; Ganushevich, Y.S.; Melnikov, E.A.; Miluykov, V.A. Generation and direct EPR spectroscopic observation of triplet arylphosphinidenes: Stabilisation versus internal rearrangements. *Phys. Chem. Chem. Phys.* **2020**, *22*, 27626–27631. [[CrossRef](#)]
13. Li, X.; Robinson, K.D.; Gaspar, P.P. A New Stereoselective Synthesis of Phosphiranes. *J. Org. Chem.* **1996**, *61*, 7702–7710. [[CrossRef](#)]
14. Luo, X.; Yuan, J.; Yue, C.-D.; Zhang, Z.-Y.; Chen, J.; Yu, G.-A.; Che, C.-M. Synthesis of peri-Substituted (Naphthalen-1-yl)phosphine Ligands by Rhodium(I)-Catalyzed Phosphine-Directed C–H Arylation. *Org. Lett.* **2018**, *20*, 1810–1814. [[CrossRef](#)]
15. Maienza, F.; Spindler, F.; Thommen, M.; Pugin, B.; Malan, C.; Mezzetti, A. Exploring Stereogenic Phosphorus: Synthetic Strategies for Diphosphines Containing Bulky, Highly Symmetric Substituents. *J. Org. Chem.* **2002**, *67*, 5239–5249. [[CrossRef](#)]
16. Haenel, M.W.; Oevers, S.; Bruckmann, J.; Kuhnigk, J.; Krüger, C. Facile Syntheses of 1,8-bis(diphenylphosphino)anthracene and 1,8-bis(dimethylamino)anthracene by nucleophilic substitution of 1,8-difluoroanthracene. *Synlett.* **1998**, *3*, 301–303. [[CrossRef](#)]
17. Musa, S.; Shaposhnikov, I.; Cohen, S.; Gelman, D. Ligand–Metal Cooperation in PCP Pincer Complexes: Rational Design and Catalytic Activity in Acceptorless Dehydrogenation of Alcohols. *Angew. Chem. Int. Ed.* **2011**, *50*, 3533–3537. [[CrossRef](#)]
18. Radchenko, Y.; Mujahed, S.; Musa, S.; Gelman, D. Synthesis and characterization of chiral enantiopure PC(sp<sup>3</sup>)P pincer ligands and their complexes. *Inorg. Chim. Acta* **2021**, *521*, 120350. [[CrossRef](#)]
19. Jiang, Z.; Xu, M.; Li, F.; Yu, Y. Red-Light-Controllable Liquid-Crystal Soft Actuators via Low-Power Excited Upconversion Based on Triplet–Triplet Annihilation. *J. Am. Chem. Soc.* **2013**, *135*, 16446–16453. [[CrossRef](#)]
20. Kilian, P.; Slawin, A.M.Z. 1,8,9-Substituted anthracenes, intramolecular phosphine donor stabilized metaphosphonate and phosphonium. *Dalton Trans.* **2007**, 3289–3296. [[CrossRef](#)]
21. Yang, B.; Wang, Z.X. Ni-Catalyzed C–P Coupling of Aryl, Benzyl, or Allyl Ammonium Salts with P(O)H Compounds. *J. Org. Chem.* **2019**, *84*, 1500–1509. [[CrossRef](#)]
22. Zhang, J.S.; Chen, T.; Han, L.B. Palladium-Catalyzed Direct Decarbonylative Phosphorylation of Benzoic Acids with P(O)–H Compounds. *Eur. J. Org. Chem.* **2020**, *2020*, 1148–1153. [[CrossRef](#)]
23. Tao, R.; Zhao, J.; Zhong, F.; Zhang, C.; Yang, W.; Xu, K. H<sub>2</sub>O<sub>2</sub>-Activated Triplet–Triplet Annihilation Upconversion via Modulation of the Fluorescence Quantum Yields of the Triplet Acceptor and the Triplet–Triplet–Energy–Transfer Efficiency. *Chem. Commun.* **2015**, *51*, 12403–12406. [[CrossRef](#)]
24. Xu, M.; Han, C.; Yang, Y.; Shen, Z.; Feng, W.; Li, F. Time-Oxygen & Light Indicating: Via Photooxidation Mediated up-Conversion. *J. Mater. Chem. C* **2016**, *4*, 9986–9992. [[CrossRef](#)]

25. Xu, H.B.; Wang, J.; Chen, X.L.; Xu, P.; Xiong, K.T.; Guan, D.B.; Deng, J.G.; Deng, Z.H.; Kurmoo, M.; Zeng, M.H. Regulating Structural Dimensionality and Emission Colors by Organic Conjugation between SmIII at a Fixed Distance. *Dalton Trans.* **2018**, *47*, 6908–6916. [[CrossRef](#)]
26. Yamaguchi, S.; Akiyama, S.; Tamao, K. The Coordination Number-Photophysical Properties Relationship of Trianthrylphosphorus Compounds: Doubly Locked Fluorescence of Anthryl Groups. *J. Organomet. Chem.* **2002**, *646*, 277–281. [[CrossRef](#)]
27. Okada, Y.; Okeya, K.; Murata, Y.; Aoki, N.; Aoki, T.; Sugitani, M.; Yasui, S.; Sawada, Y.; Ogura, F. Synthesis of Phosphine Oxide-Carboxylic Acid Esters Bearing 9,10-Dihydro-9,10-ethanoanthracene Moiety. *Phosphorus Sulfur Silicon Relat. Elem.* **2003**, *178*, 821–829. [[CrossRef](#)]
28. Katagiri, K.; Yamamoto, Y.; Takahata, Y.; Kishibe, R.; Fujimoto, N. Photoreaction of anthracenyl phosphine oxides: Usual reversible photo- and heat-induced emission switching, and unusual oxidative PC bond cleavage. *Tetrahedron Lett.* **2019**, *60*, 2026–2029. [[CrossRef](#)]
29. Schwab, G.; Stern, D.; Stalke, D. Structural and Variable-Temperature NMR Studies of 9-Diisopropylphosphanyl anthracenes and 9,10-Bis(diisopropylphosphanyl)anthracenes and Their Oxidation Products. *J. Org. Chem.* **2008**, *73*, 5242–5247. [[CrossRef](#)]
30. Chen, L.; Wang, S.; Werz, P.; Han, Z.; Gates, D.P. A “masked” source for the phosphalkene MesP=CH<sub>2</sub>: Trapping, rearrangement, and oligomerization. *Heteroat. Chem.* **2018**, *29*, e21474. [[CrossRef](#)]
31. Chen, X.; Liu, X.; Zhu, H.; Wang, Z. Palladium-catalyzed C–P bond activation of aroyl phosphine oxides without the adjacent “anchoring atom”. *Tetrahedron* **2021**, *81*, 131912. [[CrossRef](#)]
32. Chrzanowski, J.; Krasowska, D.; Urbaniak, M.; Sieroń, L.; Pokora-Sobczak, P.; Demchuk, O.M.; Drabowicz, J. Synthesis of Enantioenriched Aryl-*tert*-Butylphenylphosphine Oxides via Cross-Coupling Reactions of *tert*-Butylphenylphosphine Oxide with Aryl Halides. *Eur. J. Org. Chem.* **2018**, *2018*, 4614–4627. [[CrossRef](#)]
33. Schillmöller, T.; Ruth, P.N.; Herbst-Irmer, R.; Stalke, D. Three colour solid-state luminescence from positional isomers of facily modified thiophosphoranyl anthracenes. *Chem. Commun.* **2020**, *56*, 7479–7482. [[CrossRef](#)] [[PubMed](#)]
34. Schillmöller, T.; Ruth, P.N.; Herbst-Irmer, R.; Stalke, D. Analysis of Solid-State Luminescence Emission Amplification at Substituted Anthracenes by Host–Guest Complex Formation. *Chem. Eur. J.* **2020**, *26*, 17390–17398. [[CrossRef](#)]
35. Köhler, C.; Lübber, J.; Krause, L.; Hoffmann, C.; Herbst-Irmer, R.; Stalke, D. Comparison of different strategies for modelling hydrogen atoms in charge density analyses. *Acta Cryst. B* **2019**, *75*, 434–441. [[CrossRef](#)]
36. Niepötter, B.; Herbst-Irmer, R.; Stalke, D. Empirical correction for resolution- and temperature-dependent errors caused by factors such as thermal diffuse scattering. *J. Appl. Cryst.* **2015**, *48*, 1485–1497. [[CrossRef](#)]
37. Breshears, A.T.; Behrle, A.C.; Barnes, C.L.; Laber, C.H.; Baker, G.A.; Walensky, J.R. Synthesis, spectroscopy, electrochemistry, and coordination chemistry of substituted phosphine sulfides and selenides. *Polyhedron* **2015**, *100*, 333–343. [[CrossRef](#)]
38. Schwab, G.; Stern, D.; Leusser, D.; Stalke, D. Syntheses and Structures of 9-Bromo-10-diphenylphosphanyl anthracene and its Oxidation Products. *Z. Naturforsch. B* **2007**, *62*, 711–716. [[CrossRef](#)]
39. Fei, Z.; Kocher, N.; Mohrschladt, C.J.; Ihmels, H.; Stalke, D. Single Crystals of the Disubstituted Anthracene 9,10-(Ph<sub>2</sub>P=S)<sub>2</sub>C<sub>14</sub>H<sub>8</sub> Selectively and Reversibly Detect Toluene by Solid-State Fluorescence Emission. *Angew. Chem. Int. Ed.* **2003**, *42*, 783–787. [[CrossRef](#)]
40. Yip, J.H.K.; Prabhavathy, J. A Luminescent Gold Ring That Flips Like Cyclohexane. *Angew. Chem. Int. Ed.* **2001**, *40*, 2159–2162. [[CrossRef](#)]
41. Stephan, M.; Šterk, D.; Modéc, B.; Mohar, B. Study of the Reaction of Bulky Aryllithium Reagents with 3,4-Dimethyl-2,5-diphenyl-1,3,2-oxazaphospholidine-2-borane Derived from Ephedrine. *J. Org. Chem.* **2007**, *72*, 8010–8018. [[CrossRef](#)]
42. Watanabe, K.; Yamashita, M.; Yamamoto, Y.; Akiba, K.-y. Synthesis and Application of New Tridentate Anthracene Ligands Bearing Donative Phosphorus(III) Atoms at 1,8-Positions. *Phosphorus Sulfur Silicon Relat. Elem.* **2002**, *177*, 2047–2048. [[CrossRef](#)]
43. Müller, T.E.; Green, J.C.; Mingos, D.M.P.; McPartlin, C.M.; Whittingham, C.; Williams, D.J.; Woodroffe, T.M. Complexes of gold(I) and platinum(II) with polyaromatic phosphine ligands. *J. Organomet. Chem.* **1998**, *551*, 313–330. [[CrossRef](#)]
44. Lin, R.; Yip, J.H.K.; Zhang, K.; Koh, L.L.; Wong, K.-Y.; Ho, K.P. Self-Assembly and Molecular Recognition of a Luminescent Gold Rectangle. *J. Am. Chem. Soc.* **2004**, *126*, 15852–15869. [[CrossRef](#)]
45. Lin, R.; Yip, J.H.K. Self-Assembly, Structures, and Solution Dynamics of Emissive Silver Metallacycles and Helices. *Inorg. Chem.* **2006**, *45*, 4423–4430. [[CrossRef](#)]
46. Zhang, K.; Prabhavathy, J.; Yip, J.H.K.; Koh, L.L.; Tan, G.K.; Vittal, J.J. First Examples of AuI–X–AgI Halonium Cations (X = Cl and Br). *J. Am. Chem. Soc.* **2003**, *125*, 8452–8453. [[CrossRef](#)]
47. Ma, Z.; Xing, Y.; Yang, M.; Hu, M.; Liu, B.; Guedes da Silva, M.F.C.; Pompeiro, A.J.L. The double-helicate terpyridine silver(I) compound [Ag<sub>2</sub>L<sub>2</sub>](SO<sub>3</sub>CF<sub>3</sub>)<sub>2</sub> (L=4′-phenyl-terpyridine) as a building block for di- and mononuclear complexes. *Inorg. Chim. Acta* **2009**, *362*, 2921–2926. [[CrossRef](#)]
48. Meyer, T.G.; Jones, P.G.; Schmutzler, R. Darstellung neuer Monofluorosphine und einiger ihrer Übergangsmetallkomplexe; Einkristall-Röntgenstrukturanalyse eines Platin(II)-Komplexes/Preparation of New Monofluorophosphines and Some of their Transition Metal Complexes; Single Crystal X-ray Diffraction Study of a Platinum(II) Complex. *Z. Naturforsch. B* **1993**, *48*, 875–885. [[CrossRef](#)]
49. Romero, P.E.; Whited, M.T.; Grubbs, R.H. Multiple C–H Activations of Methyl *tert*-Butyl Ether at Pincer Iridium Complexes: Synthesis and Thermolysis of Ir(I) Fischer Carbenes. *Organometallics* **2008**, *27*, 3422–3429. [[CrossRef](#)]

50. Haenel, M.W.; Oevers, S.; Angermund, K.; Kaska, W.C.; Fan, H.; Hall, M.B. Thermally Stable Homogeneous Catalysts for Alkane Dehydrogenation. *Angew. Chem. Int. Ed.* **2001**, *40*, 3596–3600. [CrossRef]
51. Osawa, M.; Hoshino, M.; Wada, T.; Hayashi, F.; Osanai, S. Intra-Complex Energy Transfer of Europium(III) Complexes Containing Anthracene and Phenanthrene Moieties. *J. Phys. Chem. A* **2009**, *113*, 10895–10902. [CrossRef] [PubMed]
52. Kitagawa, Y.; Naito, A.; Fushimi, K.; Hasegawa, Y. Bright sky-blue fluorescence with high colour purity: Assembly of luminescent diphenyl-anthracene lutetium-based coordination polymer. *RSC Adv.* **2021**, *11*, 6604–6606. [CrossRef]
53. Chen, J.; Zhang, L.; Shi, L.; Ye, H.; Chen, Z. Preparation, characterization and redox chemistry of oxo-centered triruthenium dimers linked by bis(diphenylphosphino)anthracene and -ferrocene. *Inorg. Chim. Acta.* **2005**, *358*, 859–864. [CrossRef]
54. Deeming, A.J.; Martin, C.M. Coordination of an anthracene-derived ligand through eight carbon atoms in the pentaruthenium bow-tie clusture,  $[\text{Ru}_5(\text{CO})_{13}(\mu_5\text{-}\eta^1\text{:}\eta^2\text{:}\eta^3\text{:}\eta^3\text{-C}_{14}\text{H}_8\text{-}\eta^1\text{-PPh})]$ . *Chem. Commun.* **1996**, 53–54. [CrossRef]
55. Piche, L.; Daigle, J.-C.; Poli, R.; Claverie, J.P. Investigation of Steric and Electronic Factors of (Arylsulfonyl)phosphane-Palladium Catalysts in Ethene Polymerization. *Eur. J. Inorg. Chem.* **2010**, *2010*, 4595–4601. [CrossRef]
56. Shimizu, M.; Yamamoto, T. 9-(Diphenylphosphino)anthracene-based phosphapalladacycle catalyzed conjugate addition of arylboronic acids to electron-deficient alkenes. *Tetrahedron Lett.* **2020**, *61*, 152257. [CrossRef]
57. Burrows, A.D.; Choi, N.; McPartlin, M.; Mingos, D.M.P.; Tarlton, S.V.; Vilar, R. Syntheses and structural characterisation of the compounds  $[\text{Pd}(\text{dba})\text{L}_2]$  (where  $\text{L}=\text{PBz}_3$  and  $\text{PPh}_2\text{Np}$ ) and the novel dimer  $[\text{Pd}_2(\text{m-dba})(\text{m-SO}_2)(\text{PBz}_3)_2]$ . *J. Organomet. Chem.* **1999**, *573*, 313–322. [CrossRef]
58. Azerraf, C.; Shpruhman, A.; Gelman, D. Diels–Alder cycloaddition as a new approach toward stable  $\text{PC}(\text{sp}^3)\text{P}$ -metalated compounds. *Chem. Commun.* **2009**, 466–468. [CrossRef]
59. Haenel, M.W.; Jakubik, D.; Krüger, C.; Betz, P. 1,8-Bis(diphenylphosphino)anthracene and Metal Complexes. *Chem. Ber.* **1991**, *124*, 333–336. [CrossRef]
60. Heuer, L.; Schomburg, D.; Schmutzler, R. Dimeres 9-(Difluorophosphino)anthracen: Synthese, Eigenschaften und Struktur. *Chem. Ber.* **1989**, *122*, 1473–1476. [CrossRef]
61. Hu, J.; Yip, J.H.K. Regioselective Double Cycloplatination of 9,10-Bis(diphenylphosphino)anthracene. *Organometallics* **2009**, *28*, 1093–1100. [CrossRef]
62. Hu, J.; Lin, R.; Yip, J.H.K.; Wong, K.; Ma, D.; Vittal, J.J. Synthesis and electronic spectroscopy of luminescent cyclometalated platinum-anthracenyl complexes. *Organometallics* **2007**, *26*, 6533–6543. [CrossRef]
63. Yang, F.; Fanwick, P.E.; Kubiak, C.P. Synthesis of 1-(9-Anthracene)phosphirane and Novel Intramolecular  $\pi$ -Stacking of 1-(9-Anthracene)phosphirane Ligands in a cis-Platinum(II) Complex. *Organometallics* **1999**, *18*, 4222–4225. [CrossRef]
64. Yang, F.; Fanwick, P.E.; Kubiak, C.P. Inter- and Intramolecular  $\pi$ -Stacking Interactions in cis-Bis{1-(9-anthracene)}phosphirane Complexes of Platinum(II). *Inorg. Chem.* **2002**, *41*, 4805–4809. [CrossRef]
65. Hu, J.; Xu, H.; Nguyen, M.; Yip, J.H.K. Photooxidation of a platinum-anthracene pincer complex: Formation and structures of Pt(II)-anthrone and -ketal complexes. *Inorg. Chem.* **2009**, *48*, 9684–9692. [CrossRef]
66. Arrigo, L.M.; Galenas, M.; Bassil, D.B.; Tucker, S.A.; Kannan, R.; Katti, K.V.; Barnes, C.L.; Jurisson, S.S. Fluorescent phosphinimine as possible precursor to an anionic and fluorescent sensor for Tc-99. *Radiochim. Acta* **2008**, *96*, 835–844. [CrossRef]
67. Belyaev, A.; Cheng, Y.-H.; Liu, Z.-Y.; Karttunen, A.J.; Chou, P.-T.; Koshevoy, I.O. A Facile Molecular Machine: Optically Triggered Counterion Migration by Charge Transfer of Linear Donor- $\pi$ -Acceptor Phosphonium Fluorophores. *Angew. Chem. Int. Ed.* **2019**, *58*, 13456–13465. [CrossRef]
68. Huang, W.; Zhong, C.-H. Metal-Free Synthesis of Aryltriphenylphosphonium Bromides by the Reaction of Triphenylphosphine with Aryl Bromides in Refluxing Phenol. *ACS Omega* **2019**, *4*, 6690–6696. [CrossRef]
69. Nikitin, K.; Jennings, E.V.; Al Sulaimi, S.; Ortin, Y.; Gilheany, D.G. Dynamic Cross-Exchange in Halophosphonium Species: Direct Observation of Stereochemical Inversion in the Course of an  $\text{SN}_2$  Process. *Angew. Chem. Int. Ed.* **2018**, *57*, 1480–1484. [CrossRef]
70. Bałczewski, P.; Dudziński, B.; Koprowski, M.; Knopik, Ł.; Owsianik, K. Fused aromatic hydrocarbons substituted with organophosphorus groups, method of their production, intermediate compounds, and applications. Patent Appl. PL-438275, 26 June 2021.
71. Bałczewski, P.; Koprowski, M.; Knopik, Ł.; Dudziński, B.; Owsianik, K.; Różycka-Sokołowska, E. IL-15, P-111, P-112, P-116. In Proceedings of the International Conference on Phosphorus Chemistry (23rd ICPC), Częstochowa, Poland, 5–9 July 2021.
72. Kirst, C.; Tietze, J.; Ebeling, M.; Horndasch, L.; Karaghiosoff, K. The Formation of P–C Bonds Utilizing Organozinc Reagents for the Synthesis of Aryl- and Heteroaryl-Dichlorophosphines. *J. Org. Chem.* **2021**, *86*, 17337–17343. [CrossRef]
73. Vogt, R.; Jones, P.G.; Schmutzler, R. Darstellung, Struktur und Eigenschaften von harnstoffverbrückten cyclischen Phosphoniumsalzen mit Phosphor-Phosphor-, Phosphor-Arsen-, Phosphor-Antimon- und Phosphor-Zinn-Bindung. *Chem. Ber.* **1993**, *126*, 1271–1281. [CrossRef]
74. Tsurusaki, A.; Nagahora, N.; Sasamori, T.; Matsuda, K.; Kanemitsu, Y.; Watanabe, Y.; Hosoi, Y.; Furukawa, Y.; Tokitoh, N. Synthesis, structures, and reactivity of kinetically stabilized anthryldiphosphene derivatives. *Bull. Chem. Soc. Jpn.* **2010**, *83*, 456–478. [CrossRef]
75. Yakhvarov, D.; Trofimova, E.; Sinyashin, O.; Kataeva, O.; Budnikova, Y.; Lönnecke, P.; Hey-Hawkins, E.; Petr, A.; Krupskaya, Y.; Kataev, V.; et al. New Dinuclear Nickel(II) Complexes: Synthesis, Structure, Electrochemical, and Magnetic Properties. *Inorg. Chem.* **2011**, *50*, 4553–4558. [CrossRef]



76. Yakhvarov, D.G.; Trofimova, E.A.; Dobrynin, A.B.; Gerasimova, T.P.; Katsyuba, S.A.; Sinyashin, O.G. First neutral dinuclear cobalt complex formed by bridging  $[\mu\text{-O}2\text{P}(\text{H})\text{R}]$ -ligands: Synthesis, X-ray crystal structure and quantum-chemical study. *Mendeleev Commun.* **2015**, *25*, 27–28. [[CrossRef](#)]
77. Kalek, M.; Stawinski, J. Efficient synthesis of mono- and diarylphosphinic acids: A microwave-assisted palladium-catalyzed cross-coupling of aryl halides with phosphinate. *Tetrahedron* **2009**, *65*, 10406–10412. [[CrossRef](#)]
78. Kuimov, V.A.; Matveeva, E.A.; Telezhkin, A.A.; Malysheva, S.F.; Gusarova, N.K.; Trofimov, B.A. Reaction of 9-bromoanthracene with red phosphorus in the system KOH–DMSO. *Russ. J. Org. Chem.* **2016**, *52*, 1059–1061. [[CrossRef](#)]
79. Ishii, A.; Kikushima, C.; Hayashi, Y.; Ohtsuka, N.; Nakata, N.; Muranaka, A.; Tanaka, Y.; Uchiyama, M. 1-Phosphino-1,3-butadiene derivatives Incorporated with dibenzobarrelene skeleton: Synthesis and photophysical properties. *Bull. Chem. Soc. Jpn.* **2020**, *93*, 1430–1442. [[CrossRef](#)]
80. French, D.; Simmons, J.G.; Everitt, H.; Foulger, S.H.; Gray, G.M. Synthesis and Characterization of Amphiphilic Arenephosphonates as Water-Soluble Micellar Radioluminescent Probes. *ChemRxiv* **2020**. [[CrossRef](#)]
81. Nagode, S.B.; Kant, R.; Rastogi, N. Hantzsch Ester-Mediated Benzannulation of Diazo Compounds under Visible Light Irradiation. *Org. Lett.* **2019**, *21*, 6249–6254. [[CrossRef](#)]
82. Shu, Z.; Zhou, J.; Li, J.; Cheng, Y.; Liu, H.; Wang, D.; Zhou, Y. Rh(III)-Catalyzed Dual C–H Functionalization/Cyclization Cascade by a Removable Directing Group: A Method for Synthesis of Polycyclic Fused Pyrano[de]Isochromenes. *J. Org. Chem.* **2020**, *85*, 12097–12107. [[CrossRef](#)]
83. Nakamura, M.; Sawasaki, K.; Okamoto, Y.; Takamuku, S. Photolyses of Derivatives of Naphthyl and Anthryl Phosphates and Methylphosphonates. *Bull. Chem. Soc. Jpn.* **1995**, *68*, 3189–3197. [[CrossRef](#)]
84. Bessmertnykh, A.; Douaihy, C.M.; Guillard, R. Direct Synthesis of Amino-substituted Aromatic Phosphonates via Palladium-catalyzed Coupling of Aromatic Mono- and Dibromides with Diethyl Phosphite. *Chem. Lett.* **2009**, *38*, 738–739. [[CrossRef](#)]
85. Amicangelo, J.C.; Leenstra, W.R. Zirconium Arene-Phosphonates: Chemical and Structural Characterization of 2-Naphthyl- and 2-Anthracenylphosphonate Systems. *Inorg. Chem.* **2005**, *44*, 2067–2073. [[CrossRef](#)]
86. Amicangelo, J.C.; Leenstra, W.R. Excimer Formation in the Interlayer Region of Arene-Derivatized Zirconium Phosphonates. *J. Am. Chem. Soc.* **2003**, *125*, 14698–14699. [[CrossRef](#)]
87. Hill, S.P.; Banerjee, T.; Dilbeck, T.; Hanson, K. Photon Upconversion and Photocurrent Generation via Self-Assembly at Organic–Inorganic Interfaces. *J. Phys. Chem. Lett.* **2015**, *6*, 4510–4517. [[CrossRef](#)]
88. Zhou, Y.; Hill, S.P.; Hanson, K. Influence of meta- and para-phosphonated diphenylanthracene on photon upconversion in self-assembled bilayers. *J. Photon. Energy* **2007**, *8*, 022004. [[CrossRef](#)]
89. Yazji, S.; Westermeier, C.; Weinbrenner, D.; Sachsenhauser, M.; Liao, K.C.; Noever, S.; Postorino, P.; Schwartz, J.; Abstreiter, G.; Nickel, B.; et al. Surface-Directed Molecular Assembly of Pentacene on Aromatic Organophosphonate Self-Assembled Monolayers Explored by Polarized Raman Spectroscopy. *J. Raman Spectrosc.* **2017**, *48*, 235–242. [[CrossRef](#)]
90. Cattani-Scholz, A.; Liao, K.-C.; Bora, A.; Pathak, A.; Krautloher, M.; Nickel, B.; Schwartz, J.; Tornow, M.; Abstreiter, G. A New Molecular Architecture for Molecular Electronics. *Angew. Chem. Int. Ed.* **2011**, *50*, A11–A16. [[CrossRef](#)]
91. Kabachnik, M.; Solntseva, M.; Izmer, V.; Novikova, Z.; Beletskaya, I. Palladium-catalyzed phase-transfer arylation of dialkyl phosphonates. *Russ. J. Org. Chem.* **1998**, *34*, 93–97.
92. McDermott, J.E.; McDowell, M.; Hill, I.G.; Hwang, J.; Kahn, A.; Bernasek, S.L.; Schwartz, J. Organophosphonate Self-Assembled Monolayers for Gate Dielectric Surface Modification of Pentacene-Based Organic Thin-Film Transistors: A Comparative Study. *J. Phys. Chem. A* **2007**, *111*, 12333–12338. [[CrossRef](#)]
93. Liao, K.C.; Ismail, A.G.; Kreplak, L.; Schwartz, J.; Hill, I.G. Designed Organophosphonate Self-Assembled Monolayers Enhance Device Performance of Pentacene-Based Organic Thin-Film Transistors. *Adv. Mater.* **2010**, *22*, 3081–3085. [[CrossRef](#)] [[PubMed](#)]
94. Buckland, S.J.; Davidson, R.S. The Photooxidation of Some Anthryl Phosphorus Compounds. *Phosphorus Sulfur Relat. Elem.* **1983**, *18*, 225–228. [[CrossRef](#)]
95. Yamashita, M.; Yamamoto, Y.; Akiba, K.-Y.; Nagase, S. Synthesis of a Versatile Tridentate Anthracene Ligand and Its Application for the Synthesis of Hypervalent Pentacoordinate Boron Compounds (10-B-5). *Angew. Chem. Int. Ed.* **2000**, *39*, 4055–4058. [[CrossRef](#)]
96. Yamashita, M.; Yamamoto, Y.; Akiba, K.; Hashizume, D.; Iwasaki, F.; Takagi, N.; Nagase, S. Syntheses and Structures of Hypervalent Pentacoordinate Carbon and Boron Compounds Bearing an Anthracene Skeleton – Elucidation of Hypervalent Interaction Based on X-Ray Analysis and DFT Calculation. *J. Am. Chem. Soc.* **2005**, *127*, 4354–4371. [[CrossRef](#)]
97. Meek, J.S.; Koh, L. Syntheses and Reactions of Phosphates from Dibromoanthrone. Anthraquinone Anil, and 1,8-Dichloroanthraquinone. *J. Org. Chem.* **1970**, *35*, 153–156. [[CrossRef](#)]
98. Sasamori, T.; Tsurusaki, A.; Nagahora, N.; Matsuda, K.; Kanemitsu, Y.; Watanabe, Y.; Furukawa, Y.; Tokitoh, N. Synthesis and Properties of 9-Anthryldiphosphene. *Chem. Lett.* **2006**, *35*, 1382–1383. [[CrossRef](#)]
99. Yoshifuji, M.; Shima, I.; Inamoto, N.; Hirotsu, K.; Higuchi, T. Synthesis and structure of bis(2,4,6-tri-tert-butylphenyl)diphosphene: Isolation of a true phosphobenzene. *J. Am. Chem. Soc.* **1981**, *103*, 4587–4589. [[CrossRef](#)]
100. Tokitoh, N.; Tsurusaki, A.; Sasamori, T. A Unique Thermal Reaction of 9-Anthryldiphosphene Leading to the Formation of a Triphosphirane Derivative. *Phosphorus Sulfur Silicon Relat. Elem.* **2009**, *184*, 979–986. [[CrossRef](#)]

101. Bałczewski, P.; Kowalska, E.; Różycka-Sokołowska, E.; Skalik, J.; Owsianik, K.; Koprowski, M.; Marciniak, B.; Guziejewski, D.; Ciesielski, W. Mono-Aryl/Alkylthio-Substituted (Hetero)acenes of Exceptional Thermal and Photochemical Stability by the Thio-Friedel-Crafts/Bradsher Cyclization Reaction. *Chem. Eur. J.* **2019**, *25*, 14148–14161. [[CrossRef](#)]
102. Bałczewski, P.; Kowalska, E.; Różycka-Sokołowska, E.; Uznański, P.; Wilk, J.; Koprowski, M.; Owsianik, K.; Marciniak, B. Organosulfur Materials with High Photo- and Photo-Oxidation Stability: 10-Anthryl Sulfoxides and Sulfones and Their Photo-physical Properties Dependent on the Sulfur Oxidation State. *Materials* **2021**, *14*, 3506. [[CrossRef](#)]